5-1-2012

Mechanisms of hydrogen sulfide induced vasodilation

Olan Jackson-Weaver

Olan Jackson-Weaver

Candidate

Biomedical Sciences

Department

This dissertation is approved, and it is acceptable in quality and form for publication:

Approved by the Dissertation Committee:

Nancy Kanagy , Chairperson

Ben Walker

Laura Gonzalez Bosc

Tom Resta

Bill Shuttleworth

MECHANSIMS OF HYDROGEN SULFIDE INDUCED VASODILATION

by

OLAN JACKSON-WEAVER

B.S. Biology, B.A. Chemistry, University of New Mexico,
Albuquerque, NM, 2006

DISSERTATION

Submitted in Partial Fulfillment of the
Requirements for the Degree of

Doctor of Philosophy
Biomedical Sciences

The University of New Mexico
Albuquerque, New Mexico

May 2012

ACKNOWLEDGEMENTS

I am enormously grateful to my mentor Nancy Kanagy for giving me the opportunity to pursue my degree in her lab. Her enthusiasm and guidance has made this project and my graduate school experience successful as well as enjoyable. She has taught me more than I can express about the scientific process, not to mention giving presentations and writing logically and precisely. Her guidance and friendship will forever be a part of my life and future work.

I would also like to thank my other committee members, Drs. Ben Walker, Laura Gonzalez Bosc, Tom Resta, and Bill Shuttleworth. My project was not always straightforward, and several times became downright confusing. Their insight and guidance helped to bring it back on track and make it the success I feel it has become. They each contributed knowledge and expertise to the project which was invaluable.

I am also very grateful for the support my family has given me through this process and throughout my life. I am forever grateful to my wife Jessica for her unwavering support during even the toughest times of graduate school. Also, her questioning mind has undoubtedly made me a better scientist. And finally, I wouldn't be here without my parents, who instilled a curiosity about the natural world in me and always supported my interests in any way they could.

MECHANISMS OF HYDROGEN SULFIDE INDUCED VASODILATION

by

Olan Jackson-Weaver

B.S., Biology, B.A., Chemistry, University of New Mexico, 2006
Ph.D., Biomedical Sciences, University of New Mexico, 2012

ABSTRACT

Myogenic tone is an important regulator of blood flow and may contribute to peripheral vascular resistance and blood pressure. Myogenic tone is a luminal pressure-induced constriction of the vasculature that is mediated by a vascular smooth muscle cell (VSMC) plasma membrane potential (E_m) depolarization and Ca^{2+} influx. Ca^{2+} sparks, which are ryanodine receptor (RyR) mediated Ca^{2+} release events, oppose myogenic tone by activating large-conductance Ca^{2+}-activated K^+ channels (BK_{Ca}) to hyperpolarize VSMC E_m. The gaseous signaling molecules (gasotransmitters) NO and CO activate Ca^{2+} sparks to cause vasodilation. H_2S, a third gasotransmitter produced by cystationine γ-lyase (CSE) in the vasculature, activates several K^+ channels to promote VSMC E_m hyperpolarization. We therefore sought to determine whether H_2S inhibits the development of myogenic tone. We hypothesized that H_2S opposes myogenic tone through the activation of Ca^{2+} sparks and subsequent BK_{Ca} channel activation. We observed that in small mesenteric arteries CSE-produced H_2S reduced myogenic tone. We also found that RyR-mediated Ca^{2+} sparks and BK_{Ca} channel activity opposed tone in

these arteries. We also observed that exogenous and endogenous H_2S activates sparks and hyperpolarizes VSMC E_m. Futhermore, exogenous H_2S-mediated vasodilation, spark activation, and VSMC E_m hyperpolarization required active endothelial BK_{Ca} channels and cytochrome P450 2C. Therefore, H_2S seems to be an important regulator of myogenic tone in the mesenteric circulation. The mechanism by which H_2S causes vasodilation in this bed is an unexpectedly complex pathway, with activation of endothelial BK_{Ca} channels and cytochrome P450 with subsequent activation of VSMC Ca^{2+} sparks. The effects of H_2S here described may be an important mechanism by which this signaling molecule alters hemodynamic parameters *in vivo*.

TABLE OF CONTENTS

LIST OF FIGURES

CHAPTER 1 INTRODUCTION

CHAPTER 2

Intermittent Hypoxia in Rats Increases Myogenic Tone through Loss of Hydrogen Sulfide Activation of Large-Conductance Ca^{2+}-Activated Potassium Channels.

CHAPTER 3

Hydrogen sulfide causes vasodilation through activation of calcium sparks in small mesenteric arteries

CHAPTER 1. INTRODUCTION

Myogenic Tone

The phenomenon of tonic, as opposed to rhythmic, contractility of arteries that is enhanced by pressure was first described over 150 years ago in bat wing arteries by T. Wharton Jones (57). However, the idea that this property is inherent to the vascular smooth muscle ("myogenic"), and not a property of neural or humoral factors, was first argued by W.M Bayliss in 1902 (8). In fact, Bayliss observed the pressure-induced constriction of an isolated, cannulated artery, essentially the same technique used today to study the phenomenon (Fig. 1). Bayliss saw myogenic tone as a mechanism by which tissue perfusion would be held constant despite changes in blood pressure. The relationship

$$\Delta P = QR$$

shows that an increase in the pressure gradient (ΔP) across an arterial segment will linearly increase flow (Q), unless an increase in resistance (R) develops, which can keep flow constant. A few years later von Anrep performed similar experiments to Baliss', but attributed the effects seen in animal limbs to epinephrine release from the adrenals, and attempted to repeat Bayliss' cannulated artery experiments but failed to observe any pressure-induced constriction (108). Bayliss and von Anrep used carotid arteries in the cannulated artery experiments, which do not display as robust a myogenic response as resistance arteries, perhaps leading to this discrepancy. Von Anrep's paper had the unfortunate effect of greatly reducing investigations into the myogenic response for several decades. Research picked up again in the 1950's, with work such as Read et. al.'s study of vascular flow in perfused dogs (87). This study suggested that vascular resistance depended on three mechanisms with roughly equal contributions:

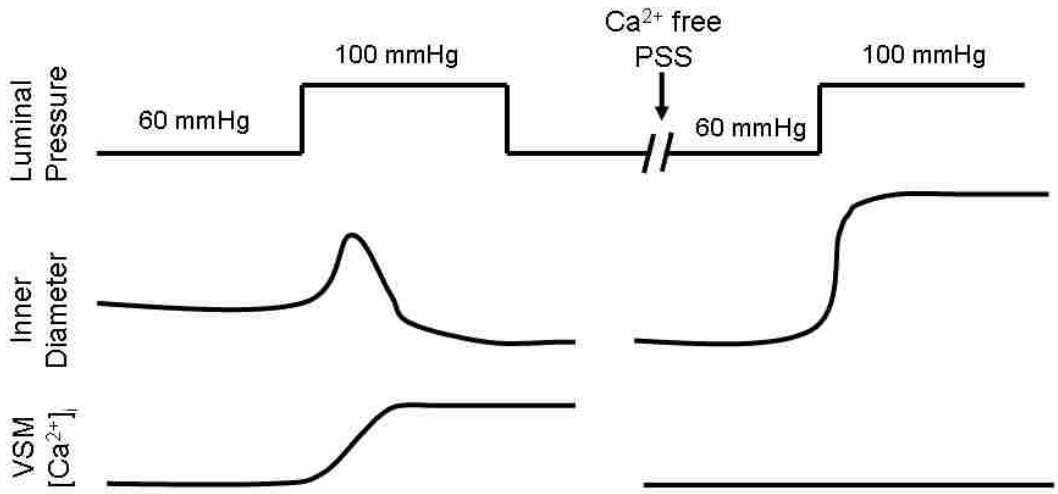

Figure 1. Method used to measure myogenic tone in isolated vessels. Step increases in luminal pressure elicit a passive distension, followed by an active constriction. If vascular smooth muscle (VSMC) Ca^{2+} is measured, it is seen to increase as the constriction develops (84).

nervous system input, myogenic mechanisms, and the inherent resistance of the vascular tree. This large effect of myogenic tone on vascular resistance implies that myogenic tone could be a significant regulator of blood pressure, as shown by the relationship:

$$MAP = CO * TPR$$

Where MAP = mean arterial pressure, CO = cardiac output, and TPR = total peripheral resistance. Thus, increases in myogenic tone could affect TPR, increasing mean arterial pressure at a constant cardiac output.

A potential role for myogenic tone in affecting TPR is observed in studies in which myogenic tone can be controlled by clamping MAP using a gravity reservoir during vasoconstrictor-medated TPR increases, essentially removing the myogenic component of the increase in TPR elicited by these agonists. It was found that approximately 50% of the increase in TPR elicited by norepinephrine or vasopressin was due to pressure-induced vascular constriction, presumably myogenic tone (78). Another study measured resistance in the hindquarter circulation of rats (iliac arteries and distal, which is primarily skeletal muscle artery beds). This study also found a large component of autoregulation in angiotensin II and phenylephrine-induced TPR increases in these beds (77). However, a much smaller autoregulatory component was found in similar experiments measuring agonist-induced TPR increases in the mesenteric circulation (76).

Myogenic tone is also thought to be a major mechanism of blood flow autoregulation, in which changes in upstream blood pressure minimally affect capillary bed perfusion because of constriction or dilation of resistance arterioles (83). In this model, increased upstream blood pressure increases myogenic tone to prevent increased capillary perfusion. Similarly, decreased upstream blood pressure reduces myogenic

tone, which, along with metabolic mechanisms (83), decreases resistance to flow and maintains capillary perfusion

Different artery beds display different levels of myogenic reactivity. The skeletal muscle arteries, for example, display much higher myogenic tone that mesenteric arteries (42). Cerebral arteries are another vascular bed that display high levels of myogenic reactivity (28). Autoregulation thus may be a more important mediator of blood flow in some tissues than others. The mesenteric arteries, for instance, are more importantly regulated by autonomic nervous system input than by autoregulatory myogenic tone (92).

Recently, research into myogenic tone has proliferated, especially into the cellular mechanisms underlying the phenomenon, which have proven to be complex and multifaceted. The sensor of luminal pressure has been particularly difficult to identify. It is thought that the vascular smooth muscle cells (VSMC) sense the stretch of the plasma membrane or cell-cell contacts that occurs when pressure distends an artery, since non-vascular smooth muscle (17) and strips of vascular smooth muscle (96) contract when mechanically stretched. It has been shown that luminal pressure and stretch of VSMC cause depolarization of the plasma membrane electrical potential (E_m) (38), suggesting stretch activates or inactivates ion channels. Various ion channels of several different families are thought to be sensitive to membrane deformation ("mechanosensitive"). These mechanosensitive channels include K^+ channels such as the TWIK-related K^+ channel 2 (TREK-2) (5), members of the transient receptor potential (TRP) family such as TRPC1 and TRPV4 (74; 117), Cl^- channels such as the cystic fibrosis transmembrane conductance regulator (CFTR) (119), members of the DEG/ENaC/ASIC family of cation channels (27), and others.

Several of these channels have been shown to play a role in the myogenic response in VSM. Blockers of the epithelial sodium channel (ENaC), amiloride and benzamil, abolished myogenic tone in mouse renal arteries (53), and genetic knock-out of the acid sensing ion channel 2 (ASIC2) reduced myogenic constriction in mouse middle cerebral arteries (36). TRPC6 antisense oligodeoxynucleotides reduced pressure-induced depolarization and eliminated myogenic tone in rat cerebral arteries (110). TRPM4 oligodeoxynucleotides had a similar effect to block pressure-induced depolarization and reduce myogenic tone in rat cerebral arteries (28) suggesting multiple channels contribute to this response. Investigating a role for mechanosensitive Cl^- channels in the myogenic response has been hampered by a lack of selective inhibitors, although a pressure-induced Cl^- efflux seen in cerebral arteries suggests that these channels could be playing a role (26). Mechanosensitive K^+ channels are expected to play no part in pressure-dependent VSMC depolarization, as opening of K^+ channels would promote hyperpolarization instead. It is possible that stretch activation of mechanosensitive K^+ channels oppose myogenic tone, although this possibility has not been investigated. Pressure-induced VSMC depolarization may be mediated by different ion channels in different vascular beds, or it may require multiple types of channels for full effect. A further possibility is that several protein subunits from different channel-coding genes form heteromultimeric channels, such as ASIC and ENaC (59) or any of a variety of TRP channels (69; 98). Regardless of the molecular identity of the mechanosensitive channel(s), it is now well accepted that the initiating event of myogenic tone is VSMC E_m depolarization.

Although some mechanosensitive ion channels conduct significant levels of Ca^{2+}, it is clear that the myogenic response requires the activation of L-type voltage-gated Ca^{2+}

channels (VGCC) (61; 111). The depolarization of the plasma membrane presumably provides the stimulus that increases the open probability of these channels and leads to a large Ca^{2+} influx. L-type VGCC in smooth muscle display an activation potential of ~-50 mV and the inward Ca^{2+} current through the channels produces a high steady state intracellular Ca^{2+} concentration ($[Ca^{2+}]$) at E_m between -30 and 0 mV (32; 35). At more positive E_m potentials, inactivation of the channels reduces steady state $[Ca^{2+}]$.

K^+ channels, due to their effect to hyperpolarize the plasma membrane E_m, would be expected to oppose myogenic tone. Voltage-gated K^+ (K_v) channels are activated by plasma membrane E_m depolarization, and so may be expected to oppose the development of myogenic tone. Kv channels in VSMC show a half-maximal activation at the depolarized E_m of -10 mV (88), a myogenically relevant activation range. Kv channels have indeed been shown to oppose myogenic tone in studies of cerebral arteries using the Kv isoform 2 channel inhibitor stromatoxin (2). Ca^{2+}-activated K^+ channels also display activation properties that make them effective negative regulators of depolarization-induced constriction. There are three types of Ca^{2+}-activated K^+ channels, large-conductance (BK_{Ca}), intermediate-conductance (IK_{Ca}), and small-conductance (SK_{Ca}). SK_{Ca} channels display a unitary conductance of ~ 10 pS (41), and are activated to 50 % of maximum by cytosolic free $[Ca^{2+}]$ of 300 nM (113). IK_{Ca} channels have a similar Ca^{2+} sensitivity as SK_{Ca} channels, but display a greater unitary conductance of ~40 pS (48). IK_{Ca} and SK_{Ca} channels are present primarily on endothelial cells (ECs), but participate in control of vascular tone by hyperpolarizing the EC E_m. This will increase the driving force for Ca^{2+} entering the EC, activating Ca^{2+}-sensitive vasodilatory pathways such as nitric oxide synthase (58; 93), or may directly cause VSMC hyperpolarization through

conducted hyperpolarization mechanisms, such as mediated by myoendothelial gap junctions or the "K^+ cloud" (23; 29).

BK_{Ca} Channels

BK_{Ca} channels, as the name suggests, display the greatest unitary conductance of the Ca^{2+}-activated K^+ channels, 150-300 pS (67). BK_{Ca} channels are composed of tetramers of the pore forming α subunit, which are the product of a single gene, Kcnma1. BK_{Ca} channel α subunits contain seven transmembrane regions, and have a large cytosolic COOH terminus (75). A stretch of aspartate residues in this cytosolic domain has been shown to mediate the channel's Ca^{2+} binding activity, and is termed the "Ca^{2+} bowl" (9). There are also two Ca^{2+}/divalent metal ion binding sites ("regulators of conductance for K^+", RCK1 and 2) that may participate in Ca^{2+} activation of the channel as well (41).

BK_{Ca} channels also display voltage sensitivity, which is mediated by transmembrane segments S2-4 (81). The presence of these two activation domains results in BK_{Ca} channels being activated by Ca^{2+} as well as voltage in a complex interdependent manner (7). At an E_m of -40 mV the channels are only activated ~5% of maximum by 100 μM cytosolic free [Ca^{2+}], but when the E_m is depolarized to 0 mV, the channel is activated ~25% of maximum by 100 μM Ca^{2+}(6). The presence of β subunits, however, greatly increases the Ca^{2+} sensitivity of the BK_{Ca} channel. In conditions of co-expression of the α (pore-forming) and β isoform 1 subunits in *Xenopus laevis* oocytes, the BK_{Ca} channel is half-maximally activated at -40 mV E_m by 10 μM Ca^{2+} and at 0 mV by ~ 3 μM Ca^{2+} (6). This enhanced Ca^{2+} sensitivity becomes relevant in the consideration of myogenic tone due to the finding that VSMC express BK_{Ca} β1 subunits (101). Mice in which the β1 gene is genetically knocked out demonstrate greatly reduced

BK_{Ca} Ca^{2+} sensitivity (16). These mice also displayed enhanced myogenic tone in cerebral arteries, and were hypertensive, illustrating the important role of the β1 subunit in cardiovascular homeostasis. The β1 subunit also slows down activation and deactivation kinetics of the BK_{Ca} channel and mediates channel sensitivity to 17 β – estradiol. Despite the interdependence of Ca^{2+} and voltage activation of the channel, it can be activated by either depolarization or [Ca^{2+}] independently as well. This is shown by the fact that [Ca^{2+}] can activate the channel at resting E_m, and E_m depolarization activates the channel in the absence of Ca^{2+} (41). This dual activation by depolarization and Ca^{2+}, in addition to its large unitary conductance, makes the BK_{Ca} channel a prime candidate for a negative regulator of myogenic tone. In support of this potential role, blockers of BK_{Ca} channels enhance myogenic tone in cerebral arteries (15; 62).

A proteomic analysis of BK_{Ca} channels was recently performed on whole brain homogenates, presumably containing neuronal and vascular channels (115). This study identified 30 serine and threonine residues that can be phosphorylated *in vivo*. This study also found three alternative splice sites in the COOH terminus of the protein, with 7 different insertions possible at these sites. Also found was a 66 amino acid extension of the N terminus. Several of these splice variants were expressed in *Xenopus* oocytes and probed for basic biophysical properties. It was found that the splice variants displayed significantly different Ca^{2+} sensitivity (107). Further elucidation of physiological differences of these splice variants has not been systematically investigated, and must await future work.

Effects of phosphorylation of the BK_{Ca} channel have been more widely explored. Phosphorylation by the cAMP-dependent protein kinase (PKA) activates BK_{Ca} channels

in inside-out patches and in cells (63). The cGMP-dependent protein kinase (PKG) has a similar effect (89). Serine 1072 has been identified as one site PKG phosphorylates to mediate this stimulation (33). In contrast to these two kinase activators of the BK_{Ca} channel, protein kinase C (PKC) has an inhibitory effect on channel activity in rat mesenteric artery smooth muscle cells (99). Presumably certain phosphorylation sites are activating, whereas others reduce channel activity. With a few exceptions, these studies of kinase effects on BK_{Ca} channels have not investigated the specific amino acids phosphorylated by each kinase. Mutation studies will be necessary to gain a comprehensive view of BK_{Ca} channel regulation, and will be an important area for future work.

In addition to voltage and Ca^{2+}, BK_{Ca} channels are also activated by cytosolic protons through the RCK1 domain. The EC_{50} of this effect is ~pH 6.5, a physiologically relevant range (4). Cell depolarization is associated with cytosolic acidification, likely due to activation of Ca^{2+}/ H^+ exchangers on mitochondria or the plasma membrane (20). Thus increased $[H^+]$ downstream of myogenic depolarization is a further mechanism by which BK_{Ca} channels actively oppose depolarization-induced Ca^{2+} influx.

Heme is a modulator of the BK_{Ca} channels through interaction with the CKACH sequence between the RCK1 and RCK2 regions (104). Heme inactivates the channel at negative E_m, but activates it at more positive voltages. The mechanism of inhibition seems to involve reduced coupling of voltage and Ca^{2+} sensors within the channel to the opening of the channel pore (43). It is unclear, however, whether this effect is physiologically relevant, as free heme seems to be low in cell cytosol. Perhaps the more relevant role of heme in BK_{Ca} channel function is that it is a substrate for the enzyme

heme oxygenase, which produces CO, now understood to be a potent activator of the BK_{Ca} channel. CO activation of BK_{Ca} channels persists even in excised membrane patches, suggesting that it is a direct effect on the channel (112). The RCK1 region of the BK_{Ca} α subunit, in particular an aspartate and two histidine residues in this region, are required for CO effects (46). This region is also involved in Ca^{2+} sensitivity of the channel, so it is possible these two activators share the same mechanism. In support of this, at saturating levels of Ca^{2+} (120 μM), CO no longer has an effect (46).

Reactive oxygen species (ROS) also affect BK_{Ca} channel function. H_2O_2 reduces channel open probability through a mechanism that involves cysteine residue 911 in the RCK2 domain (103). The effect of H_2O_2 persisted after washout, and was mimicked by the oxidizing agent 5,5'-dithiobis 2-nitrobenzoic acid (DTNB), suggesting that H_2O_2 oxidation of this cysteine causes channel inhibition. Cysteine 430 also is sensitive to oxidation to mediate an inhibition of the channel (118). Peroxynitrite ($ONOO^-$) also inhibits BK_{Ca} channels, although the precise mechanism has not been worked out yet (71). NO has also been shown to have a direct effect on BK_{Ca} channels, but this, as opposed to the inhibitory effect of other reactive oxidant species, is an activation effect (12). Application of *N*-ethylmaleimide to excised patches prevented the effect of NO, suggesting that nitrosylation of sulfhydryl groups is the mechanism responsible.

In addition to these activators, several others have been described. Certain fatty acids, phospholipids, and steroid hormones have also been shown to have a stimulatory effect on BK_{Ca} channels (45). This large and complex channel which importantly regulates E_m in a wide range of cell types may be expected to have a long list of modulators, to finely tune its function in a variety of physiological situations. Recently,

evidence has been mounting that BK_{Ca} channels may also be expressed and functional in ECs, at least under certain conditions (14; 47).

Ca^{2+} sparks

As stated above, BK_{Ca} channels are activated by cytosolic Ca^{2+}. This was worked out using inside-out patches in which the free [Ca^{2+}] at the cytosolic face of the channel was carefully controlled. But determining the [Ca^{2+}] that BK_{Ca} channels are exposed to in intact cells is a complex problem. The advent of fast Ca^{2+} indicator dyes and confocal microscopy has allowed the visualization of Ca^{2+} transients in cells and tissues that are rapid and spatially limited. It was found that the distribution of Ca^{2+} in cardiac and smooth muscle cells was not homogeneous throughout the cytosol, but exhibited periodic increases of up to 100 μM in regions as limited as 1% of the cell volume (80). These events were termed "Ca^{2+} sparks", and were found to be mediated by ryanodine receptor Ca^{2+}-release channels (RyR). These RyR channels are large ion channels that have high unitary conductance and low selectivity for Ca^{2+} (21). RyR are present on the sarcoplasmic reticulum (SR), a significant intracellular Ca^{2+} store. It has been calculated that a single Ca^{2+} spark is caused by the coordinated opening of at least 10 RyR channels (51).

In VSMC, Ca^{2+} sparks cause spontaneous transient outward currents (STOCs) as measured in cell attached patch-clamp experiments with simultaneous confocal Ca^{2+} imaging (85). These STOCs are mediated by BK_{Ca} channel opening (80), and electron microscopy studies show domains of close apposition (12-10 nM) of SR to the plasma membrane (24). Ca^{2+} sparks in VSMC have been shown to be important regulators of E_m through activation of BK_{Ca} channels (80) (Fig. 2), as blockade of sparks with the plant

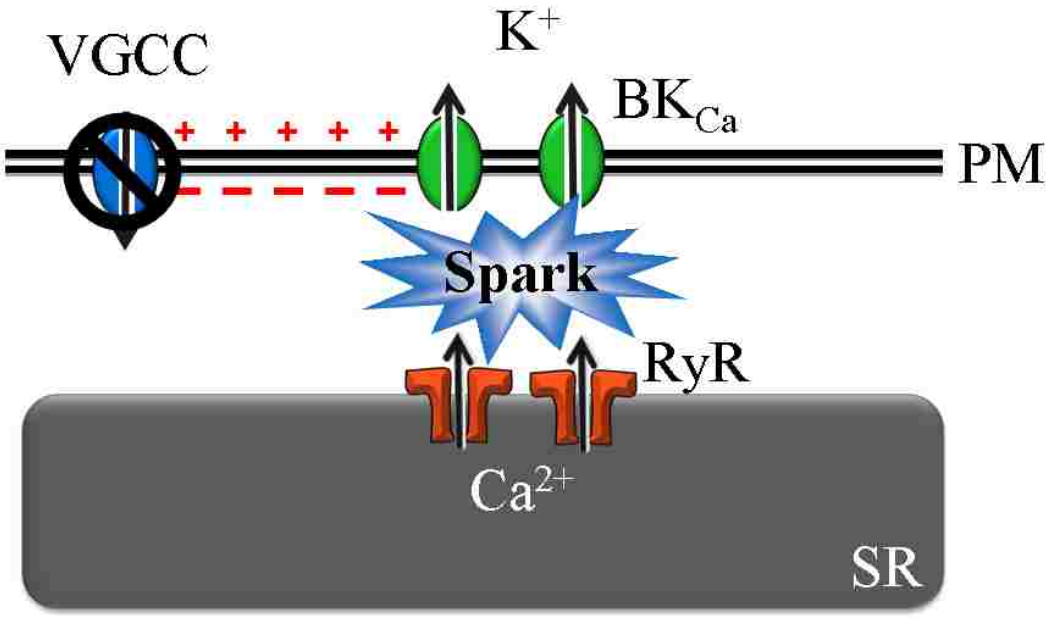

Figure 2. Ryanodine receptor (RyR) mediated Ca^{2+} sparks activate BK_{Ca} channels to cause E_m hyperpolarization and a decreased open probablilty of voltage-gated Ca^{2+} channels (VGCC).

alkaloid ryanodine abolishes STOCs and constricts arteries. It has been calculated that ~30 BK_{Ca} channels are activated per spark, increasing the open probability of the channels to ~0.6 (84). At a rate of 1 spark/cell/sec, STOCs are calculated to cause a >10 mV E_m sustained hyperpolarization, and this has been verified experimentally (62). The Ca^{2+} released by the sparks themselves is small enough that each spark increases global cytosolic [Ca^{2+}] by less than 2 nM (18). VSMC are electrically coupled by gap junctions, which may act to sum and smooth the effects of individual STOCs, leading to a relatively stable E_m as measured by sharp electrode impalement (51).

As stated above, during depolarization-induced constriction of VSMC, BK_{Ca} channels act as negative regulators of the depolarization by sensing both the depolarization and the VGCC-mediated influx of Ca^{2+}. Ca^{2+} sparks may, however, act as an amplifying mechanism of this negative regulatory response. A localized increase in [Ca^{2+}] near the membrane to levels much greater than those in the bulk cytosolic [Ca^{2+}] would enhance BK_{Ca} activation in response to depolarization. This hypothesis is based on the finding that depolarization (3; 39;52) or stretch (54) of smooth muscle cells increases Ca^{2+} sparks, and that these effects require VGCCs (49; 52). This global [Ca^{2+}]-induced increase in spark frequency may be due either to the direct effect on RyR of cytosolic Ca^{2+}, or to an increase in SR Ca^{2+} load through the sarco-endoplasmic reticulum Ca^{2+} ATPase, both of which can increase RyR activity (18; 31). Regardless of the precise mechanism, BK_{Ca} channels at spark sites should experience a much larger local increase in [Ca^{2+}] than bulk cytosolic [Ca^{2+}] measurements would suggest, and the resulting large activation of the channel would more effectively return E_m to resting levels. A recent study in airway smooth muscle cells demonstrates that RyR clusters are localized near the

plasma membrane. BK_{Ca} channels form clusters as well, which seem to be distributed randomly throughout the plasma membrane, but there are generally BK_{Ca} clusters near RyR clusters (70). The authors estimate that a single Ca^{2+} spark activates two to three clusters of BK_{Ca} channels within 600 nm of the RyR cluster, and calculate that this activation of ~ 15 BK_{Ca} channels conducts sufficient current to produce a STOC.

There are three RyR isoforms. RyR1 is the primary isoform expressed in skeletal muscle (100). In skeletal muscle, RyR1 is activated by the L-type VGCC Ca_V 1.1 independent of Ca^{2+} influx (64). The physical interaction of RyR1 to Ca_V 1.1 mediates this activation.

RyR2 is primarily expressed in cardiac myocytes. Cardiac muscle Ca^{2+} spark activity requires Ca^{2+} influx, in this case through the L-type VGCC isoform Ca_V 1.2 (10).

RyR3 is expressed in neurons and skeletal muscle, and little is known about its function (66). Vascular smooth muscle expresses all three isoforms, but it is unclear which isoform(s) are responsible for Ca^{2+} sparks in this cell type (30). In cultured rat portal vein myocytes, both RyR1 and RyR2 were shown to be required for depolarization-induced Ca^{2+} spark activation by antisense oligonucleotide injection (22). RyR3 knockdown had no effect on sparks. Thus perhaps Ca^{2+} sparks in smooth muscle are produced by an interaction between RyR1 and RyR2.

Ca^{2+} sparks are modulated by a variety of signaling mechanisms in VSMC. PKC activation with phorbol 12-myristate 13-acetate and 1,2-dioctanoyl-sn-glycerol has been shown to decrease spark frequency in cerebral artery smooth muscle cells (13). SR Ca^{2+} load was not affected by these compounds, and the effect remained in the presence of blockade of VGCC, suggesting that PKC directly affects the ryanodine receptor.

Ca^{2+} sparks have also been shown to be activated by cyclic nucleotides, through the activation of PKA and perhaps PKG. Activators of adenylyl cyclase increased spark and STOC frequency, and these effects were blocked by H-89, an inhibitor of PKA (86). This suggests that increases in cAMP activate sparks through PKA. Nitrovasodilators, which activate PKG, also increased spark and STOC frequency, although it has not been demonstrated that these effects are blocked by PKG inhibitors (73; 86). It is possible that these effects of cyclic nucleotides are through effects on phospholamban. Cerebral arteries from mice in which phospholamban was genetically ablated displayed no increase in Ca^{2+} spark frequency to forskolin-induced increases in cAMP, whereas wild type mice showed a normal increase (109). CO has also been found to have an effect on Ca^{2+} sparks. Activation of heme oxygenase with heme-L-lysinate was found to increase spark frequency as well as enhanced spark-STOC coupling (50).

A relatively recently described Ca^{2+} spark modulator is FK506 binding protein (FKBP). This protein associates with the ryanodine receptor and inhibits Ca^{2+} release. It was first described in Ca^{2+} sparks regulation in cardiomyocytes, where inhibiting FKBP with FK506 or rapamycin increased the duration of Ca^{2+} sparks (114). Evidence for FKBP inhibition of RyR Ca^{2+} release in smooth muscle comes from FKBP12.6 knockout mice, in which increased STOC frequency and spark amplitude and duration were observed in bladder smooth muscle relative to samples from wild type mice (55).

Hydrogen Sulfide

Hydrogen sulfide (H_2S) has long been known as a toxic gas, produced by geothermal activity, decomposition of eggs, and enteric bacteria. It is lethal at high concentrations through the inhibition of cytochrome *c* oxidase (72). It was found to be

produced in mammalian cells by several enzymes, but was thought to be a byproduct, with little biological function (97). Three enzymes are known to produce H_2S in mammals, cystathionine γ-lyase (CSE), cystathionine β-synthase (CBS), and 3-mercaptopyruvate sulfurtransferase (3MST) (97). CSE and CBS are both pyridoxal 5'-phosphate containing enzymes that use cysteine as a substrate. CBS is thought to be the primary source of H_2S in the central nervous system, whereas CSE is the primary source in the vasculature (11). 3MST has been shown to be expressed in endothelial cells, and may prove to be another important vascular source of H_2S (94).

A biological role for H_2S was found when it was shown that H_2S could enhance long-term potentiation in the hippocampus, and this opened the field of endogenous H_2S signaling (1). H_2S is therefore the third so called "gasotransmitter" described, after NO and CO. CSE mRNA was demonstrated to be transcribed in vascular tissue, and exogenous H_2S was shown to be a vasodilator in the thoracic aorta (44). The mechanism of H_2S-induced vasodilation appears to be independent of soluble guanylyl cyclase, and mediated by an activation of ATP-dependent K^+ channels (K_{ATP}) (120). Patch clamp studies have verified that H_2S activates K_{ATP} channels in VSMCs (102). H_2S may alter physiological pathways by protein S-sulfhydration, in which an extra sulfur atom is added to cysteine residues. K_{ATP} channel activation by H_2S is abolished by mutating cysteine residues C6 and C26 in the extracellular loop of subunit rvSUR1 (56). Furthermore, endogenous H_2S was shown to S-sulfhydrate a range of proteins in the liver as measured by a biotin switch assay selective for S-sulfhydrated cysteines (79).

Most of these studies on the biological effects of H_2S have used concentrations in the high μM range, however, and may not be physiologically relevant. Studies

performed to measure tissue [H_2S] have found high μM range concentrations (25; 37), but there has been concern that these measurements include bound as well as free H_2S, and that true tissue [H_2S] is in the nM range (34). This does not mean that subcellular [H_2S] does not ever get above the nM range, but a lack of fluorescent probes for H_2S has prevented the investigation of questions of this type. This may soon change, as probes for H_2S are currently being developed (90).

Endothelial CSE is thought to be regulated by Ca^{2+}, similar to other endothelial enzymes involved in vasodilation. The evidence for this comes from a study in which purified recombinant CSE activity was increased by addition of Ca^{2+} and calmodulin, but not by either agent alone (116). This study also demonstrated an association of CSE with calmodulin and reported that H_2S production in cultured EC was enhanced by a Ca^{2+} ionophore but reduced by chelating Ca^{2+} with [1,2-bis(2-aminophenoxy)ethane-*N*,*N*,*N′*,*N′*-tetraacetic acid (BAPTA).

H_2S has been shown to have targets other than the K_{ATP} channel in the cardiovascular system. In whole perfused mesenteric beds, EC disruption as well as application of charybdotoxin (BK_{Ca} and IK_{Ca} blocker) and apamin (SK_{Ca} blocker) were actually more effective than glibenclamide (K_{ATP} blocker) at blocking H_2S-mediated relaxation (19). This suggests that Ca^{2+}-activated K^+ channels, perhaps in ECs, mediate some of the vasodilation in this bed. In a similar whole perfused mesentery preparation, it was found that 4-(4-octadecylphenyl)-4-oxobutenoic acid (OBAA) and proadifen, inhibitors of phospholipase A2 and cytochrome P450, respectively, had a similar effect to charybdotoxin and apamin application. This suggested that following H_2S application, a

cytochrome P450 product could be either activated by, or act on, Ca^{2+}-activated K^+ channels to mediate vasodilation.

There is also evidence that BK_{Ca} channels can be activated by H_2S. In microvascular endothelial cells and pituitary tumor cells H_2S increased BK_{Ca} currents measured by patch clamp (95; 121). However, there is growing consensus that H_2S also inhibits native BK_{Ca} channels in carotid body glomus cells and recombinant BK_{Ca} channels in HEK cells (68; 105; 106). This disparity may indicate a cell-type specific effect.

H_2S has also been shown to activate Kv channels in rat aorta (91). In this study H_2S mediated vasodilation was blocked by the KCNQ-type Kv channel blocker XE991.

H_2S also has antioxidant effects and is protective for ischemia reperfusion injury (60; 65). Furthermore, H_2S has been shown to promote angiogenesis through activation of K_{ATP} channels and p38 MAPK (82). The field of biological effects of H_2S is expanding daily. The regulation of protein function by modification of cysteine residues may be a very widespread phenomenon, and thus the list of H_2S effects is predicted to continue to grow well into the future.

Summary and Hypothesis

Myogenic tone is a plasma membrane E_m depolarization-mediated vascular constriction that is importantly inhibited by K^+ channel activation. Ca^{2+} sparks, which activate VSMC BK_{Ca} channels, oppose depolarization-induced vascular constriction, including myogenic tone. As described above, H_2S has been shown to have effects on several K^+ channels. It is unknown, however, whether H_2S reduces myogenic tone in

resistance arteries. Furthermore, it is unknown whether endogenous H_2S activates Ca^{2+} sparks similarly to the two other gasotrasmitters, CO and NO. The following studies evaluated the role of endogenous H_2S on myogenic tone and Ca^{2+} spark activity in small mesenteric arteries. In addition, these studies evaluated the mechanism of H_2S mediated vasodilation in PE constricted arteries.

General Hypothesis**:** H_2S reduces myogenic tone and causes vasodilation by activating Ca^{2+} sparks in VSMC (Fig. 3).

Specific Aim 1: To determine if endogenous H_2S regulates myogenic tone.

Hypothesis: Endothelial CSE produces H_2S which inhibits myogenic tone.

Specific Aim 2: To evaluate the effect of exogenous and endogenous H_2S on VSMC membrane potential.

Hypothesis: H_2S hyperpolarizes vascular smooth muscle cells in a BK_{Ca} dependent manner.

Specific Aim 3: To evaluate exogenous and endogenous H_2S regulation of Ca^{2+} sparks.

Hypothesis: H_2S causes vasodilation through increased Ca^{2+} spark frequency.

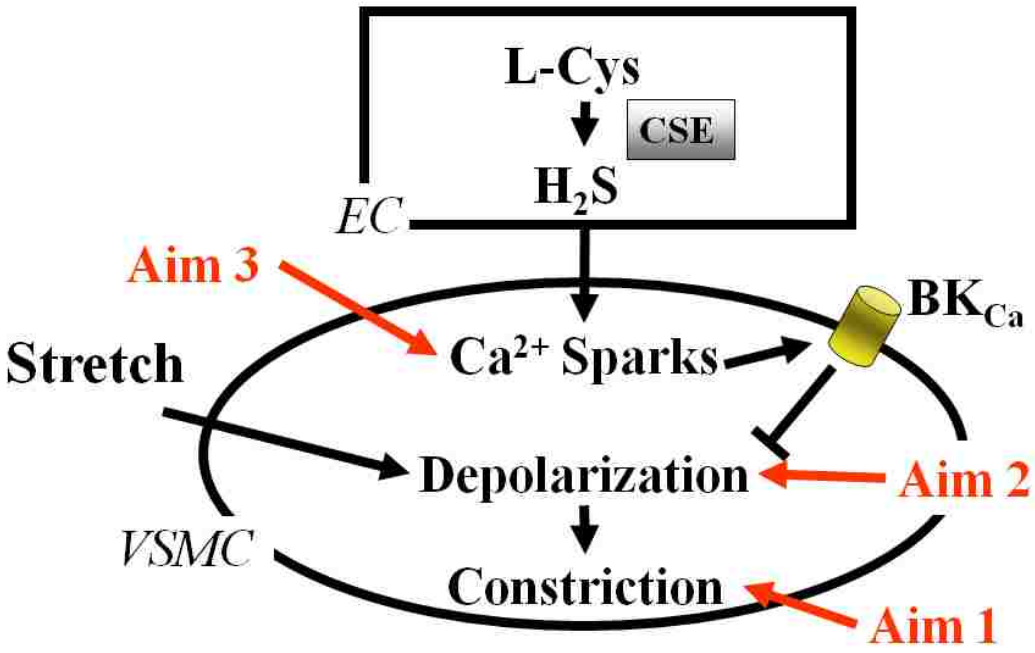

Figure 3. General hypothesis.

Reference List

1. **Abe K and Kimura H**. The possible role of hydrogen sulfide as an endogenous neuromodulator. *J Neurosci* 16: 1066-1071, 1996.

2. **Amberg GC and Santana LF**. Kv2 channels oppose myogenic constriction of rat cerebral arteries. *Am J Physiol Cell Physiol* 291: C348-C356, 2006.

3. **Arnaudeau S, Boittin FX, Macrez N, Lavie JL, Mironneau C and Mironneau J**. L-type and Ca2+ release channel-dependent hierarchical Ca2+ signalling in rat portal vein myocytes. *Cell Calcium* 22: 399-411, 1997.

4. **Avdonin V, Tang XD and Hoshi T**. Stimulatory action of internal protons on Slo1 BK channels. *Biophys J* 84: 2969-2980, 2003.

5. **Bang H, Kim Y and Kim D**. TREK-2, a new member of the mechanosensitive tandem-pore K+ channel family. *J Biol Chem* 275: 17412-17419, 2000.

6. **Bao L and Cox DH**. Gating and ionic currents reveal how the BKCa channel's Ca2+ sensitivity is enhanced by its beta1 subunit. *J Gen Physiol* 126: 393-412, 2005.

7. **Barrett JN, Magleby KL and Pallotta BS**. Properties of single calcium-activated potassium channels in cultured rat muscle. *J Physiol* 331: 211-230, 1982.

8. **Bayliss WM**. On the local reactions of the arterial wall to changes of internal pressure. *J Physiol* 28: 220-231, 1902.

9. **Berkefeld H, Fakler B and Schulte U**. Ca2+-activated K+ channels: from protein complexes to function. *Physiol Rev* 90: 1437-1459, 2010.

10. **Bers DM**. Cardiac excitation-contraction coupling. *Nature* 415: 198-205, 2002.

11. **Bhatia M**. Hydrogen sulfide as a vasodilator. *IUBMB Life* 57: 603-606, 2005.

12. **Bolotina VM, Najibi S, Palacino JJ, Pagano PJ and Cohen RA**. Nitric oxide directly activates calcium-dependent potassium channels in vascular smooth muscle. *Nature* 368: 850-853, 1994.

13. **Bonev AD, Jaggar JH, Rubart M and Nelson MT**. Activators of protein kinase C decrease Ca2+ spark frequency in smooth muscle cells from cerebral arteries. *Am J Physiol* 273: C2090-C2095, 1997.

14. **Brakemeier S, Eichler I, Knorr A, Fassheber T, Kohler R and Hoyer J**. Modulation of Ca2+-activated K+ channel in renal artery endothelium in situ by nitric oxide and reactive oxygen species. *Kidney Int* 64: 199-207, 2003.

15. **Brayden JE and Nelson MT**. Regulation of arterial tone by activation of calcium-dependent potassium channels. *Science* 256: 532-535, 1992.

16. **Brenner R, Perez GJ, Bonev AD, Eckman DM, Kosek JC, Wiler SW, Patterson AJ, Nelson MT and Aldrich RW**. Vasoregulation by the beta1 subunit of the calcium-activated potassium channel. *Nature* %19;407: 870-876, 2000.

17. **BURNSTOCK G and PROSSER CL**. Responses of smooth muscles to quick stretch: relation of stretch to conduction. *Am J Physiol* 198: 921-925, 1960.

18. **Cheng H and Lederer WJ**. Calcium sparks. *Physiol Rev* 88: 1491-1545, 2008.

19. **Cheng Y, Ndisang JF, Tang G, Cao K and Wang R**. Hydrogen sulfide-induced relaxation of resistance mesenteric artery beds of rats. *Am J Physiol Heart Circ Physiol* 287: H2316-H2323, 2004.

20. **Chesler M**. Regulation and modulation of pH in the brain. *Physiol Rev* 83: 1183-1221, 2003.

21. **Coronado R, Morrissette J, Sukhareva M and Vaughan DM**. Structure and function of ryanodine receptors. *Am J Physiol* 266: C1485-C1504, 1994.

22. **Coussin F, Macrez N, Morel JL and Mironneau J**. Requirement of ryanodine receptor subtypes 1 and 2 for Ca(2+)-induced Ca(2+) release in vascular myocytes. *J Biol Chem* 275: 9596-9603, 2000.

23. **de Wit C and Griffith TM**. Connexins and gap junctions in the EDHF phenomenon and conducted vasomotor responses. *Pflugers Arch* 459: 897-914, 2010.

24. **Devine CE, Somlyo AV and Somlyo AP**. Sarcoplasmic reticulum and excitation-contraction coupling in mammalian smooth muscles. *J Cell Biol* 52: 690-718, 1972.

25. **Dorman DC, Moulin FJ, McManus BE, Mahle KC, James RA and Struve MF**. Cytochrome oxidase inhibition induced by acute hydrogen sulfide inhalation: correlation with tissue sulfide concentrations in the rat brain, liver, lung, and nasal epithelium. *Toxicol Sci* 65: 18-25, 2002.

26. **Doughty JM and Langton PD**. Measurement of chloride flux associated with the myogenic response in rat cerebral arteries. *J Physiol* 534: 753-761, 2001.

27. **Drummond HA, Grifoni SC and Jernigan NL**. A new trick for an old dogma: ENaC proteins as mechanotransducers in vascular smooth muscle. *Physiology (Bethesda)* 23: 23-31, 2008.

28. **Earley S, Waldron BJ and Brayden JE**. Critical role for transient receptor potential channel TRPM4 in myogenic constriction of cerebral arteries. *Circ Res* 95: 922-929, 2004.

29. **Edwards G, Dora KA, Gardener MJ, Garland CJ and Weston AH**. K+ is an endothelium-derived hyperpolarizing factor in rat arteries. *Nature* %19;396: 269-272, 1998.

30. **Essin K and Gollasch M**. Role of ryanodine receptor subtypes in initiation and formation of calcium sparks in arterial smooth muscle: comparison with striated muscle. *J Biomed Biotechnol* 2009:135249. Epub;%2009 Dec 8.: 135249, 2009.

31. **Essin K, Welling A, Hofmann F, Luft FC, Gollasch M and Moosmang S**. Indirect coupling between Cav1.2 channels and ryanodine receptors to generate Ca2+ sparks in murine arterial smooth muscle cells. *J Physiol* 584: 205-219, 2007.

32. **Fleischmann BK, Murray RK and Kotlikoff MI**. Voltage window for sustained elevation of cytosolic calcium in smooth muscle cells. *Proc Natl Acad Sci U S A* 91: 11914-11918, 1994.

33. **Fukao M, Mason HS, Britton FC, Kenyon JL, Horowitz B and Keef KD**. Cyclic GMP-dependent protein kinase activates cloned BKCa channels expressed in mammalian cells by direct phosphorylation at serine 1072. *J Biol Chem* 274: 10927-10935, 1999.

34. **Furne J, Saeed A and Levitt MD**. Whole tissue hydrogen sulfide concentrations are orders of magnitude lower than presently accepted values. *Am J Physiol Regul Integr Comp Physiol* 295: R1479-R1485, 2008.

35. **Ganitkevich VY and Isenberg G**. Depolarization-mediated intracellular calcium transients in isolated smooth muscle cells of guinea-pig urinary bladder. *J Physiol* 435: 187-205, 1991.

36. **Gannon KP, Vanlandingham LG, Jernigan NL, Grifoni SC, Hamilton G and Drummond HA**. Impaired pressure-induced constriction in mouse middle cerebral arteries of ASIC2 knockout mice. *Am J Physiol Heart Circ Physiol* 294: H1793-H1803, 2008.

37. **Goodwin LR, Francom D, Dieken FP, Taylor JD, Warenycia MW, Reiffenstein RJ and Dowling G**. Determination of sulfide in brain tissue by gas dialysis/ion chromatography: postmortem studies and two case reports. *J Anal Toxicol* 13: 105-109, 1989.

38. **Harder DR**. Pressure-dependent membrane depolarization in cat middle cerebral artery. *Circ Res* 55: 197-202, 1984.

39. **Herrera GM, Heppner TJ and Nelson MT**. Voltage dependence of the coupling of Ca(2+) sparks to BK(Ca) channels in urinary bladder smooth muscle. *Am J Physiol Cell Physiol* 280: C481-C490, 2001.

40. **Hill MA, Yang Y, Ella SR, Davis MJ and Braun AP**. Large conductance, Ca2+-activated K+ channels (BKCa) and arteriolar myogenic signaling. *FEBS Lett* 584: 2033-2042, 2010.

41. **Hirschberg B, Maylie J, Adelman JP and Marrion NV**. Gating of recombinant small-conductance Ca-activated K+ channels by calcium. *J Gen Physiol* 111: 565-581, 1998.

42. **Horiguchi S, Watanabe J, Kato H, Baba S, Shinozaki T, Miura M, Fukuchi M, Kagaya Y and Shirato K**. Contribution of Na+/Ca2+ exchanger to the regulation of myogenic tone in isolated rat small arteries. *Acta Physiol Scand* 173: 167-173, 2001.

43. **Horrigan FT, Heinemann SH and Hoshi T**. Heme regulates allosteric activation of the Slo1 BK channel. *J Gen Physiol* 126: 7-21, 2005.

44. **Hosoki R, Matsuki N and Kimura H**. The possible role of hydrogen sulfide as an endogenous smooth muscle relaxant in synergy with nitric oxide. *Biochem Biophys Res Commun* 237: 527-531, 1997.

45. **Hou S, Heinemann SH and Hoshi T**. Modulation of BKCa channel gating by endogenous signaling molecules. *Physiology (Bethesda)* 24:26-35.: 26-35, 2009.

46. **Hou S, Xu R, Heinemann SH and Hoshi T**. The RCK1 high-affinity Ca2+ sensor confers carbon monoxide sensitivity to Slo1 BK channels. *Proc Natl Acad Sci U S A* 105: 4039-4043, 2008.

47. **Hughes JM, Riddle MA, Paffett ML, Gonzalez Bosc LV and Walker BR**. Novel role of endothelial BKCa channels in altered vasoreactivity following hypoxia. *Am J Physiol Heart Circ Physiol* 299: H1439-H1450, 2010.

48. **Ishii TM, Silvia C, Hirschberg B, Bond CT, Adelman JP and Maylie J**. A human intermediate conductance calcium-activated potassium channel. *Proc Natl Acad Sci U S A* 94: 11651-11656, 1997.

49. **Jaggar JH**. Intravascular pressure regulates local and global Ca(2+) signaling in cerebral artery smooth muscle cells. *Am J Physiol Cell Physiol* 281: C439-C448, 2001.

50. **Jaggar JH, Leffler CW, Cheranov SY, Tcheranova D, E S and Cheng X**. Carbon monoxide dilates cerebral arterioles by enhancing the coupling of Ca2+ sparks to Ca2+-activated K+ channels. *Circ Res* 91: 610-617, 2002.

51. **Jaggar JH, Porter VA, Lederer WJ and Nelson MT**. Calcium sparks in smooth muscle. *Am J Physiol Cell Physiol* 278: C235-C256, 2000.

52. **Jaggar JH, Stevenson AS and Nelson MT**. Voltage dependence of Ca2+ sparks in intact cerebral arteries. *Am J Physiol* 274: C1755-C1761, 1998.

53. **Jernigan NL and Drummond HA**. Vascular ENaC proteins are required for renal myogenic constriction. *Am J Physiol Renal Physiol* 289: F891-F901, 2005.

54. **Ji G, Barsotti RJ, Feldman ME and Kotlikoff MI**. Stretch-induced calcium release in smooth muscle. *J Gen Physiol* 119: 533-544, 2002.

55. **Ji G, Feldman ME, Greene KS, Sorrentino V, Xin HB and Kotlikoff MI**. RYR2 proteins contribute to the formation of Ca(2+) sparks in smooth muscle. *J Gen Physiol* 123: 377-386, 2004.

56. **Jiang B, Tang G, Cao K, Wu L and Wang R**. Molecular mechanism for H(2)S-induced activation of K(ATP) channels. *Antioxid Redox Signal* 12: 1167-1178, 2010.

57. **Jones TW**. Discovery That the Veins of the Bat's Wing (Which are Furnished with Valves) are Endowed with Rythmical Contractility, and That the Onward Flow of Blood is Accelerated by Each Contraction. *Philosophical Transactions of the Royal Society of London* 142: 131-136, 1852.

58. **Kamouchi M, Droogmans G and Nilius B**. Membrane potential as a modulator of the free intracellular Ca2+ concentration in agonist-activated endothelial cells. *Gen Physiol Biophys* 18: 199-208, 1999.

59. **Kapoor N, Lee W, Clark E, Bartoszewski R, McNicholas CM, Latham CB, Bebok Z, Parpura V, Fuller CM, Palmer CA and Benos DJ**. Interaction of ASIC1 and ENaC subunits in human glioma cells and rat astrocytes. *Am J Physiol Cell Physiol* 300: C1246-C1259, 2011.

60. **King AL and Lefer DJ**. Cytoprotective actions of hydrogen sulfide in ischaemia-reperfusion injury. *Exp Physiol* 96: 840-846, 2011.

61. **Knot HJ and Nelson MT**. Regulation of arterial diameter and wall [Ca2+] in cerebral arteries of rat by membrane potential and intravascular pressure. *J Physiol* 508 (Pt 1): 199-209, 1998.

62. **Knot HJ, Standen NB and Nelson MT**. Ryanodine receptors regulate arterial diameter and wall [Ca2+] in cerebral arteries of rat via Ca2+-dependent K+ channels. *J Physiol* 508 (Pt 1): 211-221, 1998.

63. **Kume H, Hall IP, Washabau RJ, Takagi K and Kotlikoff MI**. Beta-adrenergic agonists regulate KCa channels in airway smooth muscle by cAMP-dependent and -independent mechanisms. *J Clin Invest* 93: 371-379, 1994.

64. **Lamb GD**. Excitation-contraction coupling in skeletal muscle: comparisons with cardiac muscle. *Clin Exp Pharmacol Physiol* 27: 216-224, 2000.

65. **Lan A, Liao X, Mo L, Yang C, Yang Z, Wang X, Hu F, Chen P, Feng J, Zheng D and Xiao L**. Hydrogen Sulfide Protects against Chemical Hypoxia-Induced Injury by Inhibiting ROS-Activated ERK1/2 and p38MAPK Signaling Pathways in PC12 Cells. *PLoS One* 6: e25921, 2011.

66. **Lanner JT, Georgiou DK, Joshi AD and Hamilton SL**. Ryanodine receptors: structure, expression, molecular details, and function in calcium release. *Cold Spring Harb Perspect Biol* 2: a003996, 2010.

67. **Lee US and Cui J**. {beta} subunit-specific modulations of BK channel function by a mutation associated with epilepsy and dyskinesia. *J Physiol* 587: 1481-1498, 2009.

68. **Li Q, Sun B, Wang X, Jin Z, Zhou Y, Dong L, Jiang LH and Rong W**. A crucial role for hydrogen sulfide in oxygen sensing via modulating large conductance calcium-activated potassium channels. *Antioxid Redox Signal* 12: 1179-1189, 2010.

69. **Liapi A and Wood JN**. Extensive co-localization and heteromultimer formation of the vanilloid receptor-like protein TRPV2 and the capsaicin receptor TRPV1 in the adult rat cerebral cortex. *Eur J Neurosci* 22: 825-834, 2005.

70. **Lifshitz LM, Carmichael JD, Lai FA, Sorrentino V, Bellve K, Fogarty KE and ZhuGe R**. Spatial organization of RYRs and BK channels underlying the activation of STOCs by Ca(2+) sparks in airway myocytes. *J Gen Physiol* 138: 195-209, 2011.

71. **Liu Y, Terata K, Chai Q, Li H, Kleinman LH and Gutterman DD**. Peroxynitrite inhibits Ca2+-activated K+ channel activity in smooth muscle of human coronary arterioles. *Circ Res* 91: 1070-1076, 2002.

72. **Lloyd D**. Hydrogen sulfide: clandestine microbial messenger? *Trends Microbiol* 14: 456-462, 2006.

73. **Mandala M, Heppner TJ, Bonev AD and Nelson MT**. Effect of endogenous and exogenous nitric oxide on calcium sparks as targets for vasodilation in rat cerebral artery. *Nitric Oxide* 16: 104-109, 2007.

74. **Maroto R, Raso A, Wood TG, Kurosky A, Martinac B and Hamill OP**. TRPC1 forms the stretch-activated cation channel in vertebrate cells. *Nat Cell Biol* 7: 179-185, 2005.

75. **Meera P, Wallner M, Song M and Toro L**. Large conductance voltage- and calcium-dependent K+ channel, a distinct member of voltage-dependent ion channels with seven N-terminal transmembrane segments (S0-S6), an extracellular N terminus, and an intracellular (S9-S10) C terminus. *Proc Natl Acad Sci U S A* 94: 14066-14071, 1997.

76. **Meininger GA and Trzeciakowski JP**. Vasoconstriction is amplified by autoregulation during vasoconstrictor-induced hypertension. *Am J Physiol* 254: H709-H718, 1988.

77. **Meininger GA and Trzeciakowski JP**. Combined effects of autoregulation and vasoconstrictors on hindquarters vascular resistance. *Am J Physiol* 258: H1032-H1041, 1990.

78. **Metting PJ, Stein PM, Stoos BA, Kostrzewski KA and Britton SL**. Systemic vascular autoregulation amplifies pressor responses to vasoconstrictor agents. *Am J Physiol* 256: R98-105, 1989.

79. **Mustafa AK, Gadalla MM, Sen N, Kim S, Mu W, Gazi SK, Barrow RK, Yang G, Wang R and Snyder SH**. H2S signals through protein S-sulfhydration. *Sci Signal* 2: ra72, 2009.

80. **Nelson MT, Cheng H, Rubart M, Santana LF, Bonev AD, Knot HJ and Lederer WJ**. Relaxation of arterial smooth muscle by calcium sparks. *Science* 270: 633-637, 1995.

81. **Pantazis A, Gudzenko V, Savalli N, Sigg D and Olcese R**. Operation of the voltage sensor of a human voltage- and Ca2+-activated K+ channel. *Proc Natl Acad Sci U S A* 107: 4459-4464, 2010.

82. **Papapetropoulos A, Pyriochou A, Altaany Z, Yang G, Marazioti A, Zhou Z, Jeschke MG, Branski LK, Herndon DN, Wang R and Szabo C**. Hydrogen sulfide is an endogenous stimulator of angiogenesis. *Proc Natl Acad Sci U S A* 106: 21972-21977, 2009.

83. **Paulson OB, Strandgaard S and Edvinsson L**. Cerebral autoregulation. *Cerebrovasc Brain Metab Rev* 2: 161-192, 1990.

84. **Perez GJ, Bonev AD and Nelson MT**. Micromolar Ca(2+) from sparks activates Ca(2+)-sensitive K(+) channels in rat cerebral artery smooth muscle. *Am J Physiol Cell Physiol* 281: C1769-C1775, 2001.

85. **Perez GJ, Bonev AD, Patlak JB and Nelson MT**. Functional coupling of ryanodine receptors to KCa channels in smooth muscle cells from rat cerebral arteries. *J Gen Physiol* 113: 229-238, 1999.

86. **Porter VA, Bonev AD, Knot HJ, Heppner TJ, Stevenson AS, Kleppisch T, Lederer WJ and Nelson MT**. Frequency modulation of Ca2+ sparks is involved in regulation of arterial diameter by cyclic nucleotides. *Am J Physiol* 274: C1346-C1355, 1998.

87. **READ RC, KUIDA H and JOHNSON JA**. Effect of alterations in vasomotor tone on pressure-flow relationships in the totally perfused dog. *Circ Res* 5: 676-682, 1957.

88. **Robertson BE and Nelson MT**. Aminopyridine inhibition and voltage dependence of K+ currents in smooth muscle cells from cerebral arteries. *Am J Physiol* 267: C1589-C1597, 1994.

89. **Robertson BE, Schubert R, Hescheler J and Nelson MT**. cGMP-dependent protein kinase activates Ca-activated K channels in cerebral artery smooth muscle cells. *Am J Physiol* 265: C299-C303, 1993.

90. **Sasakura K, Hanaoka K, Shibuya N, Mikami Y, Kimura Y, Komatsu T, Ueno T, Terai T, Kimura H and Nagano T**. Development of a Highly Selective Fluorescence Probe for Hydrogen Sulfide. *J Am Chem Soc* 2011.

91. **Schleifenbaum J, Kohn C, Voblova N, Dubrovska G, Zavarirskaya O, Gloe T, Crean CS, Luft FC, Huang Y, Schubert R and Gollasch M**. Systemic

peripheral artery relaxation by KCNQ channel openers and hydrogen sulfide. *J Hypertens* 28: 1875-1882, 2010.

92. **Sieber C, Beglinger C, Jaeger K, Hildebrand P and Stalder GA**. Regulation of postprandial mesenteric blood flow in humans: evidence for a cholinergic nervous reflex. *Gut* 32: 361-366, 1991.

93. **Sheng JZ, Ella S, Davis MJ, Hill MA and Braun AP**. Openers of SKCa and IKCa channels enhance agonist-evoked endothelial nitric oxide synthesis and arteriolar vasodilation. *FASEB J* 23: 1138-1145, 2009.

94. **Shibuya N, Mikami Y, Kimura Y, Nagahara N and Kimura H**. Vascular endothelium expresses 3-mercaptopyruvate sulfurtransferase and produces hydrogen sulfide. *J Biochem* 146: 623-626, 2009.

95. **Sitdikova GF, Weiger TM and Hermann A**. Hydrogen sulfide increases calcium-activated potassium (BK) channel activity of rat pituitary tumor cells. *Pflugers Arch* 459: 389-397, 2010.

96. **SPARKS HV, Jr.** EFFECT OF QUICK STRETCH ON ISOLATED VASCULAR SMOOTH MUSCLE. *Circ Res* 15: SUPPL-60, 1964.

97. **Stipanuk MH and Beck PW**. Characterization of the enzymic capacity for cysteine desulphhydration in liver and kidney of the rat. *Biochem J* 206: 267-277, 1982.

98. **Strubing C, Krapivinsky G, Krapivinsky L and Clapham DE**. TRPC1 and TRPC5 form a novel cation channel in mammalian brain. *Neuron* 29: 645-655, 2001.

99. **Taguchi K, Kaneko K and Kubo T**. Protein kinase C modulates Ca2+-activated K+ channels in cultured rat mesenteric artery smooth muscle cells. *Biol Pharm Bull* 23: 1450-1454, 2000.

100. **Takeshima H, Iino M, Takekura H, Nishi M, Kuno J, Minowa O, Takano H and Noda T**. Excitation-contraction uncoupling and muscular degeneration in mice lacking functional skeletal muscle ryanodine-receptor gene. *Nature* 369: 556-559, 1994.

101. **Tanaka Y, Meera P, Song M, Knaus HG and Toro L**. Molecular constituents of maxi KCa channels in human coronary smooth muscle: predominant alpha + beta subunit complexes. *J Physiol* 502: 545-557, 1997.

102. **Tang G, Wu L, Liang W and Wang R**. Direct stimulation of K(ATP) channels by exogenous and endogenous hydrogen sulfide in vascular smooth muscle cells. *Mol Pharmacol* 68: 1757-1764, 2005.

103. **Tang XD, Garcia ML, Heinemann SH and Hoshi T**. Reactive oxygen species impair Slo1 BK channel function by altering cysteine-mediated calcium sensing. *Nat Struct Mol Biol* 11: 171-178, 2004.

104. **Tang XD, Xu R, Reynolds MF, Garcia ML, Heinemann SH and Hoshi T**. Haem can bind to and inhibit mammalian calcium-dependent Slo1 BK channels. *Nature* 425: 531-535, 2003.

105. **Telezhkin V, Brazier SP, Cayzac S, Muller CT, Riccardi D and Kemp PJ**. Hydrogen sulfide inhibits human BK(Ca) channels. *Adv Exp Med Biol* 648: 65-72, 2009.

106. **Telezhkin V, Brazier SP, Cayzac SH, Wilkinson WJ, Riccardi D and Kemp PJ**. Mechanism of inhibition by hydrogen sulfide of native and recombinant BKCa channels. *Respir Physiol Neurobiol* 172: 169-178, 2010.

107. **Tseng-Crank J, Foster CD, Krause JD, Mertz R, Godinot N, DiChiara TJ and Reinhart PH**. Cloning, expression, and distribution of functionally distinct Ca(2+)-activated K+ channel isoforms from human brain. *Neuron* 13: 1315-1330, 1994.

108. **von Anrep G**. On local vascular reactions and their interpretation. *J Physiol* 45: 318-327, 1912.

109. **Wellman GC, Santana LF, Bonev AD and Nelson MT**. Role of phospholamban in the modulation of arterial Ca(2+) sparks and Ca(2+)-activated K(+) channels by cAMP. *Am J Physiol Cell Physiol* 281: C1029-C1037, 2001.

110. **Welsh DG, Morielli AD, Nelson MT and Brayden JE**. Transient receptor potential channels regulate myogenic tone of resistance arteries. *Circ Res* 90: 248-250, 2002.

111. **Wesselman JP, VanBavel E, Pfaffendorf M and Spaan JA**. Voltage-operated calcium channels are essential for the myogenic responsiveness of cannulated rat mesenteric small arteries. *J Vasc Res* 33: 32-41, 1996.

112. **Xi Q, Tcheranova D, Parfenova H, Horowitz B, Leffler CW and Jaggar JH**. Carbon monoxide activates KCa channels in newborn arteriole smooth muscle cells by increasing apparent Ca2+ sensitivity of alpha-subunits. *Am J Physiol Heart Circ Physiol* 286: H610-H618, 2004.

113. **Xia XM, Fakler B, Rivard A, Wayman G, Johnson-Pais T, Keen JE, Ishii T, Hirschberg B, Bond CT, Lutsenko S, Maylie J and Adelman JP**. Mechanism of calcium gating in small-conductance calcium-activated potassium channels. *Nature* 395: 503-507, 1998.

114. **Xiao RP, Valdivia HH, Bogdanov K, Valdivia C, Lakatta EG and Cheng H**. The immunophilin FK506-binding protein modulates Ca2+ release channel closure in rat heart. *J Physiol* 500: 343-354, 1997.

115. **Yan J, Olsen JV, Park KS, Li W, Bildl W, Schulte U, Aldrich RW, Fakler B and Trimmer JS**. Profiling the phospho-status of the BKCa channel alpha subunit in rat brain reveals unexpected patterns and complexity. *Mol Cell Proteomics* 7: 2188-2198, 2008.

116. **Yang G, Wu L, Jiang B, Yang W, Qi J, Cao K, Meng Q, Mustafa AK, Mu W, Zhang S, Snyder SH and Wang R**. H2S as a physiologic vasorelaxant: hypertension in mice with deletion of cystathionine gamma-lyase. *Science* 322: 587-590, 2008.

117. **Yin J and Kuebler WM**. Mechanotransduction by TRP channels: general concepts and specific role in the vasculature. *Cell Biochem Biophys* 56: 1-18, 2010.

118. **Zhang G, Xu R, Heinemann SH and Hoshi T**. Cysteine oxidation and rundown of large-conductance Ca2+-dependent K+ channels. *Biochem Biophys Res Commun* 342: 1389-1395, 2006.

119. **Zhang WK, Wang D, Duan Y, Loy MM, Chan HC and Huang P**. Mechanosensitive gating of CFTR. *Nat Cell Biol* 12: 507-512, 2010.

120. **Zhao W, Zhang J, Lu Y and Wang R**. The vasorelaxant effect of H(2)S as a novel endogenous gaseous K(ATP) channel opener. *EMBO J* 20: 6008-6016, 2001.

121. **Zuidema MY, Yang Y, Wang M, Kalogeris T, Liu Y, Meininger CJ, Hill MA, Davis MJ and Korthuis RJ**. Antecedent hydrogen sulfide elicits an anti-inflammatory phenotype in postischemic murine small intestine: role of BK channels. *Am J Physiol Heart Circ Physiol* 299: H1554-H1567, 2010

CHAPTER 2

Intermittent Hypoxia in Rats Increases Myogenic Tone through Loss of Hydrogen Sulfide Activation of Large-Conductance Ca^{2+}-Activated Potassium Channels.

Short Title: Jackson-Weaver et. al. Intermittent hypoxia enhances myogenic tone

Olan Jackson-Weaver, Daniel A. Paredes, Laura V. Gonzalez Bosc, PhD, Benjimen R. Walker, PhD and Nancy L. Kanagy, PhD. Vascular Physiology Group, Department of Cell Biology and Physiology, School of Medicine, University of New Mexico, Albuquerque, NM

Corresponding author:

Nancy L. Kanagy, PhD, Professor

Department of Cell Biology and Physiology

MSC 08-4750

University of New Mexico

Albuquerque, NM 87131

Phone: 505-272-8814

FAX: 505-272-6649

Email: nkanagy@salud.unm.edu

Word count: 5125

Subject Codes: (130) Animal models of human disease, (152) Ion channels/membrane transport, (95) Endothelium/vascular type/nitric oxide, (149) Hypertension-basic studies.

This manuscript was published in Circulation Research, 2011 Jun 10;108(12):1439-47.

Abstract

Rationale: Myogenic tone, an important regulator of vascular resistance, is dependent on vascular smooth muscle (VSM) depolarization, can be modulated by endothelial factors and is increased in several models of hypertension. Intermittent hypoxia (IH) elevates blood pressure and causes endothelial dysfunction. Hydrogen sulfide (H_2S), a recently described endothelium-derived vasodilator, is produced by the enzyme cystathionine γ-lyase (CSE) and acts by hyperpolarizing VSM.

Objective: Determine if IH decreases endothelial H_2S production to increase myogenic tone in small mesenteric arteries.

Methods and Results: Myogenic tone was greater in mesenteric arteries from IH than Sham rats and VSM membrane potential was depolarized in IH compared to Sham arteries. Endothelium inactivation or scavenging of H_2S enhanced myogenic tone in Sham arteries to the level of IH. Inhibiting CSE also enhanced myogenic tone and depolarized VSM in Sham but not IH arteries. Similar results were seen in cerebral arteries. Exogenous H_2S dilated and hyperpolarized Sham and IH arteries and this dilation was blocked by iberiotoxin, paxilline, and KCl preconstriction but not glibenclamide or 3-isobutyl-1-methylxanthine . Iberiotoxin enhanced myogenic tone in both groups but more in Sham than IH. CSE immunofluorescence was less in the endothelium of IH compared to Sham mesenteric arteries. Endogenous H_2S dilation was reduced in IH arteries.

Conclusions: IH appears to decrease endothelial CSE expression to reduce H_2S production, depolarize VSM and enhance myogenic tone. H_2S dilation and hyperpolarization of VSM in small mesenteric arteries requires BK_{Ca} channels.

Key Words: BK_{Ca} channels, intermittent hypoxia, hydrogen sulfide, myogenic tone

Non-Standard Abbreviations and Acronyms:

3MST	3-mercaptopyruvate sulfurtransferase
AOA	amino-oxyacetate
BCA	β cyano-L-alanine
BK_{Ca}	large-conductance Ca^{2+}-activated potassium channel
BSS	Bi (III) subsalicylate
CSE	cystathionine γ-lyase
IBMX	3-isobutyl-1-methylxanthine
IbTx	iberiotoxin
i.d.	inner diameter
IH	intermittent hypoxia
IK	intermediate-conductance Ca^{2+}-activated potassium channel
K_{ATP}	ATP sensitive potassium channel
L-NNA	N^G-nitro-L-arginine
NOS	Nitric oxide synthase
PAG	DL propargylglycine
PE	phenylephrine
PSS	physiological saline solution
ROS	reactive oxygen species
SK	small-conductance Ca^{2+}-activated potassium channel
VGCC	voltage gated Ca^{2+} channel
VSM	vascular smooth muscle

Introduction

In epidemiological studies, obstructive sleep apnea (OSA) is an independent risk factor for hypertension and other cardiovascular diseases (26). Previously, we reported that exposing rats to eucapnic intermittent hypoxia (IH), a model of sleep apnea, elevates systemic blood pressure and arterial constrictor sensitivity to ET-1 (1) with an associated increase in vascular reactive oxygen species (ROS). Furthermore, the antioxidant tempol prevents IH-induced hypertension (31). These results suggest IH might also augment non-agonist induced vasoconstriction.

Myogenic, or spontaneously developed tone, can augment agonist-induced increases in blood pressure (16) through increased vascular resistance. Furthermore, myogenic tone is increased in some experimental models of hypertension (24). Myogenic tone appears to be initiated by activation of mechanosensitive cation channels leading to membrane depolarization and opening of L-type voltage-gated Ca^{2+} channels (L-type VGCC) (7). Modulation of this pathway, leading to elevated resting myogenic tone, could therefore contribute to systemic hypertension.

H_2S, a recently described vasodilator, is produced endogenously from L-cysteine by three enzymes: cystathionine β-synthase (CBS), cystathionine γ-lyase (CSE), and 3-mercaptopyruvate sulfurtransferase (3MST) (32). CSE has been reported to be the primary source of H_2S in the vasculature, although 3MST may also contribute in some vascular beds. H_2S is a reducing compound that can react with superoxide anion (O_2^-) to form sulfite (18) or with nitric oxide (NO) to form a nitrosothiol, potentially limiting the bioavailability of both gasotransmitters (33). Most studies attribute H_2S vasodilation to activation of vascular smooth muscle (VSM) ATP-sensitive potassium channels (K_{ATP})

(30), but other mechanisms have also been reported (5). Genetic deletion of CSE in mice elevates blood pressure (34). In this study, CSE expression was primarily in the endothelium of mesenteric arteries, and large mesenteric arteries from CSE -/- mice exhibited endothelial dysfunction.

We hypothesized that IH decreases endothelium-dependent H_2S generation to enhance myogenic tone in small mesenteric arteries. We observed that small mesenteric arteries from IH-exposed rats have increased myogenic tone and depolarized VSM membrane potential (E_m). Increased myogenic tone in IH arteries was mimicked in Sham arteries by disrupting the endothelium, inhibiting CSE, or scavenging H_2S. Inhibiting CSE depolarized VSM in Sham but not IH arteries. Exogenous H_2S dilated and hyperpolarized Sham and IH arteries and both effects were prevented by large-conductance Ca^{2+}-activated potassium channel (BK_{Ca}) blockade. BK_{Ca} blockade also augmented myogenic tone more in Sham than in IH arteries. These results suggest that H_2S is an endogenous endothelium-dependent regulator of myogenic tone in small mesenteric arteries that acts through the activation of BK_{Ca} channels and that IH exposure impairs this pathway.

Methods

Animals

Male Sprague Dawley rats (weighing 275 to 325 g, Harlan) were used for all studies and exposed to IH as follows. Rats were housed in Plexiglas chambers and exposed to either IH or air-air for 7 to 8 hours each day for 14 days. During exposure, the atmosphere in the boxes was controlled by a constant flow of gas through the boxes. For

the IH exposure, the atmosphere alternated every 90 seconds between compressed air (21% O_2/79% N_2) and hypoxic/hypercapnic air (5% O_2/5% CO_2/90% N_2). For control exposure, the atmosphere alternated every 90 seconds between two room air mixtures, simulating the noise and airflow disturbance associated with the protocol. O_2 and CO_2 content of the chambers was also recorded throughout the exposure period, and the inflow of gas was adjusted to achieve 5% O_2/5% CO_2 during the IH period and 21% O_2/<1% CO_2 during the air period. Gas flow in air-air exposures was equivalent to that used in the IH exposures. On the day of the experiments, animals were anesthetized with sodium pentobarbital (200 mg/kg ip) and mesenteric arteries dissected for western blot, immunofluorescence, and constrictor studies. All animal protocols were reviewed and approved by the institutional animal care and use committee of the University of New Mexico School of Medicine and conform to National Institutes of Health guidelines for animal use.

Isolated Vessel Preparation

To isolate mesenteric arteries, the intestinal arcade was removed and placed in a Silastic-coated Petri dish containing chilled HEPES buffered physiological saline solution (HEPES PSS; [in mmol/L] 134 NaCl, 6 KCl, 1 MgCl, 10 HEPES, 2 $CaCl_2$, 0.026 EDTA and 10 glucose; pH corrected to 7.4 with NaOH). Fourth or fifth-order artery segments (i.d.<100 μm) were dissected from the mesenteric vascular arcade and placed in fresh HEPES PSS. To isolate cerebral arteries, the brain was removed and placed in room temperature HEPES PSS. The middle cerebral arteries were dissected out and placed in fresh HEPES PSS. Arteries were transferred to a vessel chamber (Living Systems), cannulated with glass micropipettes, and secured with silk ligatures. The arteries were

pressurized to 60 mmHg with bicarbonate buffered physiological saline solution (PSS; [in mmol/L] 129.8 NaCl, 5.4 KCl, 0.83 $MgSO_4$, 0.43 NaH_2PO_4, 19 $NaHCO_3$, 1.8 $CaCl_2$, and 5.5 glucose) using a servo-controlled peristaltic pump (Living Systems) and superfused with warmed, oxygenated PSS at a rate of 5 mL per minute. To avoid flow-dependent changes in vessel diameter, experiments were performed with the distal cannula closed. To verify that there was no luminal flow, the servo-controlled peristaltic pump was switched to manual mode. Arterial segments that did not maintain pressure were discarded.

Endothelium Removal

The endothelium was disrupted in denuded experiments by mechanical abrasion using a strand of moose mane inserted in the distal end of the cannulated artery. Unattached endothelial cells were removed by flowing PSS through the artery for several seconds after disruption. This procedure was repeated 3 times and endothelial removal was subsequently evaluated by the loss of acetylcholine-induced dilation of constricted arteries.

Fura 2-Acetoxymethyl Ester Loading

Following a 30 minute equilibration period at 37ºC, pressurized arteries were incubated 45 minutes in the dark at room temperature in fura 2-AM solution (2 μmol/L fura 2-AM and 0.05% pluronic acid in HEPES PSS). After incubation, arteries were washed with 37°C PSS for 15 minutes to remove excess dye. Fura 2–loaded vessels were alternately excited at 340 and 380 nm at a frequency of 1 Hz with an IonOptix Hyperswitch dual-excitation light source and the respective 510-nm emissions collected with a photomultiplier tube (F_{340}/F_{380}). Background-subtracted F_{340}/F_{380} emission ratios

were calculated with IonWizard software (IonOptix) as a measure of relative vascular smooth muscle (VSM) cytoplasmic [Ca^{2+}] and recorded continuously throughout the experiment. Simultaneous measurement of inner diameter from bright-field images using video microscopy and edge-detection software (IonOptix) were recorded.

Pressure-Response Curves

Luminal pressure was increased from 20 to 180 mmHg using a servo-controlled peristaltic pump. Myogenic tone was allowed to develop for a minimum of 5 minutes at each 40 mmHg pressure step. Arteries were subsequently incubated with Ca^{2+} free physiological saline solution (Ca^{2+} free PSS; [in mmol/L] 129.8 NaCl, 5.4 KCl, 0.83 $MgSO_4$, 0.43 NaH_2PO_4, 19 $NaHCO_3$, 3.7 tetrasodium EGTA, and 5.5 glucose) for 60 minutes, and the pressure curve repeated to determine passive diameter at each pressure. Percent myogenic tone was then calculated as ((Ca^{2+} free diameter)-(Ca^{2+} containing diameter)/(Ca^{2+} free diameter))*100. Fura 2 ratio was simultaneously recorded during pressure response curves as described above. Pharmacological agents were applied during an equilibration period following fura-2 administration for a minimum of 15 minutes, and were present during the entire pressure-response curve.

Vessel Wall Thickness

Small mesenteric arteries were cannulated and pressurized to 60 mmHg as above. Arteries were maximally dilated by incubation in Ca^{2+} free PSS. Wall thickness and lumen diameter were determined using edge detection software and were expressed as the ratio (wall thickness)/(lumen diameter).

NaHS and Cysteine Dilation Curves

Small mesenteric arteries (id>100 μm) were dissected and cannulated as described above. These arteries were preconstricted with phenylephrine to 50% of resting diameter. NaHS was added in increasing concentrations from 10^{-9} to 10^{-4} mol/L and inner diameter was continuously recorded. A single bolus of cysteine (10^{-6} M) was applied for the cysteine dilation experiments and dilation in these experiments was allowed to proceed for a minimum of 20 minutes. Maximum passive diameter was recorded after both sets of dilation experiments by incubating with Ca^{2+} free PSS.

H_2S Assay

H_2S levels were determined using the Stipanuk and Beck method (29) with some modifications. Kidneys from Sham and IH rats were homogenized in phosphate buffered saline (PBS). The homogenates were added in a reaction mixture (total volume 250 μL) containing pyridoxal-5'-phosphate (8 mmol/L, 2.5 μL), L-cysteine (40 mmol/L, 2.5 μL), Complete protease inhibitor (6 μL, Roche), 100 μL tissue homogenate (190-260 mg tissue per reaction) and PBS up to volume. Some reaction mixtures contained BCA (100 mmol/L, 2.5 μL). These reaction mixtures were added to plastic center wells in 25 mL erlenmeyer flasks fitted with septum stoppers. The plastic center wells also contained small sections of Watman no. 1 filter paper wetted with PBS to trap evolved H_2S. The flasks were flushed with N_2 for 20 sec and then sealed. Reactions were allowed to proceed in an incubator at 37º C for 30 mins. H_2S was trapped by injection of ZnAc (1%, 125 μL) through the septum stopper. Reactions were stopped by injection of trichloroacetic acid (10%, 125 μL). Subsequently, 67 μL of 20 mmol/L N,N-Dimethyl-*p*-phenylenediamine sulfate in 7.2 mol/L HCl and 67 μL 30 mmol/L $FeCl_3$ in 1.2 mmol/L

HCl was added. Absorbance was measured at 670 nm after 20 minutes of incubation. The absorbance of each sample was calculated against a calibration curve of NaHS (100 nmol/L to 10 μmol/L). For determination of plasma H_2S, 100 μL of plasma was added to 150 μL PBS. The protocol proceeded as above starting with ZnAc addition.

NS1619 Dilation Curves

Small mesenteric arteries (id>100 μm) were dissected and cannulated as described above. These arteries were preconstricted with phenylephrine (PE) to 50% of resting diameter. NS1619 was added to the superfusate bath in increasing concentrations from 10-7 to 10-4 mol/L and inner diameter was continuously recorded. Maximum passive diameter was recorded after the dilation curve by incubating with Ca^{2+} free PSS.

Membrane Potential Recordings

Small mesenteric arteries (id>100 μm) were were dissected and cannulated as described above. After equilibration, vascular smooth muscle cells were impaled through the adventitia with glass intracellular microelectrodes (tip resistance 40–120 MΩ). A Neuroprobe amplifier (A-M Systems) was used for recording membrane potential (E_m). Analog output from the amplifier was low pass filtered at 1 kHz and recorded and analyzed using Axoscope software (Axon Instruments). Criteria for acceptance of E_m recordings were *1*) an abrupt negative deflection of potential as the microelectrode was advanced into a cell; *2*) stable membrane potential for at least 1 min; and *3*) an abrupt change in potential to ~0 mV after the electrode was retracted from the cell.

Immunofluorescence

Sections of mesentery were dissected as described above and placed into Histochoice (Amrefco) Mesentery was cryoprotected with 30% sucrose in PBS,

embedded in OCT medium, and frozen. Cryostat sections (10 µm) were permeabilized and blocked for nonspecific binding using donkey serum. Primary anti-CSE antibody (mouse monoclonal 1:100, Abcam) was prepared in 0.1 % gelatin with 0.2% Triton-X 100 and applied overnight at 4 ºC. Secondary antibody (anti-mouse Cy5, 1:500, Jackson ImmunoResearch Laboratories) was prepared in 0.1 % gelatin with 0.2% Triton-X 100 and applied for 1 hr at room temperature. Nuclei were stained with SYTOX green (1:5000 in PBS, Invitrogen) for 15 min at room temperature. Slides were imaged on an Olympus IX71 microscope with a 60X water-immersion lens and a spinning-disk confocal scanning unit (Andor). Nuclear morphology was used to differentiate endothelial, vascular smooth muscle, and adventitial layers of arteries. CSE expression in these cell types was separately determined using Andor iQ software with a region of interest tracing function. This method allowed measurement of fluorescence intensity per unit area in a user defined region. Areas were chosen to include only one cell type, and integrated intensity per unit area in the red fluorescence channel was used to assess CSE protein levels. A control image with the camera shutter closed was collected to determine camera noise. This background image intensity value was subtracted from all fluorescence measurements.

Western Blot Analysis

Isolated mesenteric arteries (1^{st} order to 5^{th} order) were homogenized in lysis buffer [1X RIPA lysis and extraction buffer (Pierce), 1X Complete protease inhibitor cocktail (Santa Cruz Biotechnology), 1X Halt phosphatase inhibitor cocktail (Pierce), 2 mmol/L phenylmethanesulfonylfluoride] on ice. Protein concentration was determined in the supernatant using BCA assay (Pierce) as recommended by the manufacturer.

Supernatants (5 µg/lane) were resolved by SDS-PAGE, and proteins were transferred to polyvinylidene difluoride membranes. After being blocked for nonspecific binding with blocking buffer (LI-COR), the membranes were incubated with primary anti-CSE antibody (mouse monoclonal,1 ug/mL; Abcam) or anti-β-actin antibody (1:10000; Sigma) at 4°C overnight, washed, and incubated with IRDye fluorescent secondary antibody (LI-COR) for 1 h at room temperature. Specifically bound antibody was detected using an Odyssey infrared imaging system (LI-COR). Relative content of the antigen protein was evaluated using Odyssey software (LI-COR). Band densities were normalized to total protein loaded per lane as assessed by β-Actin levels.

Quantitative Real-time Polymerase Chain Reaction (qRT-PCR)

Mesenteric Arteries from Sham and IH rats were stored in RNAlater (Ambion). Total RNA was isolated using the RNeasy Mini kit (Qiagen) following the manufacturer's protocol using the QIAcube system. Total RNA was reverse-transcribed to cDNA using High Capacity cDNA Archive Kit (Applied Biosystems). For real time detection of CSE (Rn00567128_m1) transcripts and reference gene β-actin (4352931E), TaqMan Gene Expression Assays were used. PCR was performed using Applied Biosystems 7500 Fast Real-Time PCR System. The normalized gene expression method ($2^{-\Delta\Delta CT}$) for relative quantification of gene expression was used (15).

Statistical Analysis

Data are shown as the means ± SEM of independent experiments. Constriction, fura 2 ratios, and dilation were analyzed using 2-way repeated-measures ANOVA with Student-Newman–Keuls post hoc analysis for differences between groups, concentrations, and interactions. Western blot and immunofluorescence experiments were

analyzed using Student's *t*-test. $P<0.05$ was considered statistically significant for all analyses.

Results

Myogenic tone in intact and denuded arteries

Myogenic tone was greater in mesenteric arteries from IH rats compared to arteries from Sham rats (Figure 1A, left). There was also a greater increase in VSM $[Ca^{2+}]$ in the IH arteries (Figure 1A, right). Endothelium disruption slightly elevated myogenic tone in IH arteries but greatly augmented tone in Sham arteries so that myogenic tone was not different between Sham and IH endothelium-disrupted arteries (Figure 1B, left). Endothelial disruption also elevated VSM $[Ca^{2+}]$ in both groups, and the Ca^{2+} response to pressure was not different between groups (Figure 1B, right). The enhanced myogenic tone in IH arteries was not due to vessel wall hypertrophy (Online Figure I).

Effect of inhibiting endothelial vasodilator production on myogenic tone

Myogenic tone was evaluated in arteries from Sham rats treated with the following inhibitors: 100 μmol/L N^G-nitro-L-arginine, (L-NNA, NOS inhibitor), 10 μmol/L indomethacin (cyclooxygenase blocker), 10 μmol/L SKF 525A (cytochrome p450 inhibitor), 250 units/mL PEG-catalase (H_2O_2 scavenger), 100 nmol/L apamin and 1 μmol/L TRAM-34 (SK and IK potassium channel blockers), 10 μmol/L Cr(III) mesoporphyrin IX (heme oxygenase inhibitor) (Figure 2). None had a significant effect.

H_2S regulation of myogenic tone

Arteries were treated with bismuth (III) subsalicylate (BSS,10 μmol/L) to scavenge H_2S and myogenic tone was evaluated. BSS enhanced myogenic tone in Sham

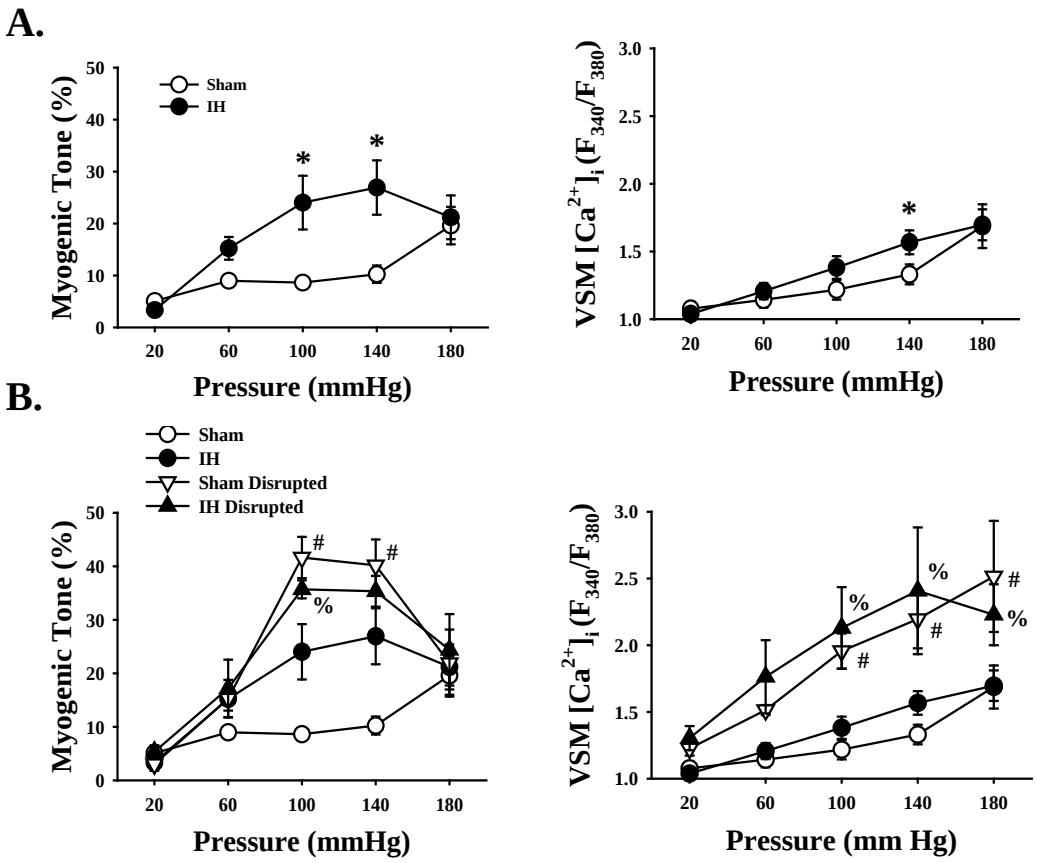

Figure 1. Myogenic tone and VSM [Ca^{2+}] in mesenteric arteries is enhanced by IH treatment **A**: myogenic tone and VSM [Ca^{2+}] in Sham and IH arteries. **B**: myogenic tone and VSM [Ca^{2+}] in Sham and IH arteries ± endothelium. n = 5-7 per group. Values are means ± SE. * $P < 0.05$ IH vs. Sham. # $P < 0.05$ Sham vs. Sham treated. % $P < 0.05$ IH vs. IH treated.

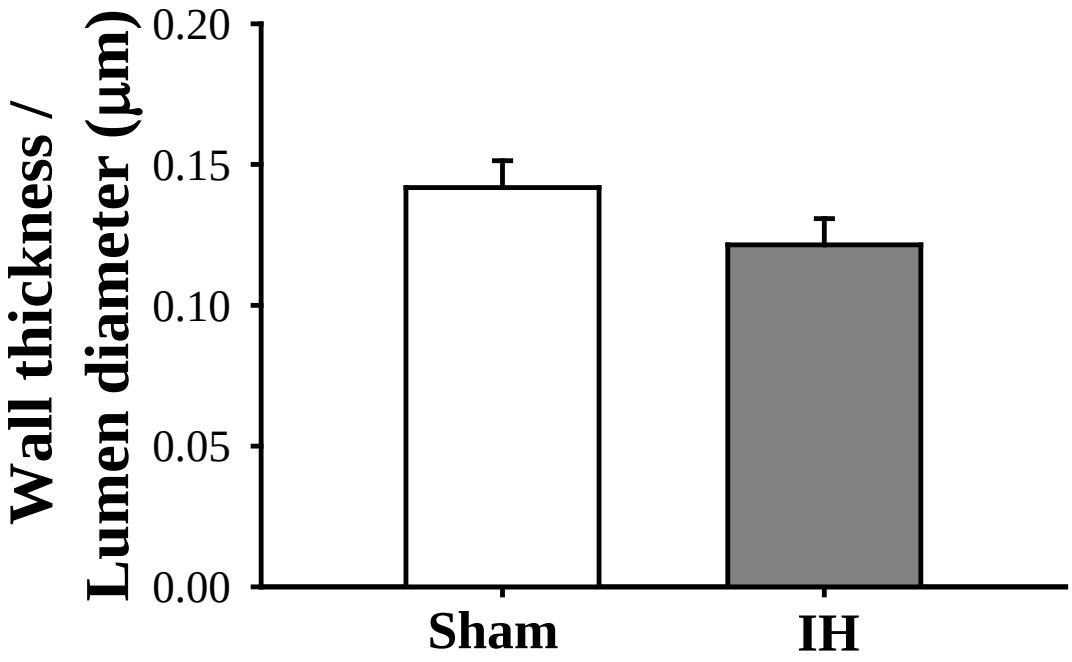

Online figure I. The ratio of wall thickness/lumen diameter in small mesenteric arteries is not altered by IH treatment. Measurements performed in maximally dilated arteries pressurized to 60 mmHg. n=8.

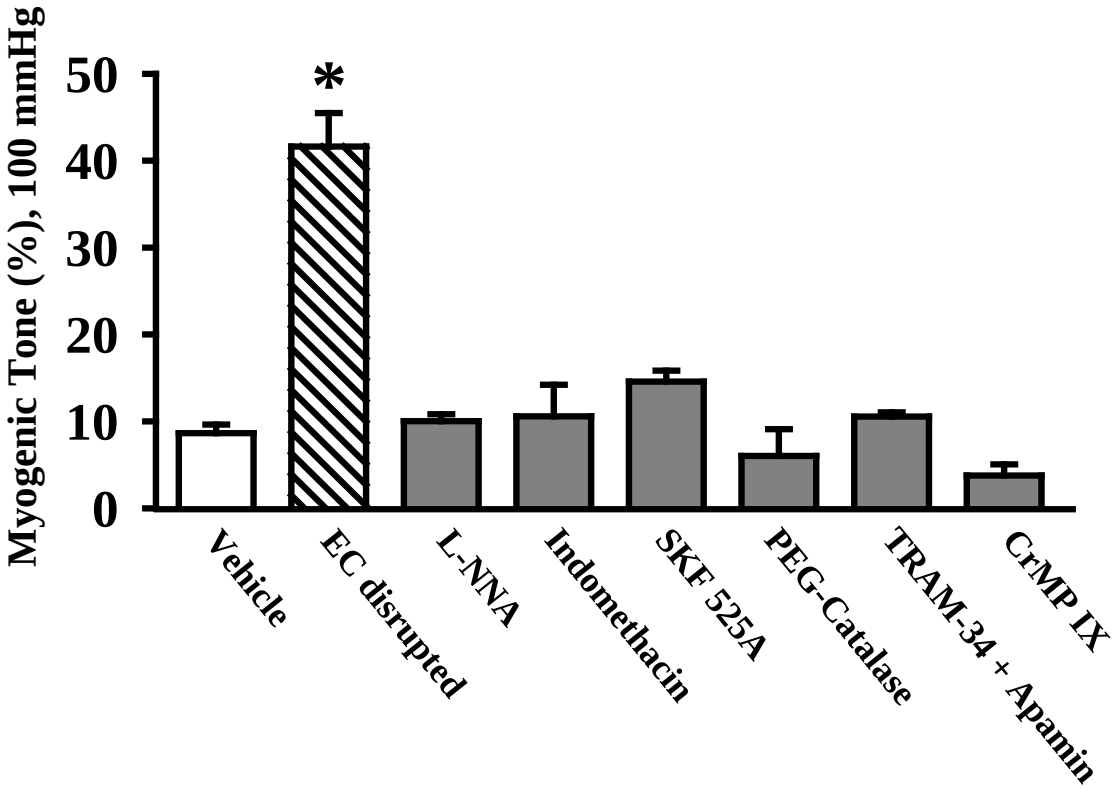

Figure 2. Inhibitors of previously-described endothelium-produced vasodilators do not affect myogenic tone in Sham arteries. Myogenic tone was assessed at 100 mmHg in untreated Sham arteries (Vehicle) or after pharmacological inhibition or endothelium disruption (EC disrupted). Values are means ± SE. n=3-6 per group. * $P < 0.05$ vs. Sham intact.

but not IH arteries, eliminating differences in pressure-induced constriction between groups (Figure 3A, left). BSS also reduced VSM [Ca^{2+}] in IH arteries but had no effect in Sham arteries (Figure 3A, right). Since BSS non-selectively scavenges H_2S and several H_2S producing enzymes are present in the vascular wall, the effect of CSE inhibitors was evaluated. The CSE inhibitor β cyano-L-alanine (BCA, 100 μmol/L) enhanced myogenic tone similarly to BSS in Sham arteries with no effect in IH arteries (Figure 3B, left). BCA also enhanced VSM [Ca^{2+}] in Sham arteries but had no effect in IH arteries, normalizing the response between groups (Figure 3B, right). A second inhibitor of CSE, DL propargylglycine (PAG, 100 μmol/L), also enhanced myogenic tone in Sham arteries but reduced myogenic tone in IH arteries (Online Figure II, left). PAG also enhanced VSM [Ca^{2+}] in Sham arteries and reduced VSM [Ca^{2+}] in IH arteries (Online Figure II, right). Myogenic curves in middle cerebral arteries from Sham and IH rats demonstrated that BCA also elevates myogenic tone in Sham but not IH cerebral arteries (Online Figure III).

Cysteine-Induced Vasodilation

The endogenous substrate cysteine increases CSE synthesis of H_2S.(3) Arteries preconstricted with PE were dilated with cysteine (1 μmol/L). Cysteine caused a greater dilation in Sham than IH arteries (Figure 4). Addition of BCA significantly reduced cysteine dilation in Sham but not IH arteries, although Sham arteries still dilated to a greater extent in the presence of BCA. Endothelium disruption likewise significantly reduced cysteine dilation in Sham but not IH arteries, normalizing the response between groups (Figure 4).

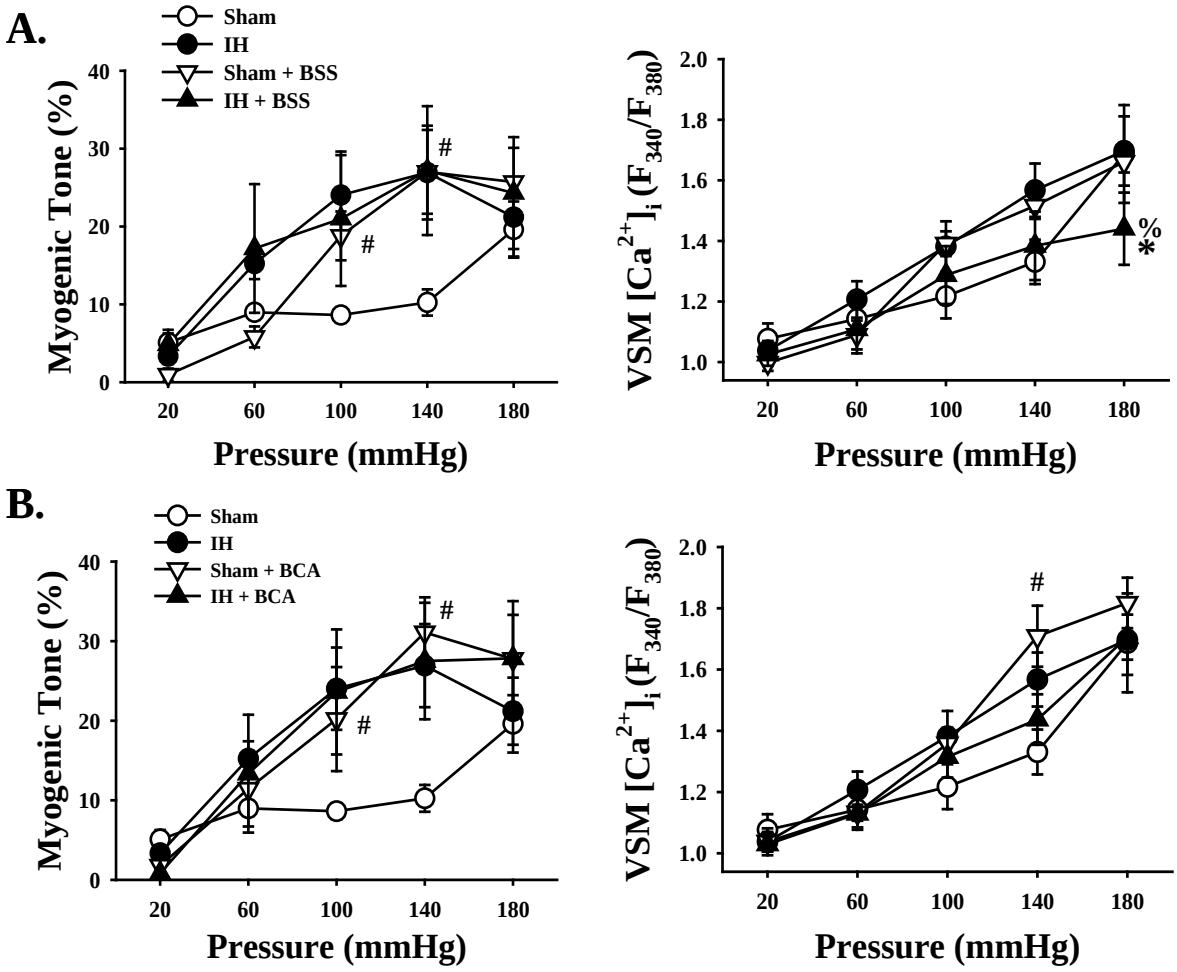

Figure 3. Myogenic tone in Sham mesenteric arteries is enhanced by treatment with H_2S antagonists bismuth (III) subsalicylate (BSS) (**A**) and β cyano-L-alanine (BCA) (**B**). n = 5-7 per group. Values are means ± SE. # $P < 0.05$ Sham vs. Sham treated. * $P < 0.05$ IH vs. Sham within treatment. % $P < 0.05$ IH vs. IH treated.

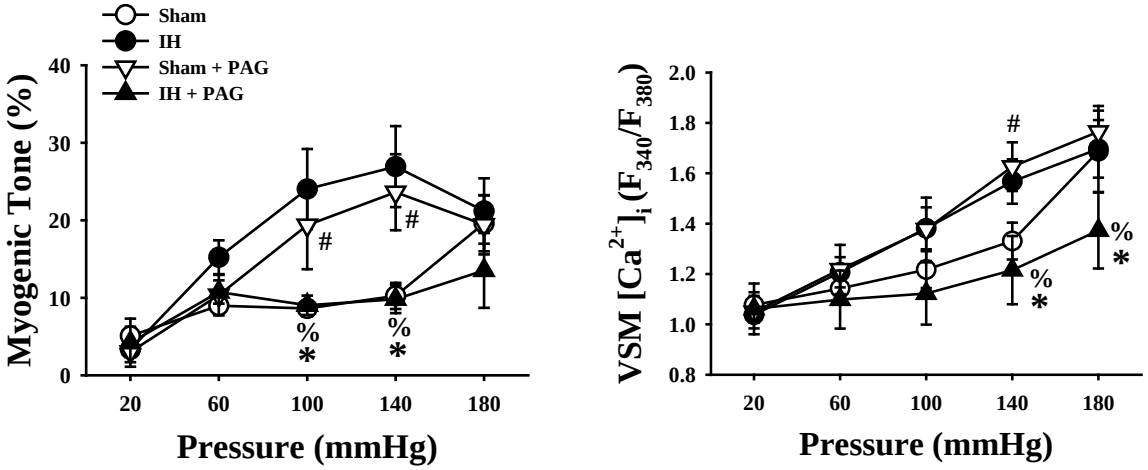

Online figure II. Myogenic tone and in Sham mesenteric arteries is enhanced by treatment with CSE antagonist DL-propargylglycine (PAG). PAG reduced myogenic tond and in IH arteries. Vessel inner diameter and fura-2 ratios were recorded during luminal pressure increases from 20 to 180 mmHg. n = 5-7 per group. Values are means ± SE. # $P < 0.05$ Sham vs Sham treated. * $P < 0.05$ IH vs Sham within PAG treated. % $P < 0.05$ IH vs IH treated.

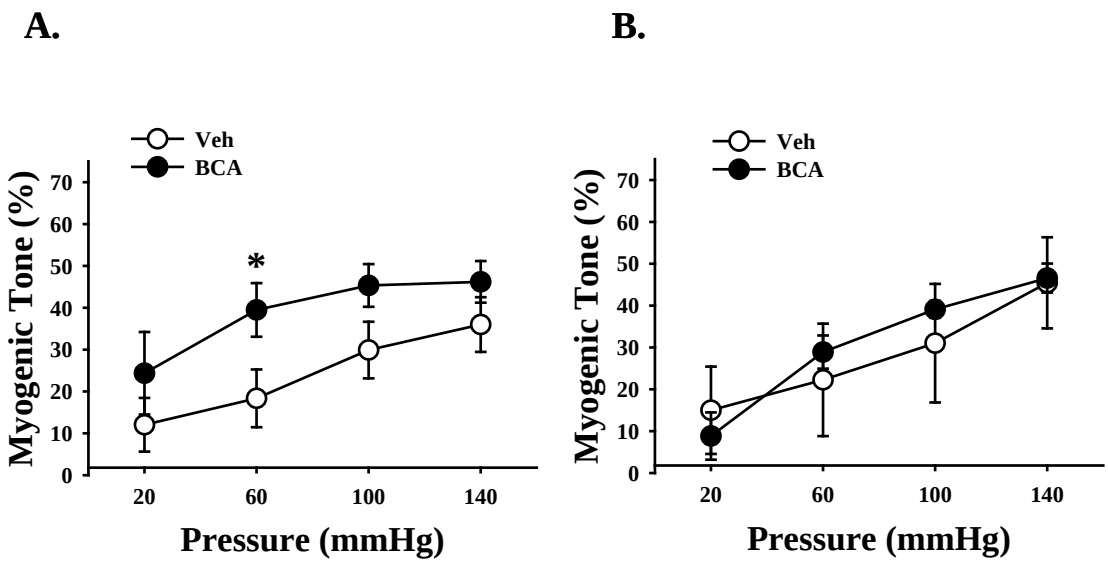

Online figure III. Myogenic tone in Sham middle cerebral arteries (**A**), but not IH middle cerebral arteries (**B**), is enhanced by treatment BCA. Vessel inner diameter was recorded during luminal pressure increases from 20 to 140 mmHg. n = 4-6 per group. Values are means ± SE. *P < 0.05 Sham vs Sham BCA.

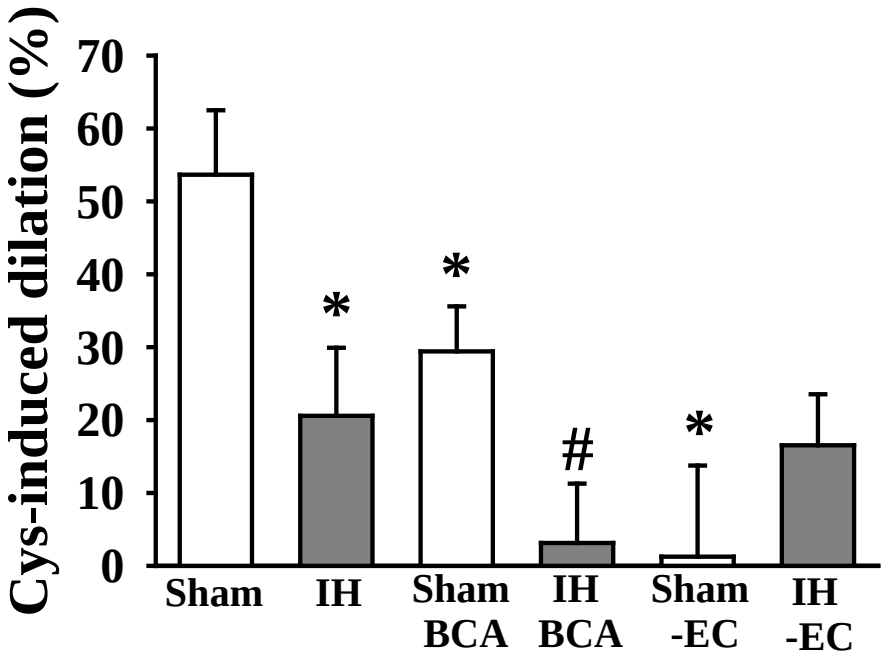

Figure 4. Endothelial CSE activity as measured by cysteine-induced dilation is reduced in IH arteries. –EC = endothelial disruption. BCA = β cyano-L-alanine. n = 5 per group. Values are means ± SE. * $P < 0.05$ vs. Sham untreated. # $P < 0.05$ Sham vs. IH within treatment.

Mechanism of H_2S-mediated vasodilation

To determine whether IH arteries have decreased sensitivity to H_2S, dilation to the H_2S donor NaHS was examined in endothelium-intact arteries constricted with PE to 50% resting diameter. NaHS dilated both Sham and IH arteries, with slightly greater dilation in IH than Sham arteries (Figure 5A). The K_{ATP} blocker glibenclamide (10 μmol/L) was used to determine if K_{ATP} channels mediate this dilation as reported in larger arteries and in the perfused mesenteric bed (30). Glibenclamide had little effect in Sham or IH arteries (Figure 5B and C), although it blocked pinacidil-induced dilation (Online figure IV). In contrast, the BK_{Ca} channel inhibitors iberiotoxin (IbTx, 100 nmol/L) and paxilline (1 μmol/L) significantly reduced NaHS dilation in both groups (Figure 5B and C and Online figure V). The phosphodiesterase inhibitor 3-isobutyl-1-methylxanthine (IBMX) did not reduce NaHS induced dilation in either group (Online figure VI). Arteries contstricted to 50% resting diameter with KCl did not dilate to NaHS (Online figure VII).

BK_{Ca} Channel Regulation of Myogenic Tone

Since the NaHS dilation experiments implicated BK_{Ca} channels as a target for H_2S, the effect of IbTx on myogenic tone was evaluated. IbTx elevated myogenic tone at all pressures in both Sham and IH arteries, and normalized myogenic tone between groups (Figure 5D). Likewise, IbTx elevated VSM $[Ca^{2+}]$ in Sham and IH arteries, eliminating differences between groups (Figure 5E). NS1619 (BK_{Ca} channel opener) dilation in arteries constricted with PE and incubated with BCA was similar in both groups. (Online Figure VIII).

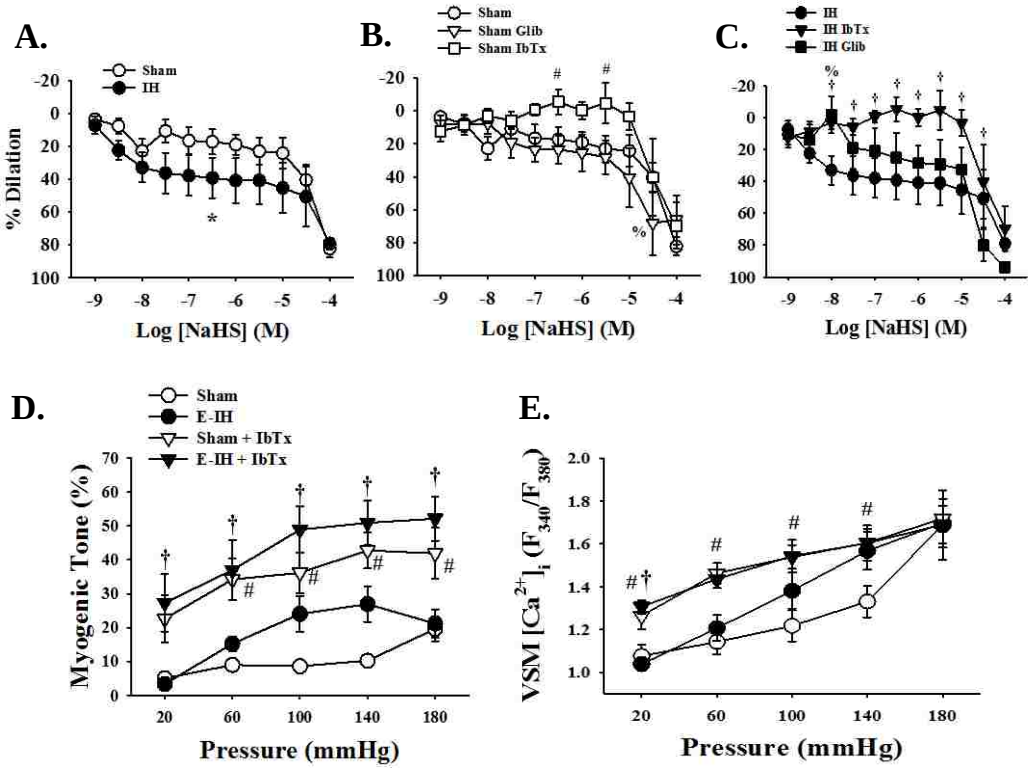

Figure 5. Blockade of BK_{Ca} channels inhibits NaHS-induced vasodilation and enhances myogenic tone in small mesenteric arteries. NaHS dilates both Sham and IH arteries (**A**). NaHS dilation in Sham arteries is inhibited by iberiotoxin (IbTx) but not glibenclamide (Glib) (**B**). NaHS dilation in IH arteries is inhibited by IbTx but not Glib (**C**). **D**: Myogenic tone in Sham and IH arteries ± IbTx. **E**: VSM $[Ca^{2+}]$ in Sham and IH arteries ± IbTx. Values are means ± SE. *P < 0.05 Sham vs. IH untreated. # P < 0.05 untreated vs. IbTx within Sham. % P < 0.05 untreated vs. Glib within group. † P < 0.05 untreated vs. IbTx within IH. IbTx =iberiotoxin,100 nmol/L Glib=glibenclamide, 10 μmol/L.

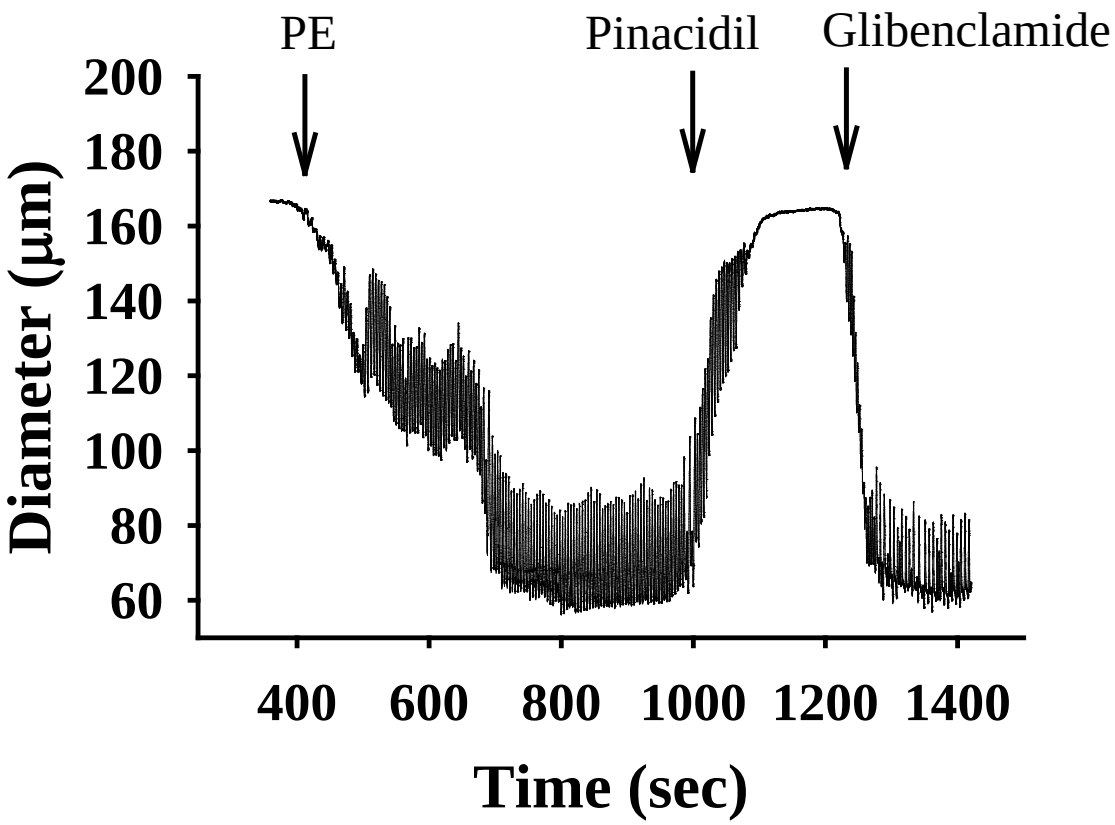

Online figure IV. Example trace of blockade of pinacidil-induced (10 µmol/L) K_{ATP} activation by glibenclamide (10 µmol/L).

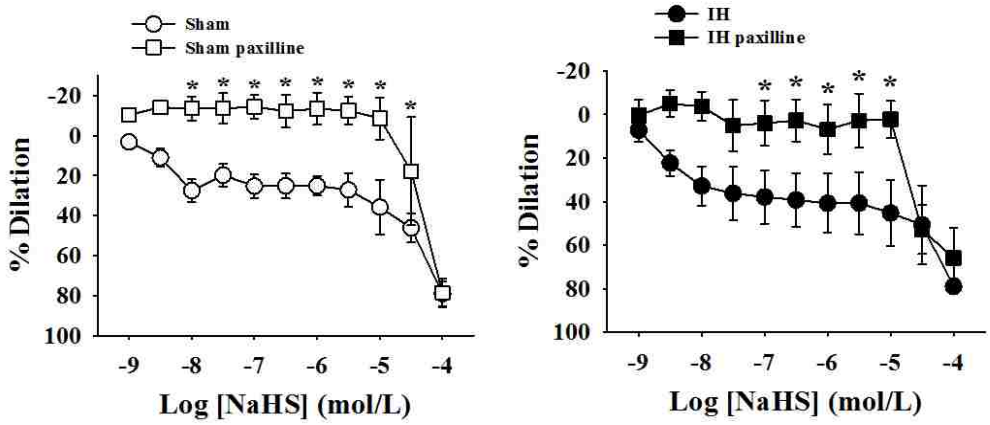

Online figure V. NaHS dilation curves in the presence and absence of the BK_{Ca} channel blocker paxilline (1 μmol/L) in Sham and IH arteries. Arteries preconstricted to 50% resting diameter with PE. n = 3-6 per group. Values are means ± SE. * $p<0.05$ vs. vehicle.

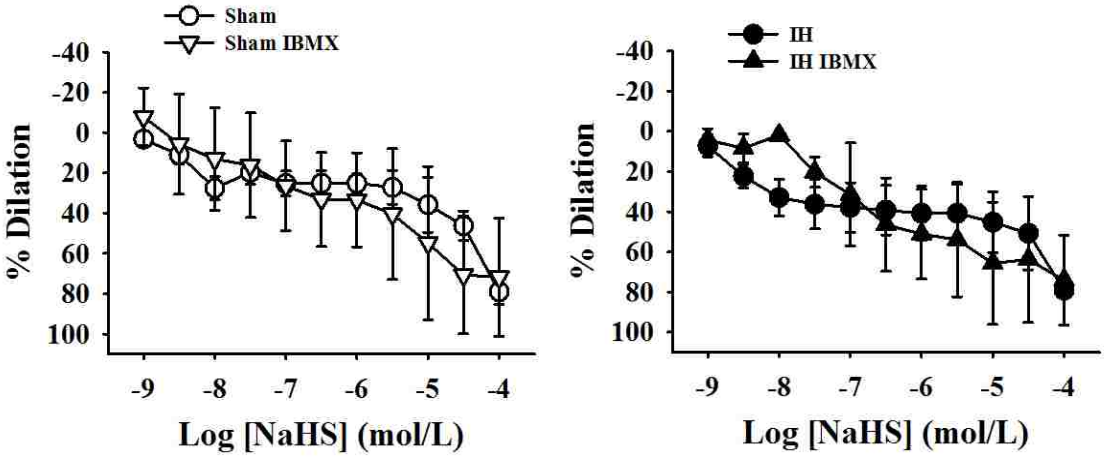

Online figure VI. NaHS dilation curves in the presence and absence of the phosphodiesterase inhibitor IBMX (40 μmol/L) in Sham and IH arteries. Arteries preconstricted to 50% resting diameter with PE. n = 3-6 per group. Values are means ± SE. No significant effect of IBMX observed.

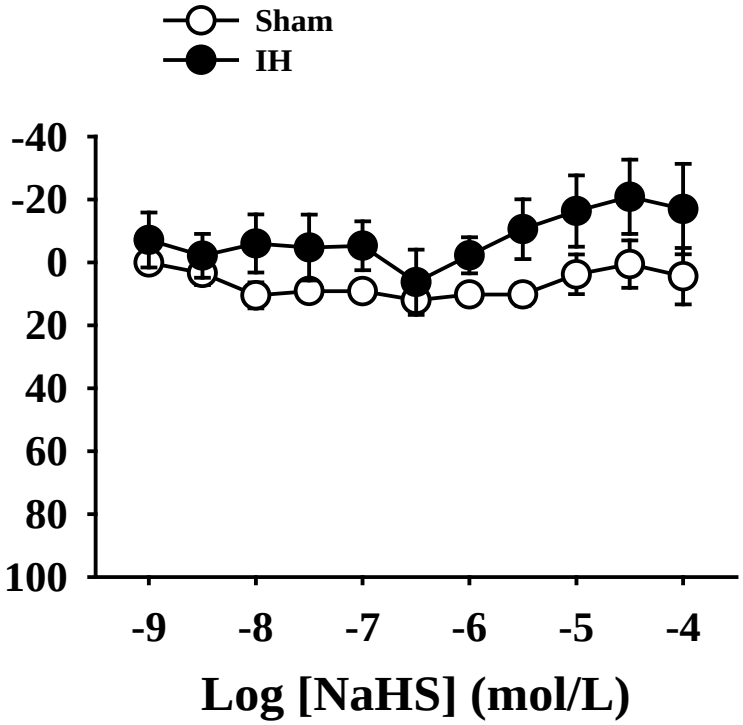

Online figure VII. NaHS dilation curves in KCl preconstricted Sham and IH arteries. Arteries preconstricted to 50% resting diameter. n = 4 per group. Values are means ± SE. No significant dilation was observed in either group.

Membrane Potential Recordings

Sharp electrodes were used to record E_m in Sham and IH arteries at 60 and 140 mmHg luminal pressure. While the increase in pressure caused a significant depolarization in both groups, IH arteries had a more depolarized E_m at both 60 and 140 mmHg compared to Sham (Figure 6A and B). Treatment with BCA depolarized only Sham arteries, normalizing E_m between groups but increased luminal pressure depolarized E_m in both groups in the presence of the inhibitor (Figure 6A and B). The H_2S donor, NaHS (10^{-5} mol/L), hyperpolarized E_m in both Sham and IH arteries constricted with 10^{-6} mol/L PE and this hyperpolarization was prevented by IbTx (Figure 6C and D).

ROS and NO Regulation of Myogenic Tone

Since H_2S reacts with superoxide to form sulfite and can also react with NO, pressure-induced constriction was evaluated in the presence of the superoxide dismutase mimetic tiron or L-NNA. Tiron slightly reduced myogenic tone in IH arteries but did not affect tone in Sham arteries (Figure 7A, left). However, myogenic tone was still greater in IH than Sham arteries at 140 mmHg. Tiron did not affect VSM $[Ca^{2+}]$ in either group, and IH arteries had a significantly higher VSM $[Ca^{2+}]$ than Sham arteries with this treatment (Figure 7A, right). L-NNA tended to reduce myogenic tone in IH arteries at 100 mmHg but had no effect on Sham arteries so that tone was greater in IH arteries at 100 mmHg but not 140 mmHg (Figure 7B, left). L-NNA had no significant effect on VSM $[Ca^{2+}]$ in either group (Figure 7B, right).

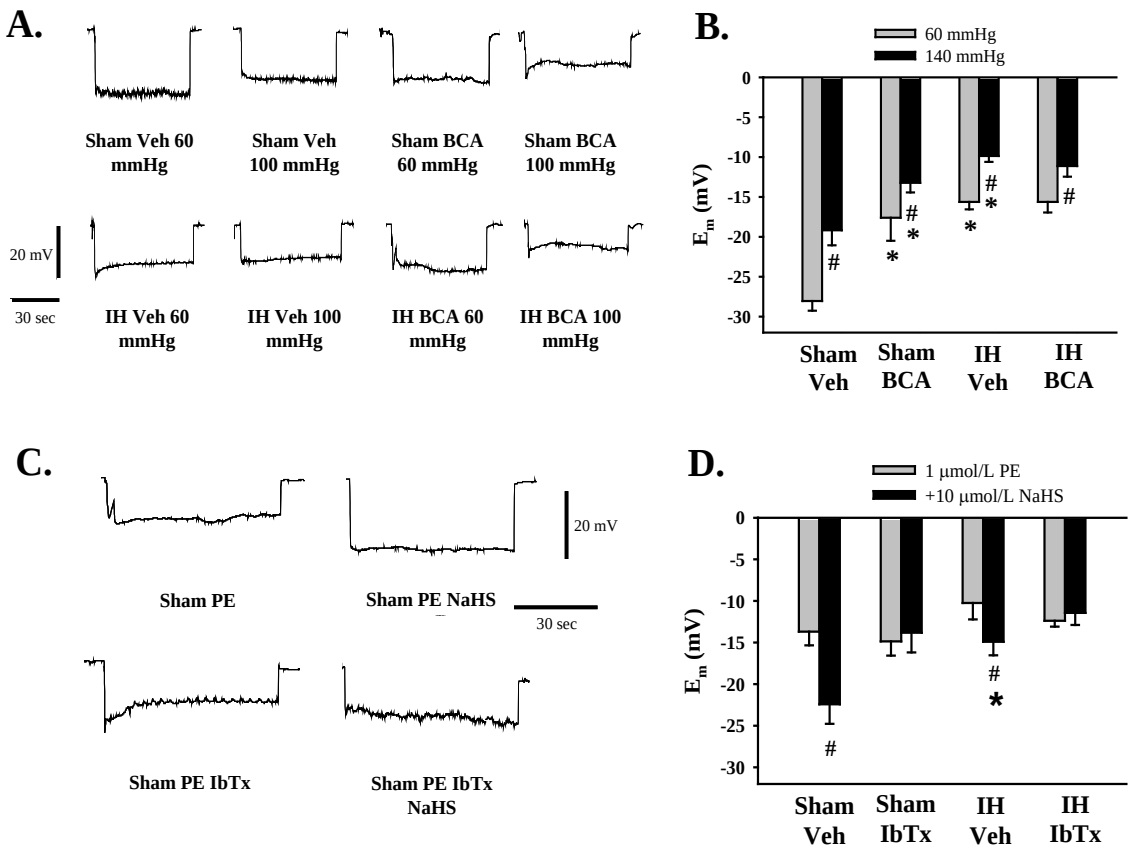

Figure 6. H_2S hyperpolarizes vascular smooth muscle cells through activation of BK_{Ca} channels and loss of endogenous H_2S depolarizes IH vascular smooth muscle cell E_m. **A:** representative traces of sharp electrode E_m measurements ± BCA. **B:** Summary data from experiments in **A**. **C:** representative traces of sharp electrode E_m measurements before and after ± NaHS addition in Sham arteries. **D**: summary data from experiments in **C**. n = 5-6 per group. Values are means ± SE. # $P < 0.05$ within group. * $P < 0.05$ vs. Sham vehicle.

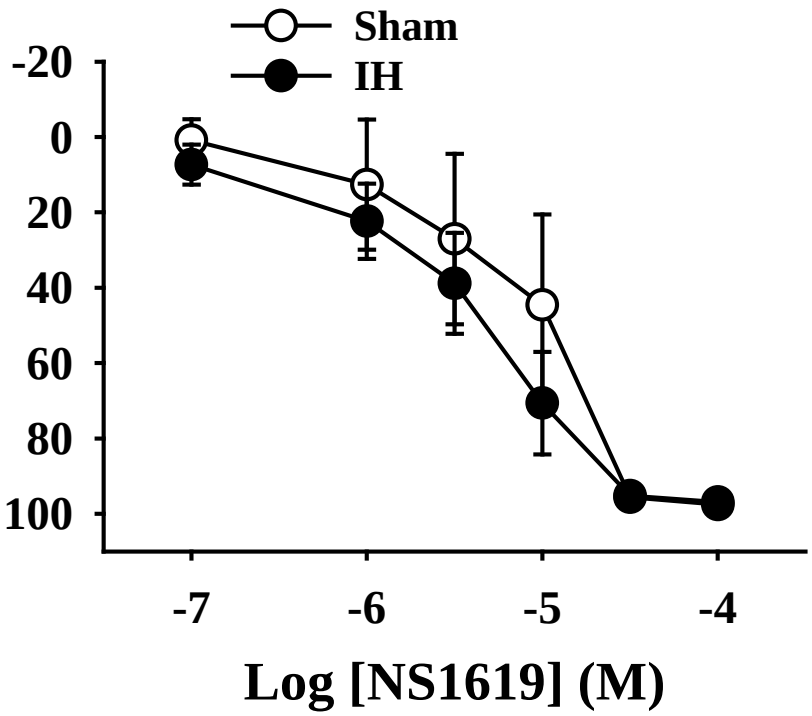

Online figure VIII. Mesenteric arteries from Sham and IH rats dilate similarly to the BK_{Ca} channel activator NS1619. Arteries preconstricted to 50% with PE. n = 5 per group. Values are means ± SE.

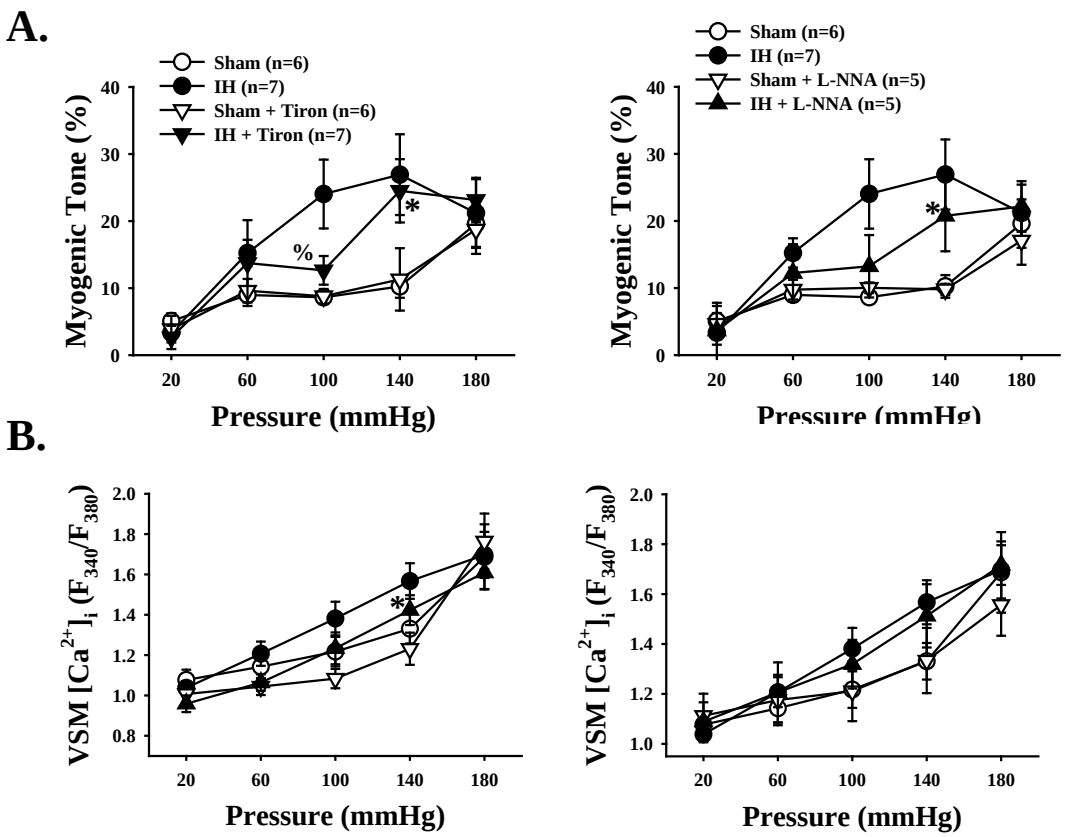

Figure 7. Tiron and L-NNA partially reduced myogenic tone in IH arteries to Sham levels. **A:** Tiron effect on Sham and IH myogenic tone. **B**: L-NNA effect on Sham and IH myogenic tone. Values are means ± SE. *P < 0.05 Sham treated vs. IH treated. % P < 0.05 IH vs. IH treated.

CSE Iimmunofluorescence, Western Blot, and qPCR

Immunofluorescence imaging in small mesenteric arteries assessed expression of CSE. Using the morphology of co-stained nuclei to assess cell type, CSE expression was apparent in endothelial, VSM and adventitia layers of small mesenteric arteries (Figure 8A). CSE expression was highest in the adventitial layer of Sham arteries. CSE expression was decreased in the endothelial layer of IH arteries vs. Sham (Figure 8B).

Western blots for CSE using tissue homogenates of 1st through 5th order mesenteric arteries showed CSE expression was actually greater in arteries from IH rats (Figure 8 C and D). To resolve this discrepancy between immunofluorescence and western blot data, immunofluorescence in 1st order mesenteric arteries was evaluated. In these larger arteries, CSE expression was greatest in the adventitia in both groups and significantly greater in IH than Sham arteries (Online figure IX). Quantitative real-time PCR of CSE mRNA using whole mesenteric artery homogenates was performed, which showed no differences between Sham and IH (Online figure X).

H_2S Assay

To verify that BCA reduces H_2S production, enzymatic production of H_2S was evaluated in kidney homogenates. Sham and IH kidney homogenates generated similar quantities of H_2S and this production was significantly reduced by either 100 µmol/L or 1 mmol/L BCA (Online figure XI). 100 µmol/L BCA reduced CSE H_2S production by ~20%, similar to the effect of 1 mmol/L BCA. Plasma levels of H_2S were also not different between Sham and IH (Online figure XII).

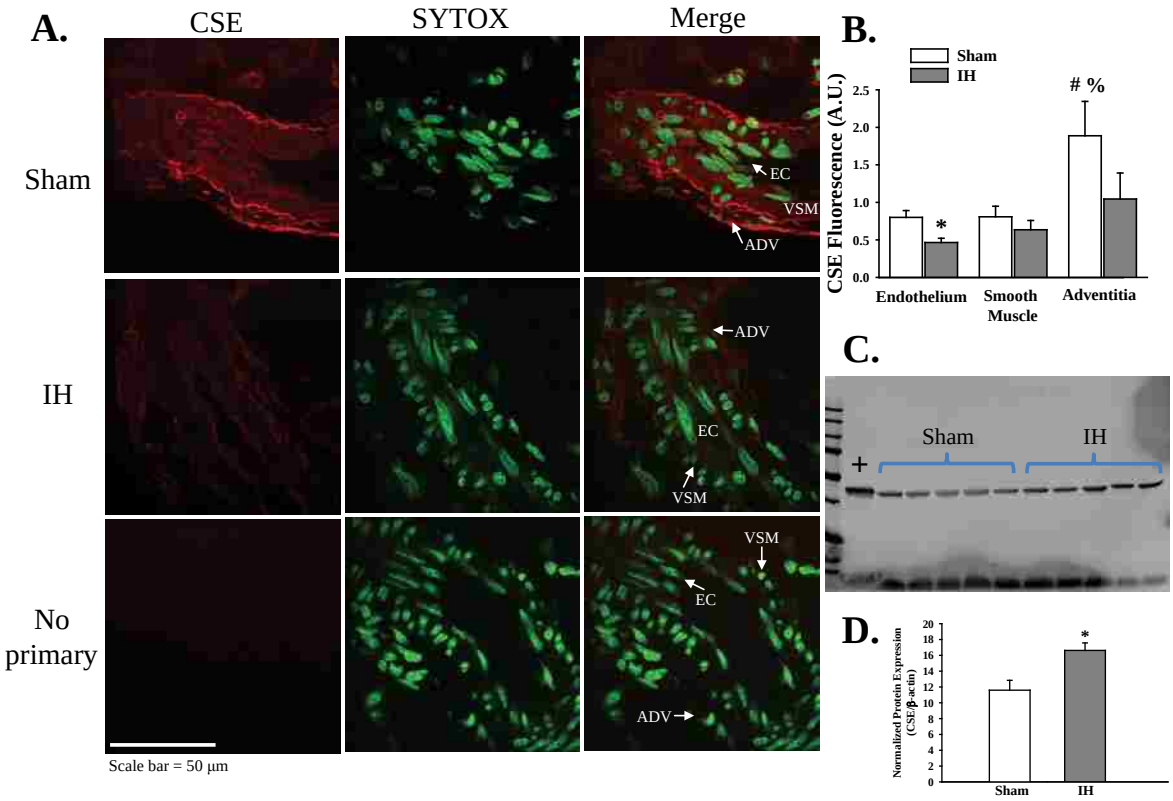

Figure 8. IH reduces endothelial cell CSE in small mesenteric arteries. **A**: representative images**. B**: Immunofluorescence summary data. n=4 per group. **C**: Western blot of CSE in 1st-5th order mesenteric arteries from Sham and IH rats. Tissue for western blot contained adventitial connective tissue but adipose tissue was removed prior to homogenization. **D**: summary data from blot in **C**. CSE expression normalized to β-actin. + positive control brain lysate. n = 5 per group. *P < 0.05 Sham vs. IH. #P < 0.05 Sham endothelium vs. Sham adventitia. %P < 0.05 Sham VSM vs. Sham endothelium

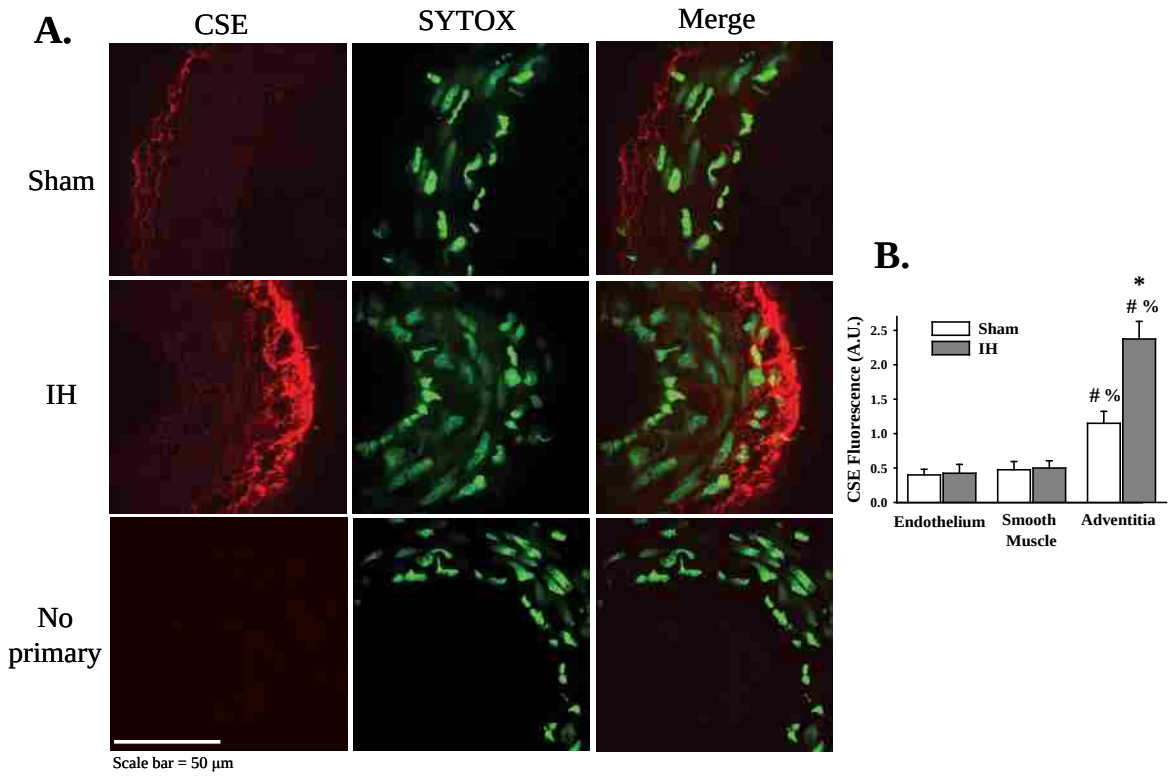

Online figure IX. IH increases adventitial CSE in large mesenteric arteries. Frozen fixed sections were probed with anti-CSE antibody (red). No primary antibody control experiments revealed no nonspecific secondary antibody binding. Nuclei stained with SYTOX green (green). Cell type was identified based on nuclear morphology. Background subtracted integrated fluorescence intensity per unit area indicated enhanced adventitial CSE in IH arteries (**B**). CSE expression was significantly higher in adventitia than in the other two layers in Sham and IH arteries. n=4 per group. *P < 0.05 Sham vs IH. #P < 0.05 endothelium vs adventitia within group. %P < 0.05 endothelium vs smooth muscle within group.

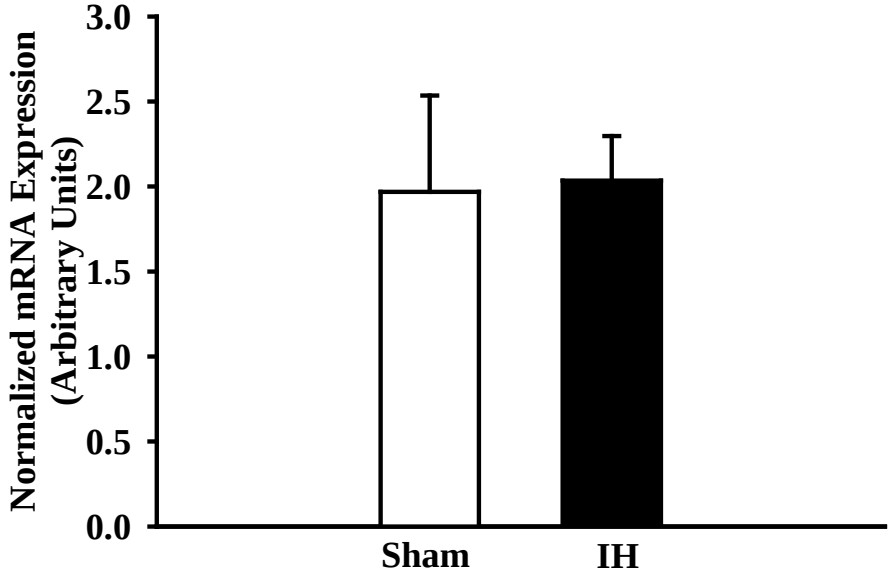

Online figure X. Real-time quantitative PCR of CSE in mesenteric arteries from Sham and IH rats. Whole mesenteric arteries were collected for this analysis. CSE expression normalized to β-actin. n = 7 Sham and 5 IH. Values are means ± SE.

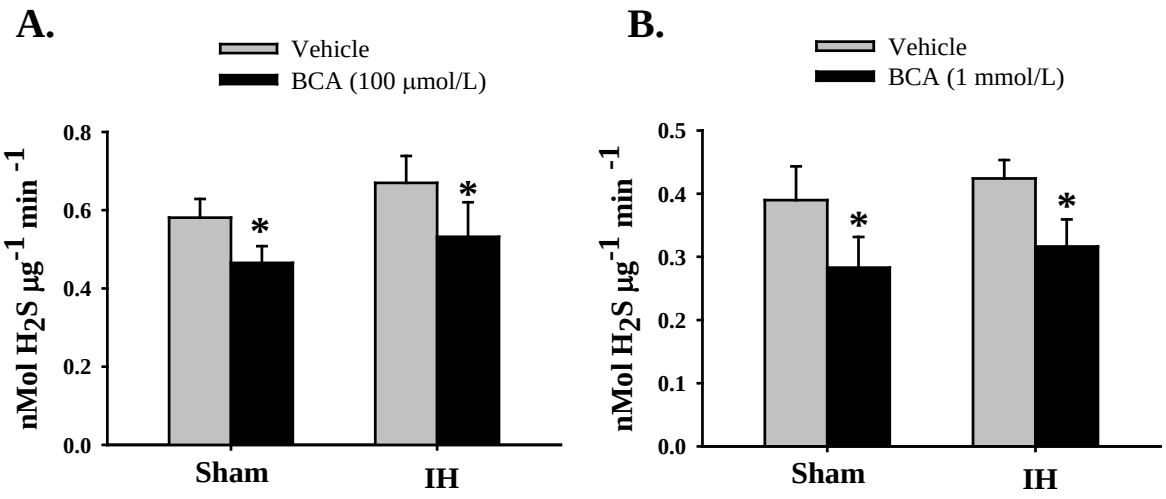

Online figure XI. H_2S production assay in kidney homogenates from Sham and IH rats. 100 μmol/L BCA reduced H_2S production in both groups (**A**) to a similar degree as 1 mmol/L BCA (**B**). n = 5-6 per group. Values are means ± SE. *P < 0.05 Veh vs BCA.

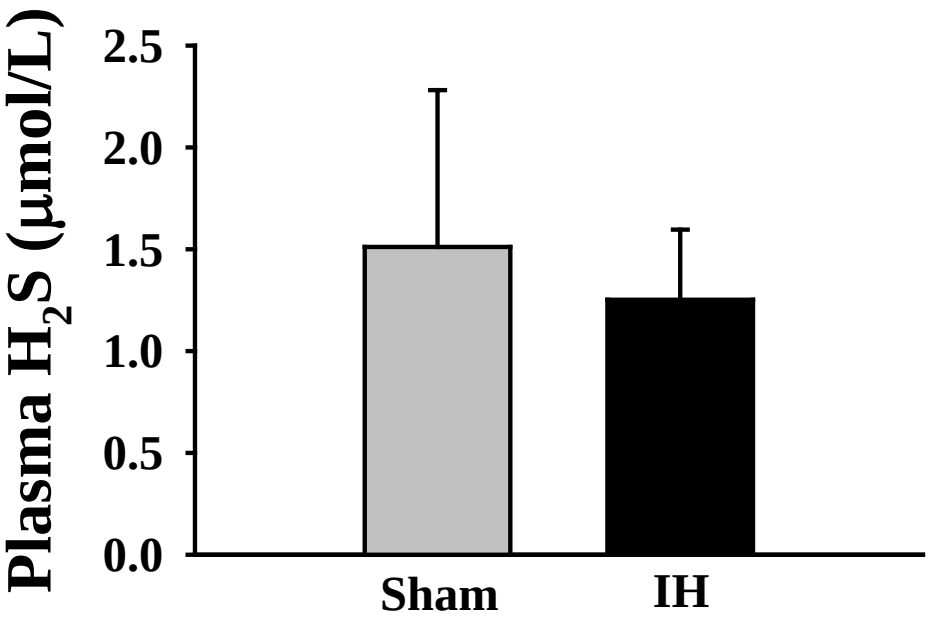

Online figure XII. Plasma H_2S concentration in Sham and IH rats. n = 5. Values are means ± SE.

Discussion

There are three major new findings from these studies. First, IH in rats enhances myogenic tone in small mesenteric arteries by decreasing H_2S-dependent dilation. Secondly, H_2S limits myogenic tone in mesenteric arteries in an endothelium-dependent manner. Third, H_2S dilation in mesenteric arteries is mediated by BK_{Ca} activation, a previously unreported mechanism of H_2S-induced vasodilation. Both functional dilation studies and recordings of VSM membrane potential support these conclusions. This is in contrast to previous reports of dilation by higher concentrations of H_2S in aorta and in larger mesenteric arteries suggesting H_2S may have dose-dependent mechanisms of action that vary in different size arteries.

Both pressure-induced increases in myogenic tone and VSM $[Ca^{2+}]$ are greater in mesenteric arteries after IH consistent with the widely accepted theory of myogenic tone in which constriction is dependent on depolarization-induced Ca^{2+} influx (7). Although myogenic tone can be increased by vessel wall hypertrophy through the "structural amplifier" mechanism (9), there was no increase in wall thickness in IH arteries suggesting functional rather than structural mechanisms account for this increased tone.

Endothelial dysfunction is a commonly reported consequence of sleep apnea (6) and the current studies suggest reduced endothelial dilation causes the enhanced myogenic tone in IH arteries. That is, endothelium inactivation increased both myogenic tone and VSM $[Ca^{2+}]$ more in Sham than in IH arteries suggesting endothelial factor(s) are reduced or do not reach the smooth muscle in IH arteries. Of interest, endothelial disruption greatly enhances VSM $[Ca^{2+}]$ in Sham arteries with only a moderate increase in tone over that in the IH endothelium-intact group while a relatively small enhancement

of tone but a large increase in VSM [Ca^{2+}] is seen in IH arteries. Thus the enhanced myogenic tone in IH arteries appears to be dependent on greater VSM [Ca^{2+}], but an element of Ca^{2+} sensitization may also contribute. In contrast to our findings, Phillips et al. observed no effect of IH on myogenic tone in gracilis arterioles (22). In this study, rats were exposed to 1 min of 10% O_2 every 4 min without supplemental CO_2 to prevent hypocapnia and no effects on arterial pressure were observed. In our study, rats were exposed to ~15 secs of O_2 < 10% every 3 min with supplemental CO_2 and experienced a sustained increase in arterial pressure suggesting different exposure paradigms may differentially affect myogenic reactivity. However, Phillips also found that their IH exposure impairs endothelium-dependent dilation in skeletal muscle arteries (23). Thus endothelial function may have a greater impact on myogenic tone in mesenteric arteries than in the more myogenically active skeletal muscle arteries.

Multiple pharmacological inhibitors were used in an attempt to identify the product or effect of the endothelium limiting myogenic tone in Sham but not in IH mesenteric arteries. Inhibiting NOS, cyclooxygenase, cytochrome P450 enzymes, heme oxygenase, scavenging H_2O_2 or blocking endothelium-derived hyperpolarization with SK and IK blockers did not mimic endothelial disruption, in contrast to studies in other vascular beds in which NO limits myogenic tone (12). These studies suggested that a novel endothelial product minimizes myogenic tone in small mesenteric arteries.

H_2S is a recently described endothelial product that mediates vasodilation and regulates blood pressure (32). In contrast to the effects of the other inhibitors, the H_2S scavenger BSS greatly increased myogenic tone in Sham but not IH arteries. The similarity of H_2S scavenging to endothelial disruption suggests endothelial H_2S

minimizes myogenic tone but is impaired by IH treatment. Although BSS tended to increase VSM [Ca^{2+}] in Sham arteries, the increase was not significant and BSS decreased VSM [Ca^{2+}] in IH arteries suggesting the scavenger may have non-specific effects such as dissociation into salicylate (2), a cyclooxygenase inhibitor.

BSS scavenges H_2S non-selectively, so pharmacological inhibitors were used to determine if H_2S production in the Sham arteries is from CSE, the reported primary vascular source (32), CSE inhibition with either BCA or PAG also elevated myogenic tone in Sham arteries but not in IH arteries, similar to BSS scavenging of H_2S. Likewise, BCA elevated VSM [Ca^{2+}] in Sham but not IH arteries so that tone and [Ca^{2+}] were not different between groups in the presence of the inhibitor. In cerebral arteries, BCA also enhanced myogenic tone in Sham but not IH arteries. The concentration of BCA used (100 μmol/L) was verified to be as effective at reducing H_2S production in kidney homogenates as a higher concentration (1 mmol/L) used in some studies. These results suggest that endothelial CSE produces H_2S to minimize myogenic tone and IH impairs this pathway in multiple vascular beds. Unexpectedly, PAG, but not BCA or BSS reduced myogenic tone and [Ca^{2+}] in IH arteries and increased VSM [Ca^{2+}] in Sham arteries. Because PAG inhibits the entire cystathionine synthase-like family of proteins and is thus not specific to CSE, it is possible that one of this large family of proteins that includes several ion channels and transporters (27) is required for myogenic tone after IH treatment, although what enzyme it is or what function it fulfills is unknown.

Dilation to excess CSE substrate cysteine was also evaluated. Cysteine dilation was greater in Sham than in IH arteries and significantly reduced by CSE inhibition in Sham but not IH arteries suggesting mesenteric arteries from IH rats have reduced CSE

function. Consistent with H_2S being endothelium-derived, endothelial disruption reduced cysteine dilation in Sham but not IH arteries.

CSE expression is reduced in the endothelium of IH arteries providing a likely cause of decreased H_2S dilation following IH treatment. In contrast to studies in mice (34), CSE was readily apparent in all three layers of the vasculature with the greatest expression in the adventitial layer. Indeed, western blot analysis of CSE protein in homogenates of the entire mesenteric vascular tree revealed a significant increase in total CSE in IH arteries compared with Sham arteries, similar to the increased immunofluoresence observed in the adventitial layer of IH 1st order mesenteric arteries. It is interesting that although CSE is expressed in all vessel wall layers, disrupting the endothelium prevents CSE's vasoregulatory function. One possibility is that CSE in smooth muscle and adventitial cells produces little vasoactive H_2S or is associated with enzymes that rapidly degrade H_2S. Alternatively, the endothelium may be the target rather than the source of the H_2S. Indeed, recent studies by Schleifenbaum et. al. (25) demonstrated vascular effects of periadventitial H_2S production in rat aorta. However, in the mesenteric arteries, endothelial CSE appears to promote vasodilation and IH appears to impair this pathway.

The H_2S donor NaHS dilated PE-constricted arteries from both groups with a slightly greater dilation in IH arteries demonstrating that IH arteries have an intact response to H_2S and loss of endogenous H_2S may even cause compensatory upregulation of H_2S targets. Similarly, mid-sized mesenteric arteries from CSE -/- mice exhibit greater dilation to exogenous H_2S compared to arteries from wild type littermates (34). Thus enhanced myogenic tone in IH arteries is likely caused by loss of production or

increased scavenging of H_2S. We observed NaHS-dependent dilation at much lower concentrations than has been previously reported with a consistent dilation in response to H_2S in the nmol/L range. This low concentration, more comparable to tissue H_2S levels measured by gas chromatography as 17 nmol/l (10), suggests small arteries may be more sensitive to H_2S than larger arteries. We found that basal and cysteine-induced H_2S production from arterial homogenates was below the detection limit of a colorometric assay capable of detecting 100 nmol/L levels, although this same assay detected BCA sensitive H_2S production in kidney homogenates. Thus exposure to high concentrations of exogenous H_2S likely elicits pharmacological rather than physiological effects of this molecule.

Although H_2S vasodilation can be mediated by activation of K_{ATP} channels (30), the K_{ATP} channel blocker glibenclamide had little effect on NaHS-induced dilation. However, H_2S dilation was prevented by constricting arteries with depolarizing concentrations of KCl confirming that H_2S activates potassium channels to cause vasodilation. BK_{Ca} channels can also limit myogenic tone (13) and H_2S activates BK_{Ca} channels in rat pituitary tumor cells (28). The selective BK_{Ca} blockers IbTx and paxilline blocked NaHS-induced dilation in both groups across the lower portion of the curve suggesting H_2S dilates small mesenteric arteries by activating BK_{Ca} channels. Vascular BK_{Ca} channels contain a redox-sensitive Ca^{2+} domain in the cytoplasmic C-terminal providing a potential mechanism for H_2S sensitivity (35). However, there have been conflicting reports of H_2S effects on BK_{Ca} channels. In pituitary tumor cells, H_2S activates BK_{Ca} channels but in carotid body glomus cells H_2S decreased BK_{Ca} mediated current (14). A recent study in vascular endothelial cells also demonstrated that BK_{Ca}

channels are activated by H_2S (36). Thus BK_{Ca} channel dependent vasodilation in small mesenteric arteries may be mediated by similar effects on the endothelium or perhaps there are regional differences in channel expression between vascular beds. Endothelial BK_{Ca}-mediated hyperpolarization could enhance production of vasoactive agents such as NO, and thus we would expect this production to be reduced in IH arteries. This loss could explain the apparent Ca^{2+} sensitization seen in the IH artery myogenic curves, due to the effect of NO to reduce Ca^{2+} sensitization (17). The depolarized state of IH arteries could also activate Rho kinase-Ca^{2+} sensitization as seen in pulmonary arteries (4).

Another reported vascular target of H_2S is the voltage dependent potassium channel, KCNQ (8; 25). Several studies suggest H_2S produced in adventitial adipocytes activates this channel to cause vasodilation. Our immunofluorescence studies revealed high expression of CSE in the adventitial layer. However, myogenic tone was augmented by endothelium disruption and cysteine-induced dilation was almost eliminated by disrupting the endothelium, suggesting adventitial CSE does not play a major role in vasodilation of small mesenteric arteries.

In addition to blocking NaHS dilation, IbTx enhanced myogenic tone and VSM $[Ca^{2+}]$ more in Sham than IH arteries, consistent with lower BK_{Ca} channel activity in IH arteries as the cause of greater pressure-induced Ca^{2+} influx and constriction. Furthermore, resting E_m was depolarized in small mesenteric arteries from IH rats compared to Sham arteries at both 60 and 140 mmHg and inhibiting CSE caused depolarization only in Sham arteries. Thus endogenous H_2S appears to contribute to resting E_m and loss of H_2S leads to depolarization in IH arteries. In parallel to the dilation studies, NaHS caused a BK_{Ca}-dependent hyperpolarization in PE treated Sham

and IH arteries, returning E_m to nearly the pre-PE potentials. Because the BK_{Ca} activator, NS1619, dilated both Sham and IH arteries similarly, reduced H_2S activation of BK_{Ca} channels is apparently not due to a lower ability of the channels to be activated.

Recent studies have demonstrated that in some arteries, ECs also express BK_{Ca} channels and these can contribute to VSMC hyperpolarization, at least in disease states such as hypoxia (11). The data presented here do not establish the cellular location of H_2S activated BK_{Ca} channels and the recent observation that H_2S activates BK_{Ca} channels in endothelial cells (36) suggests the endothelium may be the target for the IbTx-sensitive vasodilation by H_2S reported here, suggesting future studies on the site of action of H_2S. An additional potential mechanism for H_2S-induced dilation is inhibition of phosphodiesterases to elevate vascular levels of cGMP and cAMP (5). However, the phosphodiesterase inhibitor IBMX did not affect NaHS-induced dilation, suggesting inhibition of phosphodiesterase does not contribute to H_2S dilation in this vascular bed.

H_2S can combine with O_2^- and NO so that greater synthesis of either could inactivate H_2S after IH exposure (18; 33). Scavenging O_2^- with tiron or inhibiting NO with L-NNA slightly inhibited myogenic tone in IH but not Sham arteries. However, myogenic tone was still elevated in IH compared to Sham arteries. Thus increased scavenging of H_2S by endogenous reactive species may account for a small portion of the loss of H_2S inhibition of myogenic tone in IH arteries.

In light of the emerging role of H_2S as an oxygen sensor is stabilized during acute hypoxia (19-21), it is remarkable that vascular H_2S production is apparently decreased by IH. Therefore chronic IH may have a very different effect on H_2S than a single acute exposure to hypoxia. Thus one hypoxic episode may elevate H_2S but days or weeks of IH

exposure appear to downregulate CSE expression, at least in the endothelium, suggesting additional research is needed to evaluate hypoxia regulation of CSE.

In conclusion, our results suggest that in small mesenteric arteries, H_2S production by endothelial CSE maintains low myogenic tone through E_m hyperpolarization. Two weeks of IH treatment reduces H_2S modulation of both VSM E_m and myogenic tone through decreased endothelial CSE expression and through a modest increase in scavenging by reactive oxygen and nitrogen species. H_2S dilates small endothelium-intact mesenteric arteries through activation of BK_{Ca} channels, a novel mechanism of vasorelaxation for this gaseous messenger. These studies implicate a unique mechanism of endothelial dysfunction in IH, and suggest that therapies targeting the H_2S signaling could be useful in combating vascular dysfunction and hypertension in sleep apnea patients.

Acknowledgements

We would like to thank Carolyn E. Lucero for technical assistance with the intermittent hypoxia exposures.

Sources of Funding

OJW (HL7736); LGB (SDG 0535347N, American Heart Association); BRW (HL95640); NLK (EPA STAR award PHS 83186, HL82799 and is an established investigator of the American Heart Association)

Conflicts of Interests/Disclosures

None

Novelty and Significance

What is Known?

- Intermittent hypoxia (IH) is a model for sleep apnea-induced hypertension, and is associated with vascular dysfunction and elevated blood pressure in rats.
- Myogenic tone is a pressure-induced constriction of blood vessels that can be an important regulator of arterial resistance.
- Hydrogen sulfide (H_2S) is a recently described endothelium-derived vasodilator that is responsive to hypoxia.

What new information does this article contribute?

- H_2S causes vasodilation in small mesenteric arteries through the activation of large-conductance Ca^{2+}-activated K^+ channels (BK_{Ca}).
- H_2S dilation normally inhibits myogenic tone in small mesenteric arteries but loss of H_2S production after IH exposure leads to increased myogenic tone.
- IH vascular smooth muscle cells (VSMC) are depolarized relative to control cells due to this loss of H_2S.

We have reported that IH causes enhanced vascular contractility to endothelin-1, but its effect on myogenic tone was unclear. We found that myogenic tone in small mesenteric arteries was enhanced by IH, and that this effect was through loss of an endothelium-dependent effect. Furthermore, we found that H_2S reduces myogenic tone in control arteries but that this function was lost in IH arteries. This effect of H_2S to regulate myogenic tone is a novel finding and adds to the growing list of physiological functions of this molecule. Endothelial expression of cystathionine γ-lyase, an H_2S generating enzyme, was reduced in IH arteries, suggesting a mechanism for this loss of H_2S. We also established that H_2S causes vasodilation in these arteries through hyperpolarization of VSMC, and that the BK_{Ca} channel mediates this effect. BK_{Ca} channels are important regulators of vascular function, and showing that H_2S activates these channels impacts the emerging field of H_2S hypertension biology. These results establish a novel mechanism of sleep apnea-induced hypertension, but may have implications in a broad range of cardiovascular diseases that are shown to be affected by H_2S.

Reference List

1. **Allahdadi KJ, Duling LC, Walker BR and Kanagy NL**. Eucapnic intermittent hypoxia augments endothelin-1 vasoconstriction in rats: role of PKCdelta. *Am J Physiol Heart Circ Physiol* 294: H920-H927, 2008.

2. **Bierer DW**. Bismuth subsalicylate: history, chemistry, and safety. *Rev Infect Dis* 12 Suppl 1: S3-S8, 1990.

3. **Brancaleone V, Roviezzo F, Vellecco V, De Gruttola L, Bucci M and Cirino G**. Biosynthesis of H2S is impaired in non-obese diabetic (NOD) mice. *Br J Pharmacol* 155: 673-680, 2008.

4. **Broughton BR, Jernigan NL, Norton CE, Walker BR and Resta TC**. Chronic hypoxia augments depolarization-induced Ca2+ sensitization in pulmonary vascular smooth muscle through superoxide-dependent stimulation of RhoA. *Am J Physiol Lung Cell Mol Physiol* 298: L232-L242, 2010.

5. **Bucci M, Papapetropoulos A, Vellecco V, Zhou Z, Pyriochou A, Roussos C, Roviezzo F, Brancaleone V and Cirino G**. Hydrogen sulfide is an endogenous inhibitor of phosphodiesterase activity. *Arterioscler Thromb Vasc Biol* 30: 1998-2004, 2010.

6. **Carlson JT, Rangemark C and Hedner JA**. Attenuated endothelium-dependent vascular relaxation in patients with sleep apnoea. *J Hypertens* 14: 577-584, 1996.

7. **Davis MJ and Hill MA**. Signaling mechanisms underlying the vascular myogenic response. *Physiol Rev* 79: 387-423, 1999.

8. **Fang L, Zhao J, Chen Y, Ma T, Xu G, Tang C, Liu X and Geng B**. Hydrogen sulfide derived from periadventitial adipose tissue is a vasodilator. *J Hypertens* 27: 2174-2185, 2009.

9. **Folkow B**. "Structural factor" in primary and secondary hypertension. *Hypertension* 16: 89-101, 1990.

10. **Furne J, Saeed A and Levitt MD**. Whole tissue hydrogen sulfide concentrations are orders of magnitude lower than presently accepted values. *Am J Physiol Regul Integr Comp Physiol* 295: R1479-R1485, 2008.

11. **Hughes JM, Riddle MA, Paffett ML, Gonzalez Bosc LV and Walker BR**. Novel role of endothelial BKCa channels in altered vasoreactivity following hypoxia. *Am J Physiol Heart Circ Physiol* 299: H1439-H1450, 2010.

12. **Jarajapu YP, Grant MB and Knot HJ**. Myogenic tone and reactivity of the rat ophthalmic artery. *Invest Ophthalmol Vis Sci* 45: 253-259, 2004.

13. **Knot HJ, Standen NB and Nelson MT**. Ryanodine receptors regulate arterial diameter and wall [Ca2+] in cerebral arteries of rat via Ca2+-dependent K+ channels. *J Physiol* 508 (Pt 1): 211-221, 1998.

14. **Li Q, Sun B, Wang X, Jin Z, Zhou Y, Dong L, Jiang LH and Rong W**. A crucial role for hydrogen sulfide in oxygen sensing via modulating large conductance calcium-activated potassium channels. *Antioxid Redox Signal* 12: 1179-1189, 2010.

15. **Livak KJ and Schmittgen TD**. Analysis of relative gene expression data using real-time quantitative PCR and the 2(-Delta Delta C(T)) Method. *Methods* 25: 402-408, 2001.

16. **Metting PJ, Stein PM, Stoos BA, Kostrzewski KA and Britton SL**. Systemic vascular autoregulation amplifies pressor responses to vasoconstrictor agents. *Am J Physiol* 256: R98-105, 1989.

17. **Mills TM, Chitaley K, Lewis RW and Webb RC**. Nitric oxide inhibits RhoA/Rho-kinase signaling to cause penile erection. *Eur J Pharmacol* 439: 173-174, 2002.

18. **Mitsuhashi H, Yamashita S, Ikeuchi H, Kuroiwa T, Kaneko Y, Hiromura K, Ueki K and Nojima Y**. Oxidative stress-dependent conversion of hydrogen sulfide to sulfite by activated neutrophils. *Shock* 24: 529-534, 2005.

19. **Olson KR, Healy MJ, Qin Z, Skovgaard N, Vulesevic B, Duff DW, Whitfield NL, Yang G, Wang R and Perry SF**. Hydrogen sulfide as an oxygen sensor in trout gill chemoreceptors. *Am J Physiol Regul Integr Comp Physiol* 295: R669-R680, 2008.

20. **Olson KR and Whitfield NL**. Hydrogen sulfide and oxygen sensing in the cardiovascular system. *Antioxid Redox Signal* 12: 1219-1234, 2010.

21. **Olson KR, Whitfield NL, Bearden SE, St Leger J, Nilson E, Gao Y and Madden JA**. Hypoxic pulmonary vasodilation: a paradigm shift with a hydrogen sulfide mechanism. *Am J Physiol Regul Integr Comp Physiol* 298: R51-R60, 2010.

22. **Phillips SA, Olson EB, Lombard JH and Morgan BJ**. Chronic intermittent hypoxia alters NE reactivity and mechanics of skeletal muscle resistance arteries. *J Appl Physiol* 100: 1117-1123, 2006.

23. **Phillips SA, Olson EB, Morgan BJ and Lombard JH**. Chronic intermittent hypoxia impairs endothelium-dependent dilation in rat cerebral and skeletal muscle resistance arteries. *Am J Physiol Heart Circ Physiol* 286: H388-H393, 2004.

24. **Rapacon-Baker M, Zhang F, Pucci ML, Guan H and Nasjletti A**. Expression of myogenic constrictor tone in the aorta of hypertensive rats. *Am J Physiol Regul Integr Comp Physiol* 280: R968-R975, 2001.

25. **Schleifenbaum J, Kohn C, Voblova N, Dubrovska G, Zavarirskaya O, Gloe T, Crean CS, Luft FC, Huang Y, Schubert R and Gollasch M**. Systemic peripheral artery relaxation by KCNQ channel openers and hydrogen sulfide. *J Hypertens* 28: 1875-1882, 2010.

26. **Shahar E, Whitney CW, Redline S, Lee ET, Newman AB, Javier NF, O'Connor GT, Boland LL, Schwartz JE and Samet JM**. Sleep-disordered breathing and cardiovascular disease: cross-sectional results of the Sleep Heart Health Study. *Am J Respir Crit Care Med* 163: 19-25, 2001.

27. **Sile S, Vanoye CG and George AL, Jr.** Molecular physiology of renal ClC chloride channels/transporters. *Curr Opin Nephrol Hypertens* 15: 511-516, 2006.

28. **Sitdikova GF, Weiger TM and Hermann A**. Hydrogen sulfide increases calcium-activated potassium (BK) channel activity of rat pituitary tumor cells. *Pflugers Arch* 459: 389-397, 2010.

29. **Stipanuk MH and Beck PW**. Characterization of the enzymic capacity for cysteine desulphhydration in liver and kidney of the rat. *Biochem J* 206: 267-277, 1982.

30. **Tang G, Wu L, Liang W and Wang R**. Direct stimulation of K(ATP) channels by exogenous and endogenous hydrogen sulfide in vascular smooth muscle cells. *Mol Pharmacol* 68: 1757-1764, 2005.

31. **Troncoso Brindeiro CM, da Silva AQ, Allahdadi KJ, Youngblood V and Kanagy NL**. Reactive oxygen species contribute to sleep apnea-induced hypertension in rats. *Am J Physiol Heart Circ Physiol* 293: H2971-H2976, 2007.

32. **Wang R**. Hydrogen sulfide: the third Gasotransmitter in biology and medicine. *Antioxid Redox Signal* 2009.

33. **Whiteman M, Li L, Kostetski I, Chu SH, Siau JL, Bhatia M and Moore PK**. Evidence for the formation of a novel nitrosothiol from the gaseous mediators nitric oxide and hydrogen sulphide. *Biochem Biophys Res Commun* 343: 303-310, 2006.

34. **Yang G, Wu L, Jiang B, Yang W, Qi J, Cao K, Meng Q, Mustafa AK, Mu W, Zhang S, Snyder SH and Wang R**. H2S as a physiologic vasorelaxant: hypertension in mice with deletion of cystathionine gamma-lyase. *Science* 322: 587-590, 2008.

35. **Yi L, Morgan JT and Ragsdale SW**. Identification of a thiol/disulfide redox switch in the human BK channel that controls its affinity for heme and CO. *J Biol Chem* 285: 20117-20127, 2010.

36. **Zuidema MY, Yang Y, Wang M, Kalogeris T, Liu Y, Meininger CJ, Hill MA, Davis MJ and Korthuis RJ**. Antecedent hydrogen sulfide elicits an anti-inflammatory phenotype in postischemic murine small intestine: role of BK channels. *Am J Physiol Heart Circ Physiol* 299: H1554-H1567, 2010.

CHAPTER 3

Hydrogen sulfide causes vasodilation through activation of calcium sparks in small mesenteric arteries.

Olan Jackson-Weaver, BS, Melissa A. Riddle, PhD, Laura V. Gonzalez Bosc, PhD, Benjimen R. Walker, PhD, and Nancy L. Kanagy, PhD.

Vascular Physiology Group, Department of Cell Biology and Physiology, School of Medicine, University of New Mexico, Albuquerque, NM

Running head: Hydrogen sulfide, Ca^{2+} sparks

Address for correspondence: Nancy L. Kanagy, PhD, Professor

Department of Cell Biology and Physiology

MSC 08-4750

University of New Mexico

Albuquerque, NM 87131

Phone: 505-272-8814

FAX: 505-272-6649

Email: nkanagy@salud.unm.edu

Word count: 5,484

Subject codes: 95 (Endothelium/vascular type/nitric oxide), 97 (other vascular biology).

This manuscript has been submitted to circulation research.

Abstract

Rationale: We have previously shown that hydrogen sulfide (H_2S) reduces myogenic tone and causes relaxation of phenylephrine (PE) constricted mesenteric arteries. This effect of H_2S to cause vasodilation and vascular smooth muscle cell (VSMC) hyperpolarization was mediated by Ca^{2+}-activated potassium channels (BK_{Ca}). Ca^{2+} sparks are ryanodine receptor (RyR)-mediated Ca^{2+}-release events that activate BK_{Ca} channels in VSMCs to cause membrane hyperpolarization and vasodilation.

Objective: We hypothesized that H_2S activates Ca^{2+} sparks in small mesenteric arteries.

Methods and results: Ca^{2+} sparks were measured using confocal microscopy in rat mesenteric arteries loaded with the Ca^{2+} indicator Fluo-4. VSMC membrane potential (E_m) was measured in isolated arteries using sharp microelectrodes. In PE preconstricted arteries, the H_2S donor NaHS caused vasodilation that was inhibited by ryanodine (RyR blocker), bath iberiotoxin (IbTx, BK_{Ca} blocker), endothelial (EC) disruption, sulfaphenazole (cytochrome P450 2C blocker), and luminal IbTx. The H_2S donor NaHS (10 μmol/l) increased Ca^{2+} spark frequency in Fluo-4 loaded arteries imaged by confocal microscopy, which was blocked by EC disruption, sulfaphenazole, and luminal IbTx. NaHS hyperpolarized VSMC E_m in PE depolarized mesenteric arteries, and this effect was blocked by ryanodine, sulfaphenazole, bath IbTx, and luminal IbTx. Blockade of endogenous cystathionine γ-lyase-derived H_2S with β-cyano-L-alanine (BCA) reduced IbTx-sensitive K^+ currents in freshly dispersed mesenteric ECs. BCA also reduced VSMC Ca^{2+} spark frequency in mesenteric arteries, as did EC disruption.

Conclusions: These results suggest that H_2S activates Ca^{2+} sparks in mesenteric arteries through activation of endothelial BK_{Ca} channels and cytochrome P450 2C, a novel vasodilatory pathway for this emerging signaling molecule.

Key words: endothelium, BK_{Ca} channel, cytochrome P450 epoxygenase, sodium hydrosulfide.

Non-standard Abbreviations and Acronyms:

3MST	3-mercaptopyruvate sulfurtransferase
BCA	β cyano-L-alanine
BK_{Ca}	Large-conductance Ca^{2+}-activated K^+ channel
CSE	cystathionine γ-lyase
EC	endothelial cell
ECS	extracellular solution
EDHF	endothelium-derived hyperpolarizing factor
E_m	membrane potential
IbTx	Iberiotoxin
ICS	intracellular solution
PE	phenylephrine
PKA	cAMP-dependent protein kinase
PKG	cGMP-dependent protein kinase
PSS	physiological saline solution
RyR	ryanodine receptor
SR	sarcoplasmic reticulum
STOC	spontaneous transient outward current

TRPV4	transient receptor potential vanilloid type 4
VGCC	voltage-gated Ca^{2+} channels
VSMC	vascular smooth muscle cell

Introduction

Ca^{2+} sparks are spatially and temporally limited Ca^{2+} release events from ryanodine receptor Ca^{2+}-release channels (RyR) in the sarcoplasmic reticulum (SR) of cardiac and smooth muscle cells. Ca^{2+} sparks in vascular smooth muscle cells (VSMC) have been shown to activate large-conductance Ca^{2+}-activated K^+ channels (BK_{Ca}) and to cause hyperpolarization leading to a reduced open probability of L-type voltage-gated Ca^{2+} channels (VGCC) and a decrease in cytosolic [Ca^{2+}] (22). Ca^{2+} spark frequency is increased by stretch of VSMCs, and has been hypothesized to act as an intrinsic negative feedback mechanism to regulate stretch-induced VSMC depolarization and myogenic tone (13). In addition, several studies have demonstrated that endothelial cell (EC)-produced signaling compounds increase VSMC Ca^{2+} spark activity (6; 11; 21), indicating a role of endothelium-produced vasodilator molecules in the regulation of VSMC RyR. RyR activity can also be modulated by several mechanisms such as phosphorylation, cytosolic and SR [Ca^{2+}], binding of associated proteins, and redox modification of amino acid residues (16).

Hydrogen sulfide (H_2S) is a newly established vasodilator molecule produced in the vasculature by the enzymes cystathionine γ-lyase (CSE) and 3-mercaptopyruvate sulfurtransferase (3MST). H_2S causes vasodilation through a variety of mechanisms (3; 5; 27; 38) and genetic knockout of the CSE gene causes hypertension (36). H_2S is a

reducing agent and its physiological effects are thought to be mediated by reduction of redox sensitive amino acids in proteins or binding to heme-containing metalloproteins (14). We have previously reported that inhibition of CSE or endothelial disruption enhances myogenic tone in small mesenteric arteries from control rats, and that H_2S causes VSMC E_m hyperpolarization and vasodilation in these arteries through activation of BK_{Ca} channels (10). Due to the well described regulation of VSMC BK_{Ca} channels by Ca^{2+} sparks, we hypothesized that H_2S activates Ca^{2+} sparks in small mesenteric arteries to mediate VSMC hyperpolarization and vasodilation.

Methods

Animals.

Male Sprague Dawley rats (275 to 325 g) were used for all studies. Animals were housed in Plexiglas cages with free access to food and water. A continuous flow of room air was present in the cages at all times. On the day of the experiments, animals were anesthetized with sodium pentobarbital (200 mg/kg ip) and mesenteric arteries isolated for constrictor, Ca^{2+} imaging, and E_m studies. All animal protocols were reviewed and approved by the Institutional Animal Care and Use Committee of the University of New Mexico School of Medicine and conform to National Institutes of Health guidelines for animal use.

Isolated Vessel Preparation.

The intestinal arcade was removed and placed in a Silastic-coated Petri dish containing chilled physiological saline solution (PSS; [in mmol/L] 129.8 NaCl, 5.4 KCl, 0.83 $MgSO_4$, 0.43 NaH_2PO_4, 19 $NaHCO_3$, 1.8 $CaCl_2$, and 5.5 glucose). Fourth or fifth-

order artery segments (inner diameter <100 μm) were dissected from the mesenteric vascular arcade and transferred to a vessel chamber (Living Systems). Segments (1 -2 mm in length) were cannulated onto glass micropipettes and secured with silk ligatures. The arteries were pressurized to 60 mmHg with PSS using a servo-controlled peristaltic pump (Living Systems) and superfused with warmed, oxygenated PSS at a rate of 5 mL per minute.

Vasodilation studies.

Arterial inner diameter was recorded in cannulated arteries using edge-detection software (IonOptix). Arteries were equilibrated at 37°C in warmed, oxygenated PSS for 30 minutes at 60 mmHg luminal pressure prior to the start of the experiment. Following a slow increase in pressure to 100 mmHg, arteries were preconstricted to 50% resting diameter using phenylephrine (PE) and vasodilation measured during cumulative addition of the H_2S donor NaHS. Arteries were incubated with Ca^{2+}-free PSS ([in mmol/L] 129.8 NaCl, 5.4 KCl, 0.83 $MgSO_4$, 0.43 NaH_2PO_4, 19 $NaHCO_3$, 3.7 tetrasodium EGTA, and 5.5 glucose) to determine maximal, passive diameter at the end of the experiment.

Fluo-4 Imaging.

Arteries used for fluo-4 studies were incubated in a fluo-4 AM (10 μmol/L, Invitrogen) solution containing 0.25% pluronic acid in HEPES buffer ([in mmol/L] 134 NaCl, 6 KCl, 1 $MgCl_2$, 2 $CaCl_2$, 10 HEPES, 0.026 EDTA, and 10 glucose) for 60 min at 28°C prior to cannulation. After loading with fluo-4, arteries were transferred to a vessel chamber and cannulated as described above. After 10 minutes equilibration in oxygenated PSS at 32°C, luminal pressure in was increased to 100 mmHg in most experiments, some remained at 60 mmHg, and subsequently were excited at 488 nm by a

solid state laser and emitted light > 500 nm was collected using an Olympus IX71 microscope with a 60X water-immersion lens and a spinning-disk confocal scanning unit (Andor). A 75 X 50 μm area was imaged at 50-60 Hz using laser power of 30%.

Spark Analysis.

Spark movies were analyzed using SparkAn software, developed by A. D. Bonev and M. T. Nelson (University of Vermont). Ten images without spark activity were averaged to determine background fluorescence levels (F_0). Regions of interest (ROI) of 25 pixels^2 (3 μm^2) were used to detect sparks with a minimum F/F_0 of 1.2. Each image contained 15-25 cells, and spark frequency was averaged for all cells visible.

Membrane Potential Recordings.

Small mesenteric arteries were dissected and cannulated as described above. After equilibration at 60 mmHg, luminal pressure was increased to 100 mmHg for most experiments, some remained at 60 mmHg, and vascular smooth muscle cells were impaled through the adventitia with glass intracellular microelectrodes filled with 1 mol/L KCl (tip resistance 40–120 MΩ). A Neuroprobe amplifier (A-M Systems) was used for recording membrane potential (E_m). Analog output from the amplifier was low pass filtered at 1kHz and recorded and analyzed using Axoscope software (Axon Instruments). Criteria for acceptance of E_m recordings were: 1) an abrupt negative deflection of potential as the microelectrode was advanced into a cell; 2) stable membrane potential for at least 1 min; and 3) an abrupt change in potential to ~0 mV after the electrode was retracted from the cell.

Whole-Cell Patch Clamp Studies on Isolated Endothelial Cells

Mesenteric arteries were cut into 2-mm segments and exposed to mild digestion solution containing 0.2 mg/ml dithiothreitol and 0.2 mg/ml papain in HBSS for 45 min at 37°C. Arteries were removed from the digestion solution and placed in 1 ml of HBSS containing 2 mg/ml BSA. Single ECs were released by gentle trituration with a small-bore Pasteur pipette and were stored at 4°C between experiments for up to 5 h. One to two drops of the resulting cell suspension were applied to a glass cover slip mounted on an inverted fluorescence microscope (Olympus IX71) for 30 min to allow cell adhesion prior to superfusion. Single endothelial cells were identified by the selective uptake of the fluorescently labeled acylated low density lipoprotein Ac-LDL-Dil with a rhodamine filter (29) prior to each electrophysiological experiment. Freshly dispersed endothelial cells were superfused under constant flow (2 ml/min) at room temperature (22-23°C) in an extracellular solution (ECS [in mmol/L]: 141 NaCl, 4.0 KCl, 1 $MgCl_2$, 1$CaCl_2$, 10 HEPES, 10 glucose and buffered to pH 7.4 with NaOH). Whole cell current data were generated using an Axopatch 200B amplifier (Axon Instruments). Biophysical criteria: (Seal resistance > 1GΩ, series resistance <25MΩ) was checked following membrane rupture and monitored throughout the course of the experiment. Cells were held at -60mV and were dialyzed for 5 min with an intracellular solution (ICS [in mmol/L]: 140 KCl, 0.5 $MgCl_2$, 5 Mg_2ATP, 10 HEPES, 1 EGTA and adjusted to pH 7.2 with KOH). $CaCl_2$ was added to yield a free-Ca^{2+} concentration of 1 μmol/L, as calculated using WinMAXC chelator software.

Statistical Analysis.

Constriction, Ca^{2+} concentration, and spark parameters (frequency, amplitude, and duration) were analyzed using 1-way ANOVA with Student-Newman–Keuls post hoc analysis for differences between groups, concentrations, and interactions. $P<0.05$ was considered statistically significant for all analyses.

Results

Ca^{2+} spark effect on E_m in small mesenteric arteries.

In order to determine the role of Ca^{2+} spark activity to regulate VSMC E_m in small mesenteric arteries, Ca^{2+} spark frequency was increased in isolated arteries using 1 mmol/L caffeine (fig. 1*A*). Ca^{2+} sparks were verified to be RyR mediated by blockade with 10 μmol/L ryanodine (Fig. 1*A*). E_m was then measured in separate arteries at 60 mmHg luminal pressure before and after addition of 1 mmol/L caffeine using sharp electrode impalement. No effect on E_m by this level of Ca^{2+} spark activation was seen (Fig. 1*B*). However when luminal pressure was increased to 100 mmHg, 1 mmol/L caffeine evoked a significant E_m hyperpolarization (Fig. 1*C*). Subsequent experiments were performed at 100 mmHg luminal pressure.

H_2S vasodilation.

The H_2S donor NaHS produced a large vasodilation in phenylephrine preconstricted arteries at 100 mmHg luminal pressure and this effect was significantly reduced by blocking Ca^{2+} sparks with ryanodine (10 μmol/L; Fig. 2*B*). Consistent with Ca^{2+} sparks activating BK_{Ca} channels, iberiotoxin (IbTx, 100 nmol/L) applied in the bath

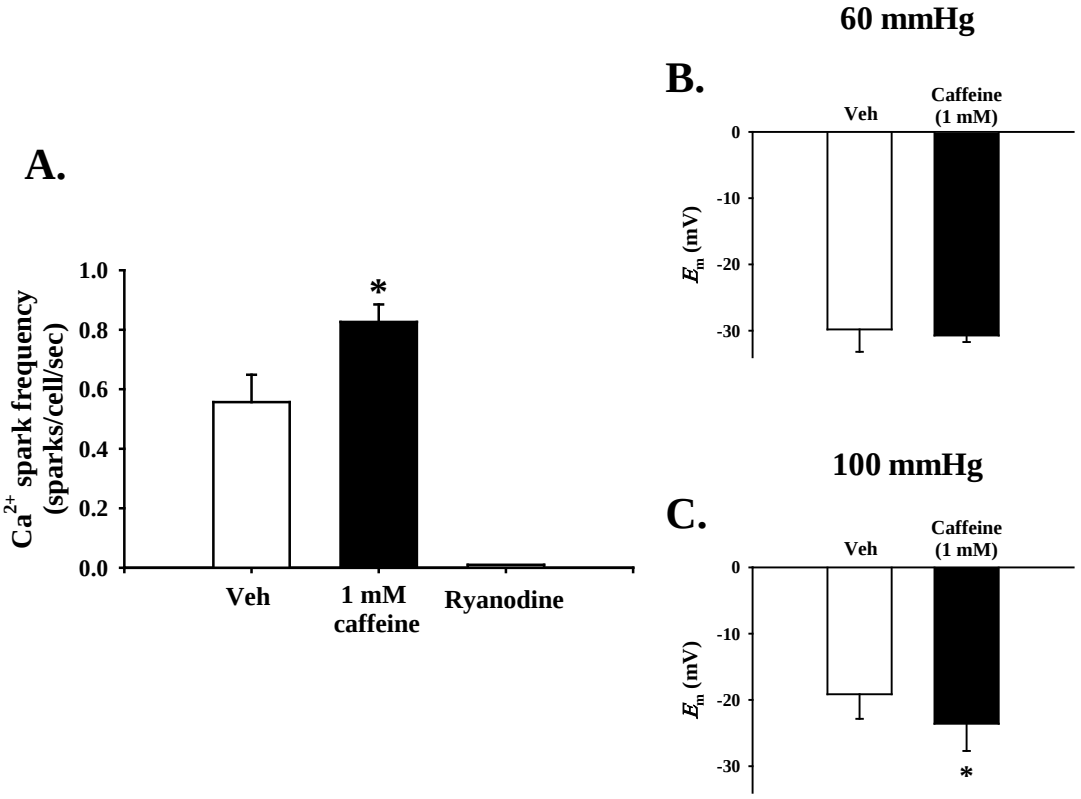

Figure 1. Effect of 1 mmol/L caffeine and 10 μmol/L ryanodine on Ca^{2+} spark frequency in cannulated small EC intact mesenteric arteries loaded with fluo-4 at 60 mmHg luminal pressure (A). Effect of 1 mmol/L caffeine on VSMC E_m in cannulated mesenteric arteries at 60 mmHg luminal pressure measured by sharp microelectrode impalement (B). Effect of 1 mmol/L caffeine on VSMC E_m in cannulated mesenteric arteries at 100 mmHg luminal pressure measured by sharp microelectrode impalement (C). n=5 per group. * $p<0.05$ vs. vehicle.

solution also reduced NaHS-induced vasodilation (Fig. 2*C*). Due to the recent evidence that H_2S can activate endothelial (EC) BK_{Ca} channels (39), we measured vasodilation in arteries with disrupted EC or with selective application of IbTx to the lumen (Fig. 3). Both treatments abolished dilation across the physiologically relevant range of $[H_2S]$. EC K^+ channel activation increases EC $[Ca^{2+}]$, which can activate several EC enzymes that produce vasodilators (28). One such EC derived vasodilator involved in activation of VSMC Ca^{2+} sparks is 11,12 EET which is produced by cytochrome P450 epoxygenase (6). Therefore NaHS vasodilation was measured in the presence of the cytochrome P450 2C inhibitor sulfaphenazole (10 μmol/L), which also reduced vasodilation (Fig. 4).

H_2S-induced Ca^{2+} spark activity.

Ca^{2+} spark activity in small mesenteric arteries was recorded at 100 mmHg luminal pressure. NaHS (10 μmol/L) significantly increased spark frequency (Fig. 5*B*), but this effect was blocked by EC disruption, sulfaphenazole, or luminal IbTx. NaHS actually reduced Ca^{2+} spark frequency in EC disrupted arteries. NaHS did not affect Ca^{2+} spark amplitude or duration (Fig. 5*C*), except in the presence of luminal IbTx, in this case reducing amplitude and extending duration. EC disruption on its own reduced spark amplitude but this effect was not increased in the presence of NaHS (Fig. 5*C*).

H_2S regulation of membrane potential and endothelial cell K^+ current.

Ca^{2+} sparks mediate their vasodilatory effect through activation of BK_{Ca} channels and subsequent E_m hyperpolarization of VSMC (22). We therefore assessed the effect of NaHS on VSMC E_m in small mesenteric arteries. Arteries were depolarized with 1 μmol/L PE and held at 100 mmHg luminal pressure during experiments. NaHS caused a hyperpolarization of mesenteric artery VSMC E_m measured by sharp electrode

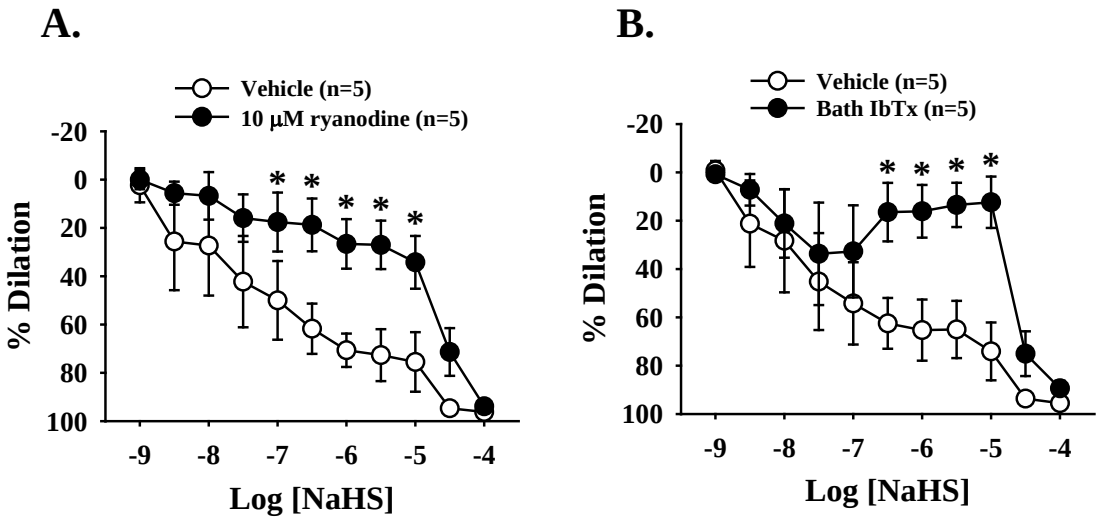

Figure 2. Small mesenteric artery dilation to increasing concentrations of H_2S donor NaHS in the presence of vehicle or 10 μmol/L ryanodine (A). NaHS dilation curves in EC intact small mesenteric arteries in the presence of vehicle or 100 nmol/L IbTx in the superfusate bath (B). Arteries pressurized to 100 mmHg and preconstricted to ~ 50 % with PE. n=5 per group. * $p<0.05$ vs. vehicle.

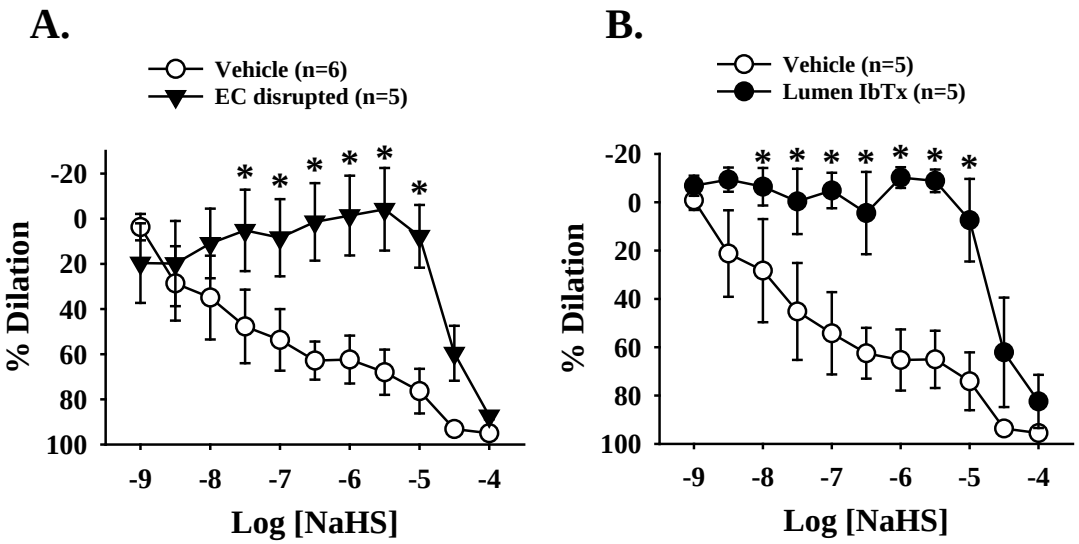

Figure 3. Small mesenteric artery dilation to increasing concentrations of H_2S donor NaHS with and without active EC (A) or lumen specific application of 100 nmol/L IbTx in EC intact arteries (B). Arteries pressurized to 100 mmHg and preconstricted to ~ 50 % with PE. n=5-6 per group. * $p<0.05$ vs. vehicle.

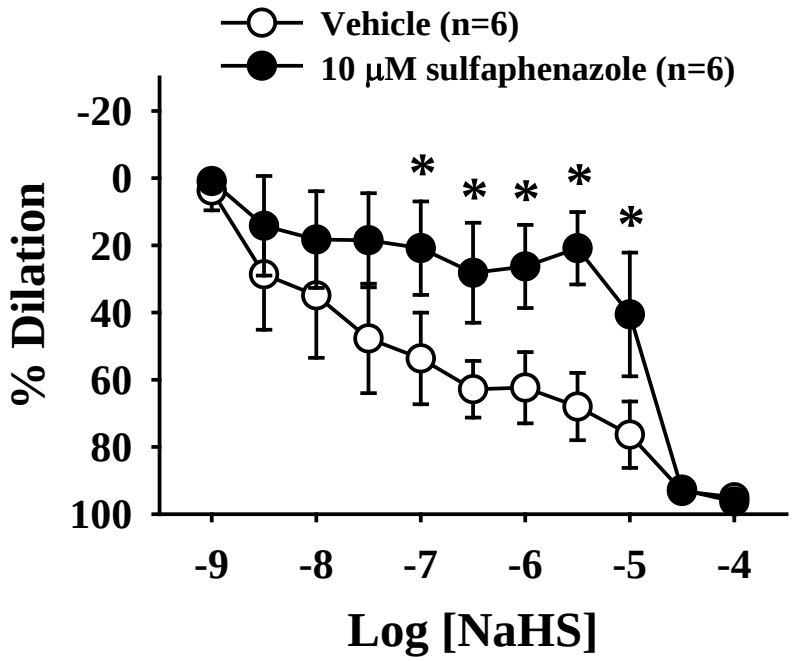

Figure 4. Small EC intact mesenteric artery dilation to increasing concentrations of H_2S donor NaHS in the presence of vehicle or 10 μmol/L sulfaphenazole. Arteries pressurized to 100 mmHg and preconstricted to ~ 50 % with PE. n=6 per group. * $p<0.05$ vs. vehicle.

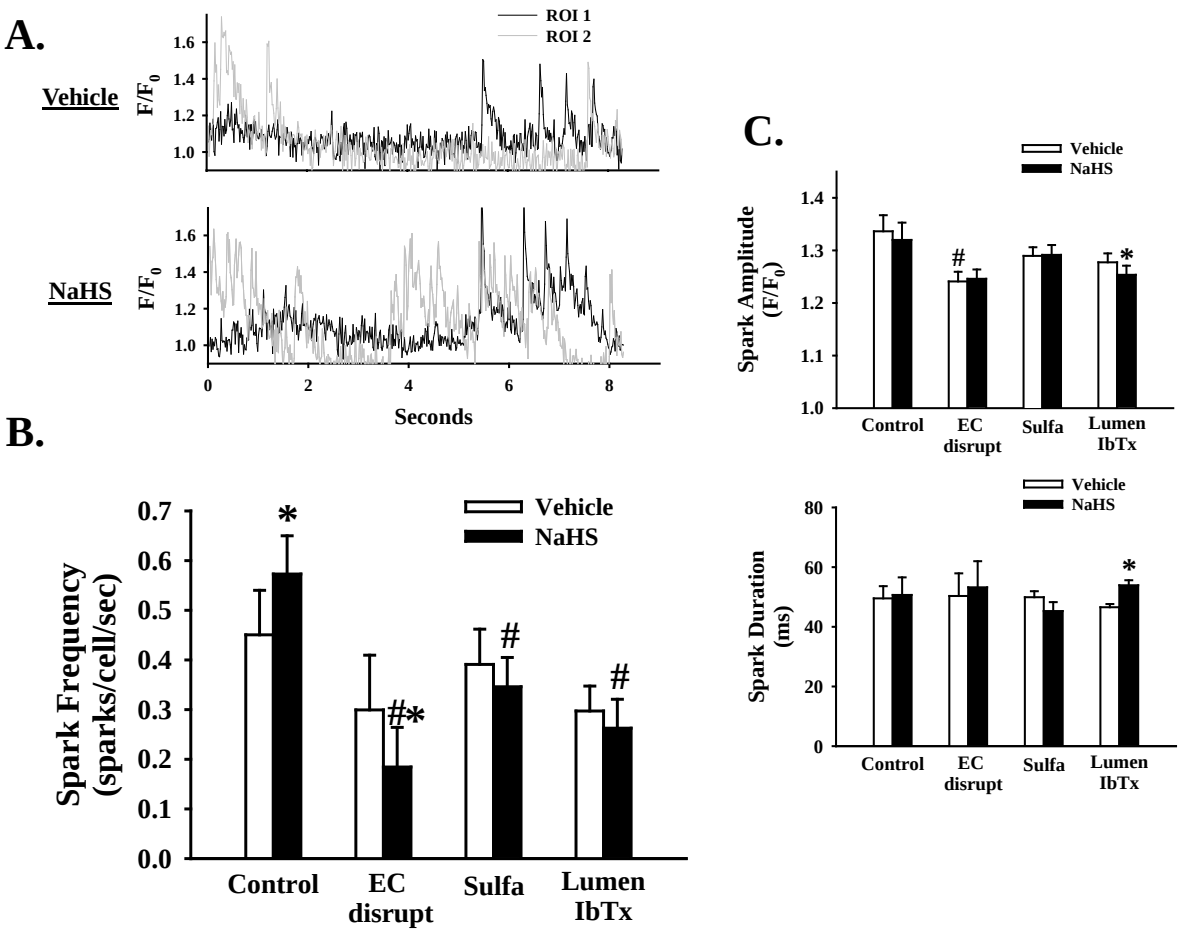

Figure 5. Example traces of Ca^{2+} spark activity in VSMC in mesenteric arteries loaded with fluo-4 and pressurized to 100 mmHg in the presence of vehicle or NaHS (A). Two example regions of interest (ROI) in the same artery shown for each condition. Summary data of Ca^{2+} spark frequency at 100 mmHg in the presence of vehicle or NaHS under EC intact control conditions, EC disruption, 10 μmol/L sulfaphenazole (EC intact), or 100 nmol/L luminal IbTx (EC intact) (B). Spark amplitude and duration at half-maximal amplitude under the same conditions as in B (C). n=5-7 per group. * $p<0.05$ vs. vehicle. #$p<0.05$ vs. control within treatment.

impalement (Fig. 6*B*). This E_m hyperpolarizing effect of NaHS was prevented with ryanodine, sulfaphenazole, bath applied IbTx, or lumen applied IbTx (Fig. 6*B*). The greater efficacy of luminal IbTx compared to bath IbTx suggested an effect of H_2S on EC BK_{Ca} channels, therefore K^+ currents were measured in EC to directly assess this possibility. Whole cell outward K^+ currents in freshly dispersed mesenteric EC were reduced by the cystathionine γ-lyase inhibitor β-cyano-L-alanine (BCA), without an additional effect of IbTx (Fig. 6*C*).

Endogenous H_2S regulation of Ca^{2+} sparks.

Endogenous H_2S produced by CSE importantly opposes myogenic tone in small mesenteric arteries (10). To determine whether endogenous H_2S activates Ca^{2+} sparks, BCA was applied to arteries held at 100 mmHg luminal pressure. BCA reduced Ca^{2+} spark frequency, as did EC disruption (Fig. 7*B*), and these effects were not additive.

Discussion

Our findings show that H_2S causes vasodilation through activation of Ca^{2+} sparks, and suggest this effect is through activation of endothelial BK_{Ca} channels and cytochrome P450 2C. H_2S is a relatively recently described vasodilatory signaling molecule, and new modes of action are being described at a rapid pace. We previously demonstrated that in small mesenteric arteries, dilation and VSMC E_m hyperpolarization by the H_2S donor NaHS requires BK_{Ca} channels (10). A major activator of VSMC BK_{Ca} channels is Ca^{2+} sparks, which are RyR mediated SR store-release events. Rather than increasing global intracellular $[Ca^{2+}]$, Ca^{2+} sparks increase $[Ca^{2+}]$ locally in the subsarcolemmal space to increase the open probability of BK_{Ca} channels (22). Therefore, the net effect of Ca^{2+}

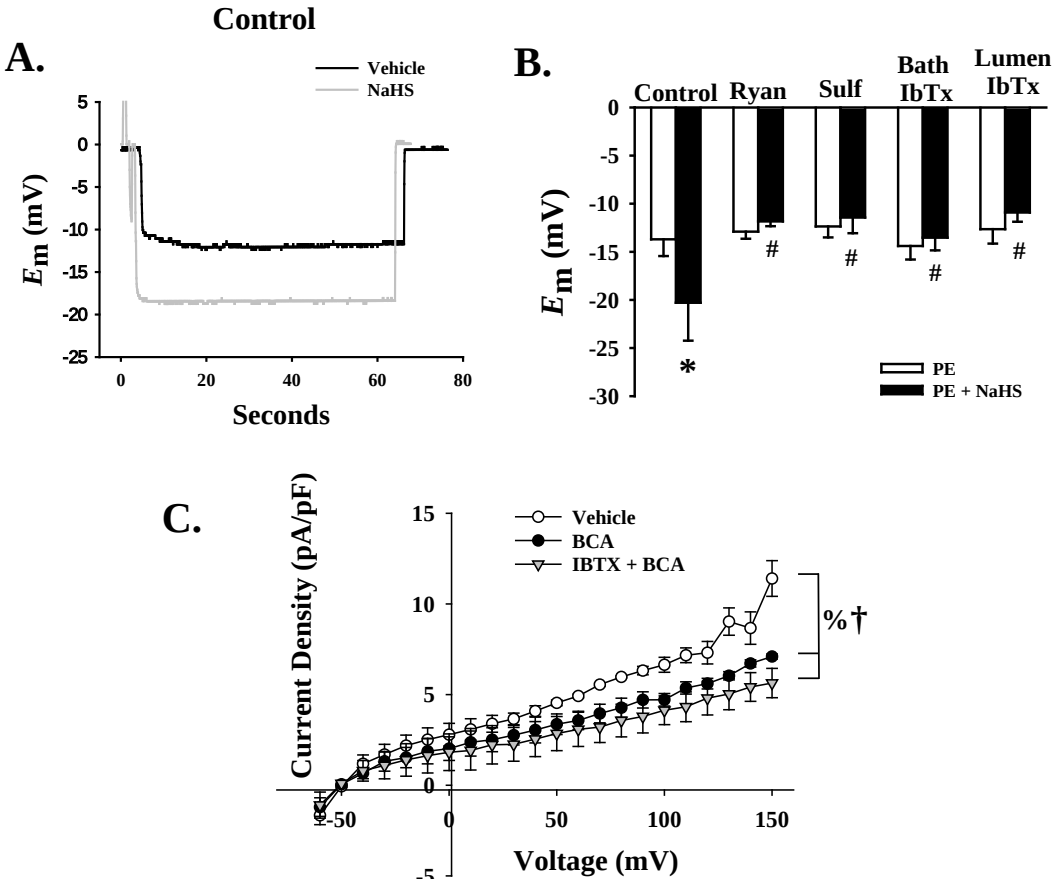

Figure 6. Example recordings of sharp microelectrode impalements of VSMC in arteries pressurized to 100 mmHg and depolarized with 1 μmol/L PE in the presence of vehicle or NaHS under control conditions (A). Negative deflection of trace indicates cell impalement; positive deflection to 0 mV indicates retraction of electrode. Summary data of E_m recordings in EC intact arteries in the presence of vehicle or NaHS under control conditions or in the presence of 10 μmol/L ryanodine, 10 μmol/L sulfaphenazole, 100 nmol/L IbTx in superfusate bath, or 100 nmol/L iberiotoxin (IbTx) in lumen (B). In freshly dispersed mesenteric EC β cyano-L-alanine (BCA) reduced IbTx sensitive K^+ currents in whole-cell patch clamp voltage step experiments (C). n=4-5 per group. * $p<0.05$ vs. PE. #$p<0.05$ vs. control within treatment. %$p<0.05$ BCA vs. vehicle. †$p<0.05$ BCA + IbTx vs. vehicle.

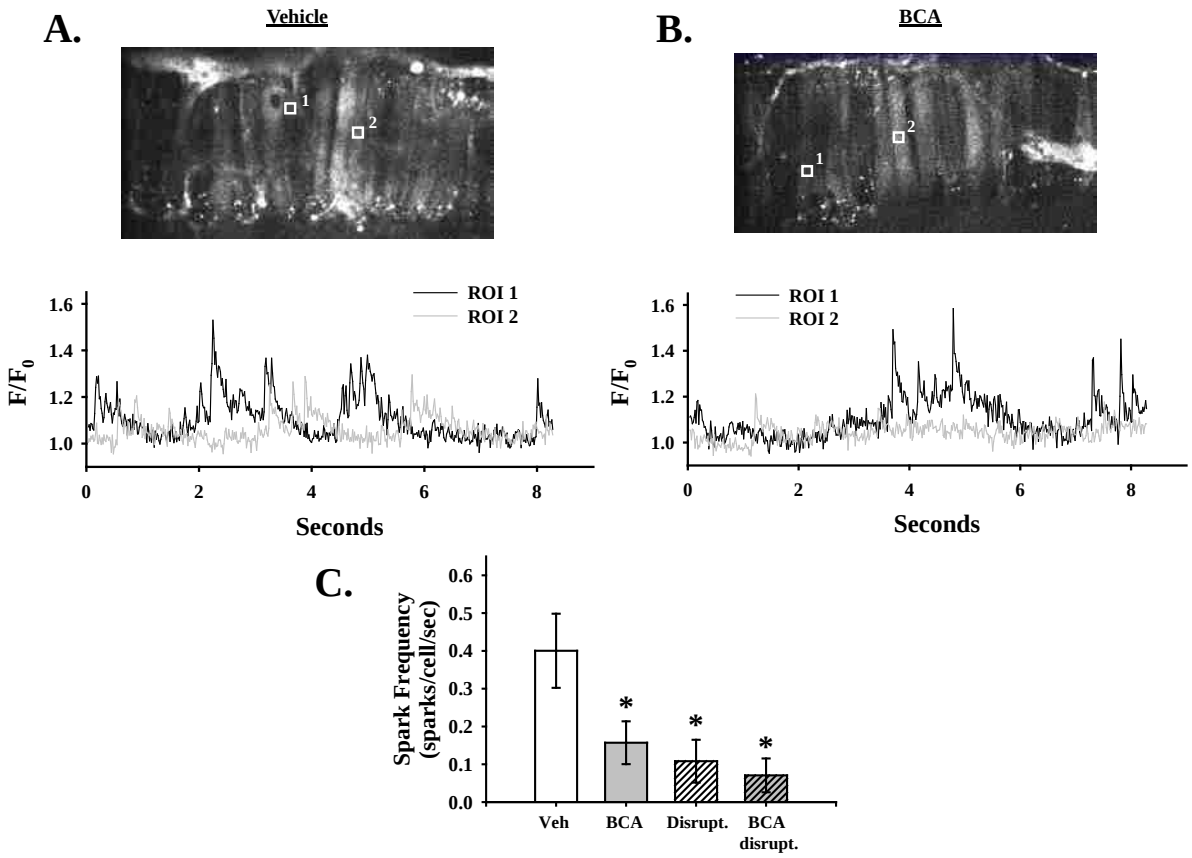

Figure 7. Example traces of Ca^{2+} spark activity in VSMC in mesenteric arteries loaded with fluo-4 and pressurized to 100 mmHg in the presence of vehicle (A) or β cyano-L-alanine (BCA; B). Two example regions of interest (ROI) shown from two separate arteries. Summary data showing Ca^{2+} spark frequency in arteries under EC intact vehicle conditions or with 100 μmol/L BCA (EC intact), disrupted EC, or both BCA and EC disruption (C). ROIs = 1.7 μm per side. n=5-6 per group. * $p<0.05$ vs. vehicle.

sparks is hyperpolarization of the plasma membrane E_m and reduced open probability of L-type voltage-gated Ca^{2+} channels, thus indirectly reducing global intracellular [Ca^{2+}] (12; 22). The distinctive outward K^+ current produced by a Ca^{2+} spark is termed a "spontaneous transient outward current" (STOC).

In small mesenteric arteries, we found that increasing Ca^{2+} spark frequency by ~ 50% with 1 mmol/L caffeine had no effect on VSMC E_m (Fig. 1 *A* and *B*) at 60 mmHg luminal pressure. If, however, we first elevated luminal pressure to 100 mmHg, 1mmol/L caffeine hyperpolarized VSMC E_m by ~ 4.5 mV. This suggests an enhanced coupling between sparks and BK_{Ca} channels at this higher pressure, although this is only speculative without simultaneous measurements of sparks and STOCs. It is unclear what mechanism may be responsible for this effect, although it is known that spark-STOC coupling can be modified by a variety of factors such as BK_{Ca} β subunit expression (37) and the presence of CO (11). This coupling of sparks to BK_{Ca} channels by pressure may be a result of pressure-induced VSMC E_m depolarization, since in isolated mesenteric VSMC, normal spark-STOC coupling was seen in cells held at 0 mV by voltage clamp (37). A potential mechanism for this effect is suggested by the fact that BK_{Ca} channels are activated by E_m depolarization as well as Ca^{2+}, and these effects interact such that a more depolarized E_m enhances Ca^{2+} sensitivity (1). Further investigation of this phenomenon is warranted. The Ca^{2+} sparks seen in these small mesenteric arteries were verified to be RyR mediated since they were abolished by 10 μmol/L ryanodine (Fig 1*A*).

In arteries held at 100 mmHg luminal pressure and preconstricted to ~50% of resting diameter with PE, NaHS induced a large dilation (~70%) at relatively low concentrations (1 μmol/L). This is a greater dilation than in our previous studies

conducted in arteries pressurized to 60 mmHg luminal pressure (10). This enhancement of H_2S-induced vasodilation with increasing luminal pressure is consistent with our previous characterization of H_2S as an endogenous inhibitor of myogenic tone (10). That is, since myogenic tone is stimulated by increasing luminal pressure, H_2S production may not be actively augmented by increases in luminal pressure, but the vasodilatory response is amplified at higher pressures. In agreement with this, our previous results showed no effect of endogenous H_2S to diminish myogenic tone at 60 mmHg, but a significant effect at 100 mmHg (10).

Because ryanodine largely blocked NaHS-induced vasodilation (Fig. 2*B*), Ca^{2+} sparks appear to mediate the dilation. Additionally, bath applied IbTx blocked dilation across much of the curve (Fig. 2*C*) consistent with our previous results at 60 mmHg luminal pressure (10). It is of note that the large dilation seen above 10 μmol/L NaHS is not greatly affected by these treatments. This is similar to our results seen previously at 60 mmHg luminal pressure (10). These may be supraphysiological effects, since endogenous tissue [H_2S] is thought to be in the nmol/L range (8).

The effect of H_2S on the activity of BK_{Ca} channels is a contentious issue. Although some studies suggest activation of the channel by H_2S (10; 20; 30; 39), others find H_2S inhibits BK_{Ca} activity (18; 31; 32). Because the cell types investigated in these two groups of studies do not overlap, it is possible that tissue specific expression of subunits or other associated proteins modify the effect of H_2S on BK_{Ca} channels. The demonstration that H_2S activates EC BK_{Ca} channels by Zuidema et. al. (39) led us to test whether EC BK_{Ca} channels were the target of H_2S to dilate small mesenteric arteries. Luminal application of IbTx specifically targets endothelial cell BK_{Ca} channels (9). We

found that luminal IbTx was even more effective at blocking NaHS-induced dilations than bath applied IbTx (Fig. 3*B*). Furthemore, EC disruption was similarly effective at blocking dilation (Fig. 3*A*) suggesting that endothelial BK_{Ca} channels are critically important in the vasodilatory response of small mesenteric arteries to H_2S.

K^+ channel activation has been demonstrated to increase EC [Ca^{2+}] (15; 28) with subsequent activation of Ca^{2+} sensitive second messenger pathways. In support of this, a recent study demonstrated that NaHS increases microvascular EC [Ca^{2+}] (24). This in turn should elevate the production of endothelial dilators, several of which have been shown to affect Ca^{2+} spark signaling. For example, NO increases spark frequency and EC denudation decreases basal spark activity in cerebral artery VSMC (21). The EC product CO has also been shown to modestly increase spark frequency and to enhance spark-STOC coupling in cerebral artery VSMCs (11). Finally, the EC-derived cytochrome P450 2C product 11,12 EET also increases spark frequency downstream of transient receptor potential vanilloid type 4 (TRPV4) cation channel activation in cerebral artery VSMCs (6). Because previous studies have implicated cytochrome P450 enzymes in NaHS mediated relaxation in whole perfused mesenteric beds (5). cytochrome P450 epoxygenase is a logical link between EC E_m and VSMC Ca^{2+} spark activity. The current studies demonstrate that inhibiting cytochrome P450 2C with sulfaphenazole blocks NaHS-induced dilation similarly to ryanodine (Fig. 4). Although EC BK_{Ca} channels in these experiments would seem to be causing activation of second messenger systems, mesenteric arteries do display myoendothelial gap junctions (26), and a directly conducted hyperpolarization may contribute to H_2S-induced vasodilation in this bed. The sensitivity of the dilation to ryanodine, however, suggests a large VSMC BK_{Ca} channel

contribution, since EC BK_{Ca} channels seem not to require RyR Ca^{2+} release (25), nor have sparks been reported in ECs.

In fluorescent imaging studies in this work, NaHS increased Ca^{2+} spark frequency by ~25% in EC intact but not in EC disrupted arteries. Furthermore, sulfaphenazole administration and luminal IbTx administration also abolished NaHS stimulation of spark frequency (Fig. 5*B*). Thus NaHS dilation in small mesenteric arteries is at least partly mediated through an enhancement of Ca^{2+} spark activity that requires cytochrome P450 2C and EC BK_{Ca} channels. In EC disrupted arteries, NaHS in fact reduced Ca^{2+} spark frequency, suggesting EC may also regulate sparks separate from effects of EC BK_{Ca} channels and cytochrome P450 2C. Because spark kinetics were minimally affected by the experimental perturbations, the Ca^{2+} conductance properties, clustering of the RyR channels, and duration of opening events appears to be largely unaffected by these manipulations (Fig. 5*C*).

VSMC Ca^{2+} sparks promote vasodilation through activation of BK_{Ca} channels resulting in plasma membrane E_m hyperpolarization. In studies directly measuring VSMC E_m in cannulated arteries using sharp electrode impalement, 1 μmol/L PE caused depolarization, approximating the conditions of the dilation study. In these arteries, 10 μmol/L NaHS hyperpolarized VSMC E_m by ~7 mV (Fig. 6*B*). Consistent with this effect being mediated by Ca^{2+} spark activation, ryanodine as well as bath applied IbTx abolished this effect (Fig. 6*B*). Furthermore, sulfaphenazole or lumen applied IbTx also prevented this effect, suggesting BK_{Ca} channels and cytochrome P450 2C in the EC are required to cause this VSMC hyperpolarization. In order to directly assess the possibility of H_2S activation of EC BK_{Ca} channels, whole-cell K^+ currents were measured in freshly

dispersed mesenteric EC. BCA reduced outward K^+ currents, without an additional effect of IbTx (Fig. 6*C*), suggesting that endogenous H_2S activates EC K^+ channels.

Spark frequency in arteries at 100 mmHg transmural pressure was reduced by BCA and EC disruption by about 60% (Fig 7*C*) while BCA had no additional effect in endothelium-disrupted arteries. Thus endogenous H_2S activation of Ca^{2+} sparks in small mesenteric arteries requires active EC. This is in agreement with our previous finding that inhibiting CSE with BCA as well as disrupting the endothelium enhanced myogenic tone at 100 mmHg (10).

Based on these studies, we propose that H_2S activates EC BK_{Ca} channels in small mesenteric arteries increasing EC $[Ca^{2+}]$, to activate cytochrome P450 2C production of 11,12-EET which causes TRPV4 channel activation of Ca^{2+} sparks (6). These sparks activate VSMC BK_{Ca} channels to promote vasodilation (Fig. 8). This hypothesized pathway explains several apparently disparate observations of H_2S dilation in small arteries. Specifically, it has been observed that H_2S 1) activates BK_{Ca} channels in microvascular EC (39), 2) increases $[Ca^{2+}]$ in microvascular EC (24), 3) dilates perfused mesenteric beds in a cytochrome P450, Ca^{2+}-activated K^+ channel, and endothelium-dependent manner (4; 5), and 4) hyperpolarizes small mesenteric VSMC E_m in a BK_{Ca}-dependent manner (10). In this model, EC BK_{Ca} channels are the primary target of H_2S in small mesenteric arteries.

It is not clear why bath applied NaHS activates EC BK_{Ca} channels but does not directly activate VSMC BK_{Ca} channels. H_2S may target some associated protein that is only expressed in EC. Because BK_{Ca} channel activity can be modified by several protein phosphatases and kinases including cAMP-dependent protein kinase (PKA) and cGMP-

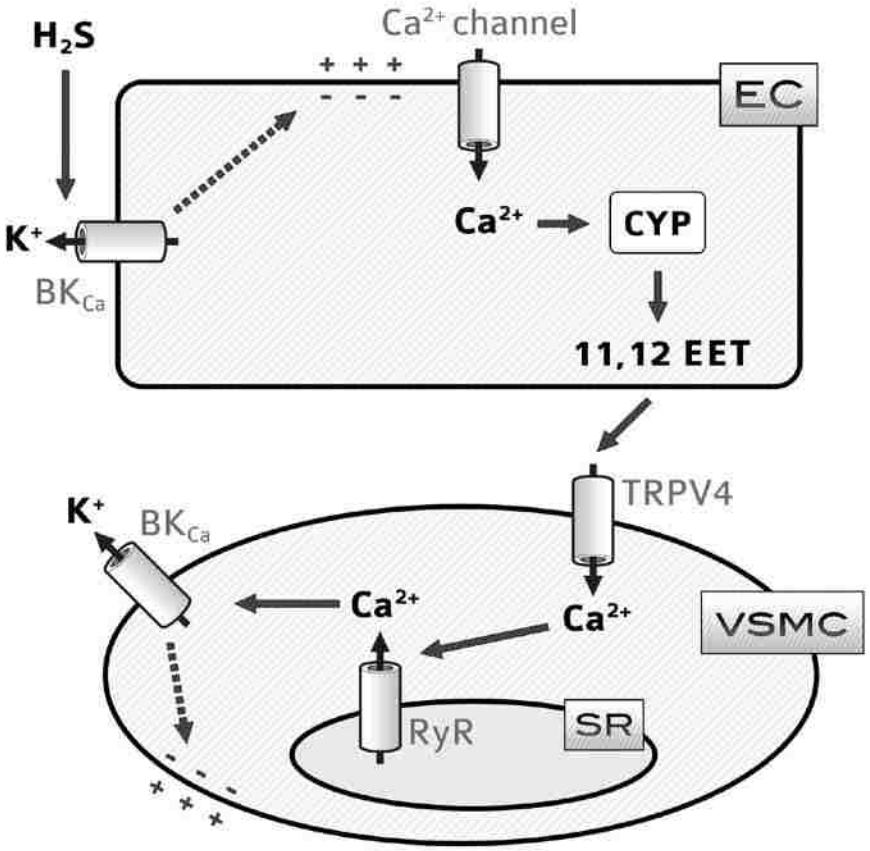

Figure 8. Proposed mechanism for H_2S-mediated VSMC plasma membrane E_m hyperpolarization and dilation in small mesenteric arteries. Effect of 11,12 EET on TRPV4 channels and Ca^{2+} sparks adapted from Earley et. al. (6).

dependent protein kinase (PKG) (17; 19), these enzymes may modify the sensitivity of BK_{Ca} channels to H_2S in VSMC. Differences in channel sensitivity to H_2S may alternatively be caused by splice variants in the BK-α subunit (17). Therefore the differential effects of H_2S on BK_{Ca} in EC and VSMC may be due to differences in associated proteins, BK-α splice variants, or both. Riddle et. al. (25) have described differences in Ca^{2+} sensitivity of BK_{Ca} channels in EC and VSMC, directly demonstrating the functional non-equivalence of BK_{Ca} channels in these cell types. Specifically, EC BK_{Ca} channels displayed a greater Ca^{2+} sensitivity than VSMC BK_{Ca} channels, despite the apparent lack of functional BK-β1 subunits in the ECs, so perhaps whatever molecular effects cause this enhanced Ca^{2+} sensitivity in EC BK_{Ca} channels is the target of H_2S effects. Future studies investigating the mechanism of H_2S activation of BK_{Ca} channels and the molecular differences between VSMC and EC BK_{Ca} channels are needed to resolve these questions.

Several studies propose that CSE and 3MST are expressed primarily in the endothelium, making H_2S a classical endothelium-derived hyperpolarizing factor (EDHF) (29; 36). Other studies have suggested that H_2S can be produced in VSMC (38) or in periadventital adipose tissue (7; 27). Although our previous results demonstrated CSE expression in all three layers of small mesenteric arteries (EC, VSMC, and adventitia) (10), the current finding that CSE in isolated EC activate BK_{Ca} channels suggests that this may be the source for vasoactive H_2S. Therefore, although it is possible that EC CSE exerts the greatest physiological effect due to its proximity to EC BK_{Ca} channels, additional studies are needed to resolve whether VSMC and adventitial CSE contribute as well.

The current work demonstrates for the first time that VSMC Ca^{2+} sparks are activated by exogenous and endogenous H_2S, which adds to and complements the growing list of physiological functions of this molecule in the vasculature. Alterations in H_2S signaling have been implicated in both human patients and animal models of cardiovascular disease (2; 10; 23; 33-36). Therefore, a comprehensive understanding of the modes of action of H_2S will be of critical importance in developing novel H_2S-based therapies for these diseases.

Acknowledgements: We are grateful to Mark Jackson-Weaver for assistance with design of the summary figure (Fig. 8).

Sources of Funding

OJW (HL7736, 10PRE4050028, American Heart Association); MAR (HL95640); LGB (HL088151); BRW (HL95640); NLK (EPA STAR award PHS 83186, HL82799 and is an established investigator of the American Heart Association)

Conflicts of Interests/Disclosures

None

Reference List

1. **Barrett JN, Magleby KL and Pallotta BS.** Properties of single calcium-activated potassium channels in cultured rat muscle. *J Physiol* 331: 211-230, 1982.

2. **Brancaleone V, Roviezzo F, Vellecco V, De Gruttola L, Bucci M and Cirino G.** Biosynthesis of H2S is impaired in non-obese diabetic (NOD) mice. *Br J Pharmacol* 155: 673-680, 2008.

3. **Bucci M, Papapetropoulos A, Vellecco V, Zhou Z, Pyriochou A, Roussos C, Roviezzo F, Brancaleone V and Cirino G.** Hydrogen sulfide is an endogenous inhibitor of phosphodiesterase activity. *Arterioscler Thromb Vasc Biol* 30: 1998-2004, 2010.

4. **Cheng Y, Ndisang JF, Tang G, Cao K and Wang R.** Hydrogen sulfide-induced relaxation of resistance mesenteric artery beds of rats. *Am J Physiol Heart Circ Physiol* 287: H2316-H2323, 2004.

5. **d'Emmanuele d, V, Sorrentino R, Coletta C, Mitidieri E, Rossi A, Vellecco V, Pinto A, Cirino G and Sorrentino R.** Hydrogen sulfide-induced dual vascular effect involves arachidonic acid cascade in rat mesenteric arterial bed. *J Pharmacol Exp Ther* 337: 59-64, 2011.

6. **Earley S, Heppner TJ, Nelson MT and Brayden JE.** TRPV4 forms a novel Ca2+ signaling complex with ryanodine receptors and BKCa channels. *Circ Res* 97: 1270-1279, 2005.

7. **Fang L, Zhao J, Chen Y, Ma T, Xu G, Tang C, Liu X and Geng B.** Hydrogen sulfide derived from periadventitial adipose tissue is a vasodilator. *J Hypertens* 27: 2174-2185, 2009.

8. **Furne J, Saeed A and Levitt MD.** Whole tissue hydrogen sulfide concentrations are orders of magnitude lower than presently accepted values. *Am J Physiol Regul Integr Comp Physiol* 295: R1479-R1485, 2008.

9. **Hughes JM, Riddle MA, Paffett ML, Gonzalez Bosc LV and Walker BR.** Novel role of endothelial BKCa channels in altered vasoreactivity following hypoxia. *Am J Physiol Heart Circ Physiol* 299: H1439-H1450, 2010.

10. **Jackson-Weaver O, Paredes DA, Gonzalez Bosc LV, Walker BR and Kanagy NL.** Intermittent hypoxia in rats increases myogenic tone through loss of hydrogen sulfide activation of large-conductance Ca(2+)-activated potassium channels. *Circ Res* 108: 1439-1447, 2011.

11. **Jaggar JH, Leffler CW, Cheranov SY, Tcheranova D, E S and Cheng X.** Carbon monoxide dilates cerebral arterioles by enhancing the coupling of Ca2+ sparks to Ca2+-activated K+ channels. *Circ Res* 91: 610-617, 2002.

12. **Jaggar JH, Porter VA, Lederer WJ and Nelson MT.** Calcium sparks in smooth muscle. *Am J Physiol Cell Physiol* 278: C235-C256, 2000.

13. **Ji G, Barsotti RJ, Feldman ME and Kotlikoff MI.** Stretch-induced calcium release in smooth muscle. *J Gen Physiol* 119: 533-544, 2002.

14. **Kabil O and Banerjee R.** Redox biochemistry of hydrogen sulfide. *J Biol Chem* 285: 21903-21907, 2010.

15. **Kamouchi M, Droogmans G and Nilius B.** Membrane potential as a modulator of the free intracellular Ca2+ concentration in agonist-activated endothelial cells. *Gen Physiol Biophys* 18: 199-208, 1999.

16. **Lanner JT, Georgiou DK, Joshi AD and Hamilton SL.** Ryanodine receptors: structure, expression, molecular details, and function in calcium release. *Cold Spring Harb Perspect Biol* 2: a003996, 2010.

17. **Ledoux J, Werner ME, Brayden JE and Nelson MT.** Calcium-activated potassium channels and the regulation of vascular tone. *Physiology (Bethesda)* 21: 69-78, 2006.

18. **Li Q, Sun B, Wang X, Jin Z, Zhou Y, Dong L, Jiang LH and Rong W.** A crucial role for hydrogen sulfide in oxygen sensing via modulating large

conductance calcium-activated potassium channels. *Antioxid Redox Signal* 12: 1179-1189, 2010.

19. **Lin MT, Longo LD, Pearce WJ and Hessinger DA.** Ca2+-activated K+ channel-associated phosphatase and kinase activities during development. *Am J Physiol Heart Circ Physiol* 289: H414-H425, 2005.

20. **Liu Y, Kalogeris TJ, Wang M, Zuidema MY, Wang Q, Dai H, Davis MJ, Hill MA and Korthuis RJ.** Hydrogen Sulfide Preconditioning or Neutrophil Depletion Attenuates Ischemia/Reperfusion-Induced Mitochondrial Dysfunction in Rat Small Intestine. *Am J Physiol Gastrointest Liver Physiol* 2011.

21. **Mandala M, Heppner TJ, Bonev AD and Nelson MT.** Effect of endogenous and exogenous nitric oxide on calcium sparks as targets for vasodilation in rat cerebral artery. *Nitric Oxide* 16: 104-109, 2007.

22. **Nelson MT, Cheng H, Rubart M, Santana LF, Bonev AD, Knot HJ and Lederer WJ.** Relaxation of arterial smooth muscle by calcium sparks. *Science* 270: 633-637, 1995.

23. **Perna AF, Sepe I, Lanza D, Capasso R, Di M, V, De Santo NG and Ingrosso D.** The gasotransmitter hydrogen sulfide in hemodialysis patients. *J Nephrol* 23 Suppl 16: S92-S96, 2010.

24. **Pupo E, Fiorio PA, Avanzato D, Moccia F, Avelino Cruz JE, Tanzi F, Merlino A, Mancardi D and Munaron L.** Hydrogen sulfide promotes calcium signals and migration in tumor-derived endothelial cells. *Free Radic Biol Med* 51: 1765-1773, 2011.

25. **Riddle MA, Hughes JM and Walker BR.** Role of Caveolin-1 in Endothelial BKCa Channel Regulation of Vasoreactivity. *Am J Physiol Cell Physiol* 2011.

26. **Sandow SL, Tare M, Coleman HA, Hill CE and Parkington HC.** Involvement of myoendothelial gap junctions in the actions of endothelium-derived hyperpolarizing factor. *Circ Res* 90: 1108-1113, 2002.

27. **Schleifenbaum J, Kohn C, Voblova N, Dubrovska G, Zavarirskaya O, Gloe T, Crean CS, Luft FC, Huang Y, Schubert R and Gollasch M.** Systemic peripheral artery relaxation by KCNQ channel openers and hydrogen sulfide. *J Hypertens* 28: 1875-1882, 2010.

28. **Sheng JZ, Ella S, Davis MJ, Hill MA and Braun AP.** Openers of SKCa and IKCa channels enhance agonist-evoked endothelial nitric oxide synthesis and arteriolar vasodilation. *FASEB J* 23: 1138-1145, 2009.

29. **Shibuya N, Mikami Y, Kimura Y, Nagahara N and Kimura H.** Vascular endothelium expresses 3-mercaptopyruvate sulfurtransferase and produces hydrogen sulfide. *J Biochem* 146: 623-626, 2009.

30. **Sitdikova GF, Weiger TM and Hermann A.** Hydrogen sulfide increases calcium-activated potassium (BK) channel activity of rat pituitary tumor cells. *Pflugers Arch* 459: 389-397, 2010.

31. **Telezhkin V, Brazier SP, Cayzac S, Muller CT, Riccardi D and Kemp PJ.** Hydrogen sulfide inhibits human BK(Ca) channels. *Adv Exp Med Biol* 648: 65-72, 2009.

32. **Telezhkin V, Brazier SP, Cayzac SH, Wilkinson WJ, Riccardi D and Kemp PJ.** Mechanism of inhibition by hydrogen sulfide of native and recombinant BKCa channels. *Respir Physiol Neurobiol* 172: 169-178, 2010.

33. **Whiteman M, Gooding KM, Whatmore JL, Ball CI, Mawson D, Skinner K, Tooke JE and Shore AC.** Adiposity is a major determinant of plasma levels of the novel vasodilator hydrogen sulphide. *Diabetologia* 53: 1722-1726, 2010.

34. **Xiaohui L, Junbao D, Lin S, Jian L, Xiuying T, Jianguang Q, Bing W, Hongfang J and Chaoshu T.** Down-regulation of endogenous hydrogen sulfide pathway in pulmonary hypertension and pulmonary vascular structural remodeling induced by high pulmonary blood flow in rats. *Circ J* 69: 1418-1424, 2005.

35. **Yan H, Du J and Tang C.** The possible role of hydrogen sulfide on the pathogenesis of spontaneous hypertension in rats. *Biochem Biophys Res Commun* 313: 22-27, 2004.

36. **Yang G, Wu L, Jiang B, Yang W, Qi J, Cao K, Meng Q, Mustafa AK, Mu W, Zhang S, Snyder SH and Wang R.** H2S as a physiologic vasorelaxant: hypertension in mice with deletion of cystathionine gamma-lyase. *Science* 322: 587-590, 2008.

37. **Zhao G, Zhao Y, Pan B, Liu J, Huang X, Zhang X, Cao C, Hou N, Wu C, Zhao KS and Cheng H.** Hypersensitivity of BKCa to Ca2+ sparks underlies hyporeactivity of arterial smooth muscle in shock. *Circ Res* 101: 493-502, 2007.

38. **Zhao W, Zhang J, Lu Y and Wang R.** The vasorelaxant effect of H(2)S as a novel endogenous gaseous K(ATP) channel opener. *EMBO J* 20: 6008-6016, 2001.

CHAPTER 4. DISCUSSION

Myogenic tone may be one of the more complex phenomena investigated in the physiology of the cardiovascular system. The sheer number of studies carried out, the numerous signaling mechanisms implicated in its regulation, and the long history of these investigations attest to this. The studies in this work now add H_2S to the list of factors that regulate myogenic tone, a factor previously overlooked due to its relatively recent discovery as an endogenous signaling molecule, and also perhaps due to this finding being restricted to certain beds or artery sizes, although our finding that CSE activity reduces myogenic tone in both mesenteric and middle cerebral arteries argues against this idea.

Our exogenous H_2S dilation experiments revealed that there are at least two different vasodilatory mechanism that can be activated by H_2S. Concentrations at or below 10 μM produced a dilation that was sensitive to IbTx, whereas the response to concentrations greater than this were unaffected by either IbTx or glibenclamide. Preconstriction with KCl did, however, block the dilation at all concentrations. This suggests that H_2S-induced dilaiton is mediated by the opening of a K^+ channel of some type. It could be mediated by Kv channels, which have been shown to mediate H_2S dilation in the aorta (28). As stated in chapter 3, tissue levels of H_2S have been measured by gas chromatography in the nM range (10), nowhere near the high μM concentrations that cause the non-IbTx sensitive dilation. This does not mean that microdomains of H_2S do not reach these concentrations in localized subcellular regions, however. Interestingly, the dilation at these high μM H_2S concentrations is nearly complete, reversing even resting tone, so that at 100 μM the artery diameter is nearly the same as

the Ca^{2+} free diameter. This suggests that endogenous [H_2S] does not reach these levels, as basal tone in these arteries is 5-10% of resting diameter. Thus the more physiologically relevant [H_2S] may be in the IbTx-sensitive portion of the curve. At this point this is only speculation, however.

Identification of potential H_2S microdomains must await methods to measure H_2S dynamically and microscopically, such as with H_2S-selective fluorescent intracellular probes. Commercially available H_2S probes may be available soon. The compound HSip-1 is selective and sensitive to H_2S (10 μM H_2S elicited a 50-fold increase in fluorescence), and can be made cell permeant by diacetylation (27), thus this may soon be possible.

Microdomains have been seen for other enzymatically produced and rapidly degraded signaling molecules such as superoxide ($O_2^{\cdot-}$) (35). In this 2008 study, a $O_2^{\cdot-}$-selective fluorescent probe, cp-YFP, was targeted to mitochondria by attaching the cytochrome C oxidase subunit IV. Large increases in $O_2^{\cdot-}$ were observed in individual mitochondria, which lasted ~10-20 seconds, termed “superoxide flashes”. It is possible that H_2S production shows similar subcellular localization and thus ion channels may experience much higher [H_2S] than whole tissue measurements would suggest.

The hypothesis of subcellular H_2S domains affecting vascular function is predicated on the idea that CSE is localized in close proximity to its primary cellular target, which seems to be EC BK_{Ca} channels. The locality of vasoactive CSE in small mesenteric arteries is, however, not entirely clear. The patch clamp data in chapter 3 suggest that EC do express CSE that activates K^+ channels. But this may not be the only source of H_2S that activates EC BK_{Ca} channels in the intact artery. Immunofluorescence

studies in chapter 2 show that the greatest CSE expression is in adventitial cells. However, the observation that CSE expression is selectively reduced in EC in arteries from IH rats, and this apparently abrogates H_2S regulation of myogenic tone, suggests that EC CSE may indeed be the primary source for vasoactive H_2S. EC-specific knockout of the CSE gene would be an ideal way to test this hypothesis. If EC CSE is the primary source of vasoactive H_2S, then knockout of the gene in these cells should mimic the pharmacologic inhibition of the enzyme in the present studies, namely that it would increase myogenic tone. Alternatively, it is possible that luminal application of inhibitors of CSE would preferentially inhibit the enzyme in EC.

It is interesting that although we only see apparent coupling of Ca^{2+} sparks to membrane potential in these arteries at 100 mmHg, H_2S causes a significant hyperpolarization and dilation that is IbTx sensitive at 60 mmHg. This suggests that there is some activation of BK_{Ca} channels independent of sparks by H_2S that produces vasodilation. It is possible that this dilation is due to activation of EC BK_{Ca} channels, and that conducted hyperpolarization through gap junctions is responsible. We did not measure H_2S vasodilation or VSMC E_m hyperpolarization at this lower pressure in the presence of luminal IbTx, but this seems the most direct way to test this hypothesis. Alternatively, gap junction inhibitors could be used to see if these channels play a role. It is possible that the conducted hyperpolarization is not mediated through gap junctions, though myoendothelial gap junctions are present in the mesenteric arteries (26). It is of note that in arteries at 100 mmHg luminal pressure, H_2S still caused a small dilation in the presence of ryanodine, even though luminal IbTx completely blocked this dilation below the "supraphysiological" H_2S concentrations. This residual dilation in the

presence of ryanodine is of roughly the same magnitude as the dilation at 60 mmHg. This suggests that perhaps activation of EC BK_{Ca} channels can cause ~20% dilation through conducted hyperpolarization.

The mesenteric circulation is highly innervated by autonomic fibers, and neural control is thought to be the primary mechanism of regulation of arterial contractility in this bed. Blood flow in mesenteric arteries is decreased during exercise (24) and increased after a meal (29), due to the skeletal muscle blood demands in the former case and intestinal blood flow demands in the latter case. It is therefore perhaps unsurprising that the mesenteric circulation displays so little myogenic tone, since a large myogenic response would impair its blood reservoir function and reduce the large vasodilation necessary for postprandial intestinal perfusion. Other beds with greater myogenic tone such as the cerebral vasculature do dilate to match blood flow to tissue metabolism (7), but these beds do not perform two such functions with greatly opposed blood flow requirements as nutrient absorption and reservoir mobilization. Another vascular bed with somewhat analogous functions is the pulmonary circulation. During exercise, cardiac output can increase 3 to 4 fold (15), increasing pressure and flow in the pulmonary circulation to maintain blood oxygen levels. On the other hand, pulmonary arteries constrict in response to local hypoxia, effectively matching perfusion to ventilation (19). Thus pulmonary arteries constrict or remain dilated somewhat irrespective of perfusion pressure, similar to the mesenteric circulation. As predicted by these similar functions, the pulmonary circulation displays very little myogenic tone under normal conditions (3). In small mesenteric arteries, it seems that a large cause of this decreased myogenicity is basal production of H_2S.

Due to the apparent EC dependence of H_2S vasodilation in mesenteric arteries and the EC dysfunction seen in several cardiovascular diseases including sleep apnea, it is interesting to consider how an increase in myogenic tone might affect the functions of the mesenteric circulation. A reduction in blood reservoir function could result from enhanced tone, redistributing blood to the skeletal muscle circulation and perhaps enhancing central arterial pressure. This would perhaps mimic enhanced sympathetic outflow to the mesentery, which also is itself associated with cardiovascular diseases such as sleep apnea (1; 23). Thus the combination of enhanced mesenteric myogenic tone and sympathetic nervous system activity could act synergistically to enhance central blood pressure in diseases such as sleep apnea-induced hypertension.

This synergism of sympathetic neurotransmitter release and myogenic tone would occur at the level of isolated arteries. G-protein coupled receptor ligands such as norephinephrine potentiate myogenic tone, even at subconstrictor concentrations (18; 20). Thus the loss of H_2S control of myogenic tone could be a significant factor in hypertension, both in sleep apnea complicated cases and perhaps more broadly as well.

Enhanced myogenic tone in the mesenteric arteries could also interfere with the vasodilation seen postprandially that is important in nutrient uptake. It is possible that enhanced myogenic tone contributes to chronic mesenteric ischemic disease, a disease in which normal postprandial hyperemia in the mesenteric bed is prevented. This condition causes abdominal pain 30-45 minutes after eating, sometimes associated with nausea, vomiting, diarrhea, or malabsorption (33). The most common cause is atherosclerotic narrowing of large arteries feeding the mesentery such as the superior mesenteric artery. Some cases, however, are the result of vasoconstricting medications (33), suggesting that

myogenic tone or other processes that influence mesenteric VSMC constriction may be a possible factor. If sleep apnea enhances myogenic tone in mesenteric arteries similar to our results in IH-exposed rats (Chapter 2), perhaps this could lead to mesenteric ischemic disease. There have not been any reports of sleep apnea as a risk factor for chronic mesenteric ischemic disease, but due to the association of sleep apnea with atherosclerosis (6), and atherosclerosis being a major cause of mesenteric ischemic disease, only a large study designed to look for sleep apnea as an independent risk factor for the ischemic disease could find such a link.

It is interesting to note that non-selective cytochrome P450 inhibition with SKF-525A had no effect on myogenic tone, despite the fact that inhibition of H_2S production did. If H_2S causes vasodilation through activation of cytochrome P450 2C, why did SKF-525A not have an effect? Sulfaphenazole inhibits only a small subclass of P450 enzymes, including those known to be involved in vasodilation. There are other cytochrome P450 products thought to be vasoconstrictors, however, such as 20-HETE produced by cytochrome P450 type 4 ω-hydroxylase activity. This cytochrome product has indeed been shown to be necessary for the development of myogenic tone in renal and cerebral arteries (12). The mechanisms responsible for this effect of 20-HETE include inhibition of BK_{Ca} channels and activation of protein kinase C. Thus by blocking cytochrome P450 enzymes non-selectively, a necessary step in the myogenic tone pathway may be inhibited. Studies have shown that 20-HETE contributes to mesenteric artery myogenic tone in the spontaneously hypertensive rat, but it is unknown whether it plays a role in wild type rat mesenteric arteries under normal physiological conditions (34).

H_2S at 10 μM applied to arteries pressurized to 100 mmHg causes a large dilation that is ~60% inhibited by ryanodine, indicating a large role for Ca^{2+} sparks in mediating this relaxation. Furthermore, H_2S at this concentration causes ~5 mV E_m hyperpolarization that is blocked by ryanodine, IbTx, and sulfaphenazole. Together these data support a role for H_2S activating Ca^{2+} sparks through 11,12 EET production to cause vasodilation through activation of plasma membrane BK_{Ca} channels. However, the increase in spark frequency by the addition of H_2S is modest, only going from 0.45 to 0.55 Hz. This suggests that perhaps a secondary effect may be to increase the coupling of sparks to BK_{Ca} channels. The effect of 11,12 EET to increase Ca^{2+} spark frequency and cause dilation has been attributed to an increase in spark frequency alone (8). However, in this Earley et. al. paper, 11,12 EET increases spark frequency from 0.18 to 0.3 Hz, a 66% increase, but increased STOC frequency by 120%. This also suggests a potential enhancement of spark to STOC coupling. However, without a careful study using patch clamp and confocal microscopy simultaneously to directly measure spark-STOC coupling, this must remain speculation.

Our results suggest H_2S directly activates EC BK_{Ca} channels. However, H_2S has previously been shown to inhibit BK_{Ca} channels in carotid body glomus cells, mediating hypoxia-induced cell depolarization (17). BK_{Ca} channels in these cells were inhibited by 100 μM NaHS, which is above the range that produces an IbTx-sensitive dilation in mesenteric arteries. Perhaps H_2S has different effects on the channel dependent on concentration. A later study found similar results, with the threshold for inhibition of glomus cell BK_{Ca} channels around 100 μM and an IC_{50} of around 300 μM (31). The Telezhkin study also reported the inhibition of recombinant BK_{Ca} channels in HEK 293

cells with 1.2 mM H_2S. Interestingly, chimeric BK_{Ca} channels in which the cytoplasmic tail was replaced with the tail from the KSper pH sensitive K^+ channel retained sensitivity to H_2S inhibition. This chimeric channel is completely insensitive to both Ca^{2+} and CO, suggesting H_2S inhibition of the BK_{Ca} channel does not function through a modulation of these C-terminal activation regions, at least at this high concentration.

If H_2S acts on the transmembrane regions of the BK_{Ca} channel to exert its inhibitory effect, perhaps the proposed activation by H_2S occurs in the cytoplasmic C-terminal. This possibility is interesting because the c-terminus of EC BK_{Ca} channels may be quite different functionally from VSMC channels. This hypothesis comes from the observation that EC BK_{Ca} channels do not seem to have functional β1 subunits, due to the fact that the channels are not activated by tamoxifen (25). Nevertheless, EC BK_{Ca} channels display greater Ca^{2+} sensitivity than VSMC BK_{Ca} channels, which do express functional β1 subunits that enhance Ca^{2+} sensitivity of the channel (2). Thus it is possible that EC BK_{Ca} channels have a unique cytoplasmic tail, which confers highly sensitive Ca^{2+} sensing even in the absence of functional β1 subunits. If this is true, then perhaps this unique C-terminus contains an H_2S sensitive region that VSMC BK_{Ca} channels do not express.

The hypoxia-induced depolarization of glomus cells mediated by H_2S inhibition of BK_{Ca} channels is potentially mediated by a reduced oxidation of H_2S leading to an increased intracellular [H_2S]. Mitochondrial consumption of H_2S, one of the main mechanisms of H_2S breakdown, is indeed dependent on oxygen (21). This raises the question of how repeated hypoxic exposures during IH could reduce endogenous production of H_2S, as is proposed in Chapter 2. Much of the conclusion in this chapter

that IH causes a loss of H_2S production is based on evidence that exogenous H_2S robustly dilates arteries from IH rats, but there is no apparent reduction of myogenic tone in these arteries by endogenous H_2S. Endothelial CSE expression is also reduced in arteries from IH rats. Enhancing endogenous H_2S dilation through cysteine addition also caused less vasodilation in arteries from IH rats. However, in the appendix we see that H_2S does not activate Ca^{2+} sparks in arteries from IH rats. Much of the dilation at 100 mmHg luminal pressure is dependent on Ca^{2+} sparks in Sham rat arteries, as ryanodine has a large effect to reduce dilation to exogenous H_2S. Furthermore, 100 mmHg is the first pressure at which we see greater myogenic tone in IH and BCA treated arteries. Thus it is unclear how relevant dilation at 60 mmHg is for the regulation of myogenic tone. Due to the lack of Ca^{2+} spark activation by H_2S in arteries from IH rats, it is possible that dilation to exogenous H_2S is reduced in these arteries relative to Sham at 100 mmHg. This would completely change our conclusion that IH reduces H_2S production, and it would then seem more likely that the switch in RyR expression in IH prevents dilation to H_2S, regardless of endogenous levels. This seems an important distinction to investigate, and may point to the altered RyR isoform expression in IH arteries as a unifying mechanism for the various types of vascular dysfunction observed. The results in chapter 2 showing that plasma H_2S and kidney H_2S production are not affected by IH treatment, seem to support the idea that endogenous H_2S production may not be altered by IH, but it is rather an alteration in expression of the H_2S target.

The data in the appendix manuscript suggest that H_2S activates RyR1 to produce Ca^{2+} sparks, since IH arteries showed reduced RyR1 expression and enhanced RyR2 expression and were not responsive to H_2S. This leads to the question as to why RyR1

may be activated by H_2S but RyR2 is not. As discussed in the appendix, both RyR1 and RyR2 were shown to be required for depolarization-induced Ca^{2+} spark activation in cultured rat portal vein myocytes, whereas RyR3 was not required (5). Thus the phenomenon of vascular Ca^{2+} sparks may be mediated by an interaction between RyR1 and RyR2. This seems to fit with our data, as basal Ca^{2+} spark parameters are not affected significantly by IH treatment in this size artery, at least at 60 mmHg luminal pressure. Therefore it seems that although either RyR1 or RyR2 can generate sparks, RyR1 may be the sensor for H_2S activation of Ca^{2+} sparks. The model described in chapter 3 for the activation of Ca^{2+} sparks by H_2S suggested that TRPV4-mediated Ca^{2+} influx was the direct activator of Ca^{2+} sparks. Thus we may hypothesize that RyR1 is better coupled to this TRPV4 Ca^{2+} influx than RyR2. Why this would be the case is not clear. Perhaps it is due to the sensitive activation of RyR1 by calmodulin at 100 nM Ca^{2+}, whereas RyR2 does not show activation by calmodulin at this Ca^{2+} concentration (9). Later work demonstrated a concentration-dependent effect of calmodulin on RyR2, with low concentrations (50-100 nM) activating the channel but higher concentrations (500 nM) inhibiting it (30). So the lack of activation of RyR2 by TRPV4-mediated Ca^{2+} influx would only be feasible at certain calmodulin concentrations in mesenteric VSMC. Clearly further work would be needed to explore this hypothesis.

We see a major switch in function of Ca^{2+} sparks from 60 to 100 mmHg luminal pressure in these small mesenteric arteries (see appendix). This raises the question as to what pressures are in this branch of the mesenteric tree *in vivo*. In anesthetized cats, pressure in small mesenteric arteries (80-100 μm, the size used in this work) was 75-80 mmHg (11). However, a more recent study in conscious rats measured pressures in

mesenteric arteries of about 100 μm inner diameter to be 70-75 mmHg (8). This was quite different from the results seen immediately after surgery, where in the same sized arteries pressure was 90-100 mmHg, despite aortic pressure being about the same as several hours after surgery. Thus it may be that anesthesia has a large effect on the pressure profile in the mesenteric arcade. Furthermore, continuous recordings over two hours showed that pressure at the small mesenteric arteries varied fairly widely, from ~65 to ~90 mmHg. This may be expected for an artery bed in which resistance is altered by a variety of physiological stimuli such as exercise and feeding. Thus the pressure at which isolated artery experiments are performed should perhaps depend on what phenomenon is being studied. Myogenic tone is studied by step increases in pressure, so the range of pressures used should include the lowest and highest pressures present in the arterial bed during a range of physiological conditions. Pressures of 60 mmHg and 100 mmHg seem to be at these high and low extremes, thus validating the inclusion of these pressures in the myogenic curves in chapter 2. Thus the experiments in chapter 3, which were performed at 100 mmHg, are near the maximum of the observed physiological range and therefore probably quite relevant for the study of signaling pathways that regulate myogenic tone.

As stated in the discussion of chapter 3, the enhancement of H_2S vasodilatory function when luminal pressure is increased from 60 to 100 mmHg, potentially through enhanced coupling of Ca^{2+} sparks to E_m, means that H_2S can act as a negative feedback regulator of myogenic tone without H_2S production being altered by pressure. It seems possible that other negative feedback mechanisms in control of vascular contractility could share a similar mechanism. For instance, does arterial constriction enhance the

effect of NO without enhancing NO production, perhaps though enhanced sensitivity of soluble guanylyl cyclase (sGC) activation by NO in the presence of Ca^{2+}? This turns out not to be the case. sGC is in fact inhibited by Ca^{2+} (14; 22). So the question arises, why might NO and H_2S effects be regulated in opposite directions by the vascular function that they oppose? Perhaps myogenic tone, as a pressure-induced constriction, initiates a positive feedback loop, whereby increased blood pressure augments myogenic tone, etcetera. Therefore H_2S, as a modulator of myogenic tone, participates in a negative feedback mechanism to end this cycle. The enhancement of H_2S effect at higher pressures supplies this negative feedback on myogenic tone. But agonist-mediated vasoconstriction such as that induced by norepinephrine does not have a positive feedback loop, and all that is necessary to reduce contractility is a reduction in agonist release. In fact, the baroreceptor reflex is already its own negative feedback regulator, in that a sympathetic-mediated increase in vasoconstriction and blood pressure activates baroreceptors leading to reduced sympathetic activity (13). Thus NO-induced dilation is more effectively overcome by agonists involved in neural control of blood pressure and blood flow and this is in fact what is seen *in vivo*. Norepinephrine release from forearm nerves overwhelms NO-induced vasodilation in humans (32). Alternatively, NO may have so many modes of action, both sGC-dependent and independent (4; 36), that negative regulators of NO action are necessary to produce constriction in the presence of basal NO levels. Ca^{2+} inhibition of sGC may act in this way to reduce the potent vasodilatory action of NO.

Figure 1 shows the proposed overall hypothesis for H_2S regulation of myogenic tone. It includes the hypothesis that EC Ca^{2+} activates a Ca^{2+}-dependent phospholipase

(PLA2) to liberate arachidonic acid (16), which is converted to 11, 12 EET by cytochrome P450 2C. This diffusible product then activates TRPV4 to activate Ca^{2+} sparks in VSMC. Included in the figure is the speculative activation of primarily RyR1 by TRPV4-mediated Ca^{2+} influx, but subsequent activation of RyR2 to generate a Ca^{2+} spark, since RyR1 and RyR2 are necessary for spark production in smooth muscle (5). It also includes a potential effect of stretch-induced depolarization to enhance spark coupling to membrane potential, perhaps through an increased BK_{Ca} Ca^{2+} sensitivity as discussed previously. Further work will be necessary to establish all the links proposed here, but based on our work and the work of others, this seems the most likely pathway for the effect of H_2S to inhibit myogenic tone in small mesenteric arteries.

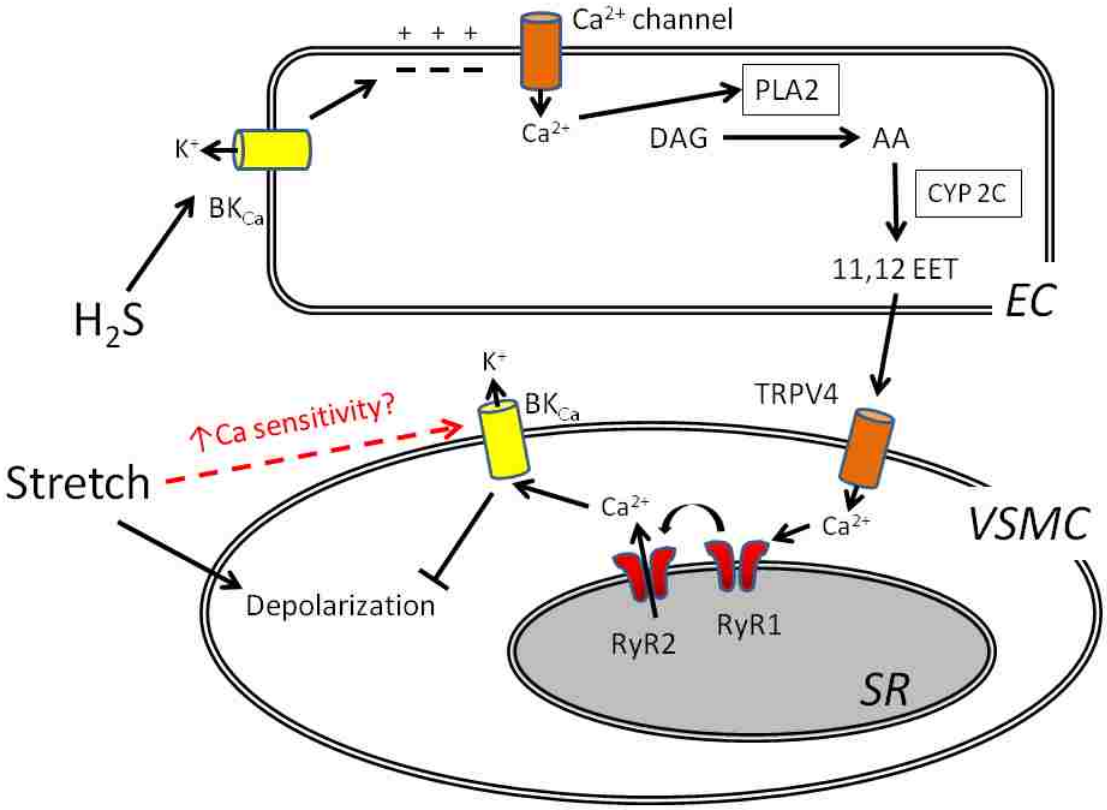

Figure 1. Proposed pathway for H_2S inhibition of myogenic tone. Myogenic tone is shown here as a stretch-induced depolarization of VSMC. This stretch also is proposed to enhance the Ca^{2+} sensitivity of BK_{Ca} channels. EC BK_{Ca} channels may increase EC Ca^{2+} to activate phospholipase A2 (PLA2), causing the production of arachidonic acid (AA), the substrate for cytochrome P450 2C which produces 11,12 EET. The activation of Ca^{2+} sparks is here hypothesized to be mediated by RyR1, but spark production also requires RyR2. Sparks then hyperpolarize the VSMC to oppose myogenic tone.

Reference List

1. **Bao G, Metreveli N, Li R, Taylor A and Fletcher EC**. Blood pressure response to chronic episodic hypoxia: role of the sympathetic nervous system. *J Appl Physiol* 83: 95-101, 1997.

2. **Brenner R, Perez GJ, Bonev AD, Eckman DM, Kosek JC, Wiler SW, Patterson AJ, Nelson MT and Aldrich RW**. Vasoregulation by the beta1 subunit of the calcium-activated potassium channel. *Nature* %19;407: 870-876, 2000.

3. **Broughton BR, Walker BR and Resta TC**. Chronic hypoxia induces Rho kinase-dependent myogenic tone in small pulmonary arteries. *Am J Physiol Lung Cell Mol Physiol* 294: L797-L806, 2008.

4. **Carvajal JA, Germain AM, Huidobro-Toro JP and Weiner CP**. Molecular mechanism of cGMP-mediated smooth muscle relaxation. *J Cell Physiol* 184: 409-420, 2000.

5. **Coussin F, Macrez N, Morel JL and Mironneau J**. Requirement of ryanodine receptor subtypes 1 and 2 for Ca(2+)-induced Ca(2+) release in vascular myocytes. *J Biol Chem* 275: 9596-9603, 2000.

6. **Drager LF, Polotsky VY and Lorenzi-Filho G**. Obstructive sleep apnea: an emerging risk factor for atherosclerosis. *Chest* 140: 534-542, 2011.

7. **Dunn KM and Nelson MT**. Potassium channels and neurovascular coupling. *Circ J* 74: 608-616, 2010.

8. **Earley S, Heppner TJ, Nelson MT and Brayden JE**. TRPV4 forms a novel Ca2+ signaling complex with ryanodine receptors and BKCa channels. *Circ Res* 97: 1270-1279, 2005.

9. **Fenger-Gron J, Mulvany MJ and Christensen KL**. Mesenteric blood pressure profile of conscious, freely moving rats. *J Physiol* 488: 753-760, 1995.

10. **Fruen BR, Black DJ, Bloomquist RA, Bardy JM, Johnson JD, Louis CF and Balog EM**. Regulation of the RYR1 and RYR2 Ca2+ release channel isoforms by Ca2+-insensitive mutants of calmodulin. *Biochemistry* 42: 2740-2747, 2003.

11. **Furne J, Saeed A and Levitt MD**. Whole tissue hydrogen sulfide concentrations are orders of magnitude lower than presently accepted values. *Am J Physiol Regul Integr Comp Physiol* 295: R1479-R1485, 2008.

12. **Gore RW**. Pressures in cat mesenteric arterioles and capillaries during changes in systemic arterial blood pressure. *Circ Res* 34: 581-591, 1974.

13. **Harder DR, Narayanan J and Gebremedhin D**. Pressure-induced myogenic tone and role of 20-HETE in mediating autoregulation of cerebral blood flow. *Am J Physiol Heart Circ Physiol* 300: H1557-H1565, 2011.

14. **Joyner MJ, Charkoudian N and Wallin BG**. A sympathetic view of the sympathetic nervous system and human blood pressure regulation. *Exp Physiol* 93: 715-724, 2008.

15. **Kazerounian S, Pitari GM, Ruiz-Stewart I, Schulz S and Waldman SA**. Nitric oxide activation of soluble guanylyl cyclase reveals high and low affinity sites that mediate allosteric inhibition by calcium. *Biochemistry* 41: 3396-3404, 2002.

16. **Kovacs G, Berghold A, Scheidl S and Olschewski H**. Pulmonary arterial pressure during rest and exercise in healthy subjects: a systematic review. *Eur Respir J* 34: 888-894, 2009.

17. **Leslie CC**. Properties and regulation of cytosolic phospholipase A2. *J Biol Chem* 272: 16709-16712, 1997.

18. **Li Q, Sun B, Wang X, Jin Z, Zhou Y, Dong L, Jiang LH and Rong W**. A crucial role for hydrogen sulfide in oxygen sensing via modulating large conductance calcium-activated potassium channels. *Antioxid Redox Signal* 12: 1179-1189, 2010.

19. **Liu J, Hill MA and Meininger GA**. Mechanisms of myogenic enhancement by norepinephrine. *Am J Physiol* 266: H440-H446, 1994.

20. **Mark A**. Hypoxic pulmonary vasoconstriction. *Essays Biochem* 43:61-76.: 61-76, 2007.

21. **Meininger GA and Faber JE**. Adrenergic facilitation of myogenic response in skeletal muscle arterioles. *Am J Physiol* 260: H1424-H1432, 1991.

22. **Olson KR, Healy MJ, Qin Z, Skovgaard N, Vulesevic B, Duff DW, Whitfield NL, Yang G, Wang R and Perry SF**. Hydrogen sulfide as an oxygen sensor in trout gill chemoreceptors. *Am J Physiol Regul Integr Comp Physiol* 295: R669-R680, 2008.

23. **Parkinson SJ, Jovanovic A, Jovanovic S, Wagner F, Terzic A and Waldman SA**. Regulation of nitric oxide-responsive recombinant soluble guanylyl cyclase by calcium. *Biochemistry* 38: 6441-6448, 1999.

24. **Prabhakar NR and Kumar GK**. Mechanisms of sympathetic activation and blood pressure elevation by intermittent hypoxia. *Respir Physiol Neurobiol* 174: 156-161, 2010.

25. **Qamar MI and Read AE**. Effects of exercise on mesenteric blood flow in man. *Gut* 28: 583-587, 1987.

26. **Riddle MA, Hughes JM and Walker BR**. Role of Caveolin-1 in Endothelial BKCa Channel Regulation of Vasoreactivity. *Am J Physiol Cell Physiol* 2011.

27. **Sandow SL, Tare M, Coleman HA, Hill CE and Parkington HC**. Involvement of myoendothelial gap junctions in the actions of endothelium-derived hyperpolarizing factor. *Circ Res* 90: 1108-1113, 2002.

28. **Sasakura K, Hanaoka K, Shibuya N, Mikami Y, Kimura Y, Komatsu T, Ueno T, Terai T, Kimura H and Nagano T**. Development of a Highly Selective Fluorescence Probe for Hydrogen Sulfide. *J Am Chem Soc* 2011.

29. **Schleifenbaum J, Kohn C, Voblova N, Dubrovska G, Zavarirskaya O, Gloe T, Crean CS, Luft FC, Huang Y, Schubert R and Gollasch M**. Systemic peripheral artery relaxation by KCNQ channel openers and hydrogen sulfide. *J Hypertens* 28: 1875-1882, 2010.

30. **Sieber C, Beglinger C, Jaeger K, Hildebrand P and Stalder GA**. Regulation of postprandial mesenteric blood flow in humans: evidence for a cholinergic nervous reflex. *Gut* 32: 361-366, 1991.

31. **Sigalas C, Bent S, Kitmitto A, O'Neill S and Sitsapesan R**. Ca(2+)-calmodulin can activate and inactivate cardiac ryanodine receptors. *Br J Pharmacol* 156: 794-806, 2009.

32. **Telezhkin V, Brazier SP, Cayzac SH, Wilkinson WJ, Riccardi D and Kemp PJ**. Mechanism of inhibition by hydrogen sulfide of native and recombinant BKCa channels. *Respir Physiol Neurobiol* 172: 169-178, 2010.

33. **Tschakovsky ME, Sujirattanawimol K, Ruble SB, Valic Z and Joyner MJ**. Is sympathetic neural vasoconstriction blunted in the vascular bed of exercising human muscle? *J Physiol* 541: 623-635, 2002.

34. **Walker TG**. Mesenteric ischemia. *Semin Intervent Radiol* 26: 175-183, 2009.

35. **Wang MH, Zhang F, Marji J, Zand BA, Nasjletti A and Laniado-Schwartzman M**. CYP4A1 antisense oligonucleotide reduces mesenteric vascular reactivity and blood pressure in SHR. *Am J Physiol Regul Integr Comp Physiol* 280: R255-R261, 2001.

36. **Wang W, Fang H, Groom L, Cheng A, Zhang W, Liu J, Wang X, Li K, Han P, Zheng M, Yin J, Wang W, Mattson MP, Kao JP, Lakatta EG, Sheu SS, Ouyang K, Chen J, Dirksen RT and Cheng H**. Superoxide flashes in single mitochondria. *Cell* 134: 279-290, 2008.

37. **Wanstall JC, Homer KL and Doggrell SA**. Evidence for, and importance of, cGMP-independent mechanisms with NO and NO donors on blood vessels and platelets. *Curr Vasc Pharmacol* 3: 41-53, 2005.

APPENDIX

Intermittent Hypoxia in Rats Reduces Activation of Ca^{2+} Sparks in Mesenteric Arteries

O Jackson-Weaver, DA Paredes, A. Martin-Ivins, LV Gonzalez-Bosc, BR Walker, NL Kanagy

Vascular Physiology Group, Department of Cell Biology and Physiology, School of Medicine, University of New Mexico, Albuquerque, NM

Running head: Intermittent hypoxia, Ca^{2+} sparks

Address for correspondence: Nancy L. Kanagy, PhD, Professor

Department of Cell Biology and Physiology

MSC 08-4750

University of New Mexico

Albuquerque, NM 87131

Phone: 505-272-8814

FAX: 505-272-6649

Email: nkanagy@salud.unm.edu

This manuscript is in preparation for submission to Hypertension.

Abstract

Ca^{2+} sparks are vascular smooth muscle cell Ca^{2+}-release events mediated by ryanodine receptors (RyR) that promote vasodilation through the activation of large-conductance Ca^{2+}-activated potassium channels and inhibit myogenic tone. We have previously reported that simulating sleep apnea in rats with intermittent hypoxia (IH) augments myogenic tone in mesenteric arteries and that hydrogen sulfide (H_2S) increases Ca^{2+} spark frequency in arteries from control (Sham) rats. We therefore hypothesized that IH reduces Ca^{2+} spark activity, and that this loss of activity enhances myogenic tone in IH mesenteric arteries. We measured Ca^{2+} spark frequency in Fluo-4 loaded arteries during stimulation with transmural pressure increases, the H_2S donor NaHS, KCl-induced depolarization, and the phosphodiesterase inhibitor IBMX. Elevating transmural pressure (20 to 100 mmHg), H_2S, and KCl depolarization increased Ca^{2+} spark frequency in Sham but not IH arteries. IBMX increased spark frequency similarly in Sham and IH arteries. In western blots, RyR1 protein expression was reduced in IH compared to Sham arteries, while expression of RyR2 was increased. mRNA transcripts of RyR1 and RyR2 were similarly affected by IH. Ryanodine blockade of RyRs enhanced myogenic tone only in Sham arteries. Therefore Ca^{2+} sparks appear to cause dilation which opposes myogenic tone in Sham but not IH arteries. Furthermore, IH decreases Ca^{2+} spark activation by H_2S, KCl, and transmural pressure increases, but leaves intact activation by cyclic nucleotides. These effects may be due to a switch from RyR1 to RyR2 isoforms, and potentially contribute to the enhanced myogenic tone in mesenteric arteries from IH rats.

Introduction

Epidemiological studies have established obstructive sleep apnea (OSA) as an independent risk factor for cardiovascular disease, in particular hypertension (31). Potential mechanisms to explain this association include increased sympathetic activity (2), activation of the renin-angiotensin system (RAS) (9), endothelial dysfunction (19), systemic inflammation (36), and increased circulating levels of the vasoactive peptide endothelin-1 (11). We have previously reported that exposing rats to 14 days of eucapnic intermittent hypoxia (IH) elevates systemic blood pressure and arterial constrictor sensitivity to ET-1 (1) with an associated increase in vascular reactive oxygen species (ROS). Furthermore, administering the antioxidant tempol *in vivo* prevented IH induced hypertension (35). We have also shown that IH enhances myogenic tone and causes vascular smooth muscle cell (VSMC) membrane potential (E_m) depolarization in small mesenteric arteries through apparent loss of production of the vasodilator H_2S (13).

Ca^{2+} sparks are spatially and temporally limited Ca^{2+} release events from ryanodine receptor Ca^{2+} channels (RyR) in the sarcoplasmic reticulum (SR) of cardiac and smooth muscle cells. In cerebral artery VSMC, Ca^{2+} sparks activate large-conductance Ca^{2+}-activated K^+ (BK_{Ca}) channels and to cause E_m hyperpolarization followed by decreased activity of L-type voltage-gated calcium channels (VGCC) and a decrease in cytosolic [Ca^{2+}] (27). Ca^{2+} spark frequency is increased by stretch of VSMC as well as E_m depolarization, and has been hypothesized to act an intrinsic negative feedback mechanism to regulate stretch-induced VSM cell depolarization and myogenic tone (12; 15). Ca^{2+} sparks are also regulated by cyclic nucleotides through the activation of protein kinases. Both cAMP-dependent protein kinase (PKA) and cGMP-dependent

protein kinase (PKG) have been shown to increase spark frequency (30). We have recently shown that in mesenteric arteries, the gasotransmitter H_2S is another activator of Ca^{2+} sparks (Jackson-Weaver et. al., in review).

There are three RyR isoforms, each with distinct patterns of expression. RyR1 is the primary isoform involved in skeletal muscle excitation-contraction coupling (34). RyR1 is activated by the L-type VGCC Ca_V 1.1 independent of Ca^{2+} influx (21). The physical interaction of RyR1 to Ca_V 1.1 is responsible for the coupling of membrane E_m depolarization to Ca^{2+} store release. RyR2 is primarily expressed in cardiac myocytes. Cardiac excitation-contraction coupling, unlike skeletal muscle, requires Ca^{2+} influx, in this case through the L-type VGCC Ca_V 1.2 (3). RyR3 is expressed in neurons and skeletal muscle, and does not play a critical role in excitation-contraction physiology (22). Vascular smooth muscle expresses all three isoforms, but it is unclear which isoform(s) are responsible for Ca^{2+} sparks in this cell type (7).

The previously observed effects of IH to enhance myogenic tone through loss of H_2S and of H_2S to activate Ca^{2+} sparks led us to hypothesize that IH in rats reduces Ca^{2+} spark activity leading to enhanced myogenic tone in mesenteric arteries.

Methods

Animals

Male Sprague Dawley rats (275 to 325 g) were used for all studies and exposed to IH as described previously (18). Briefly, animals were housed in Plexiglas boxes with free access to food and water and exposed to either IH at a rate of 20 cycles per hour (nadir 5% O_2:5% CO_2 to peak 21% O_2:0% CO_2), or air–air cycling (alternating streams of

21% O_2:0% CO_2) for 7 hours per day as described previously (18). This IH protocol reduces PO_2 to ~35 mmHg and maintains PCO_2 at ~ 30 mmHg (32). On the day of the experiments, animals were anesthetized with sodium pentobarbital (200 mg/kg i.p.) and mesenteric arteries dissected for constrictor and Ca^{2+} imaging studies. All animal protocols were reviewed and approved by the institutional animal care and use committee of the University of New Mexico School of Medicine and conform to National Institutes of Health guidelines for animal use.

Isolated Vessel Preparation

The intestinal arcade was removed and placed in a Silastic-coated Petri dish containing chilled physiological saline solution (PSS; [in mmol/L] 129.8 NaCl, 5.4 KCl, 0.83 $MgSO_4$, 0.43 NaH_2PO_4, 19 $NaHCO_3$, 1.8 $CaCl_2$, and 5.5 glucose). Fourth or fifth-order artery segments were dissected from the mesenteric vascular arcade and placed in fresh PSS. Arteries were transferred to a vessel chamber (Living Systems), cannulated with glass micropipettes, and secured with silk ligatures. The arteries were pressurized to 60 mmHg with PSS using a servo-controlled peristaltic pump (Living Systems) and superfused with warmed, oxygenated PSS at a rate of 5 mL per minute.

Fura 2-Acetoxymethyl Ester Loading

Pressurized arteries were incubated 45 minutes in the dark at room temperature in fura 2-AM solution (2 µmol/L fura 2-AM and 0.05% pluronic acid in HEPES buffer). After incubation, arteries were washed with 37°C PSS for 15 minutes to remove excess dye. Fura 2–loaded vessels were alternately excited at 340 and 380 nm at a frequency of 1 Hz with an IonOptix Hyperswitch dual-excitation light source and the respective 510-nm emissions collected with a photomultiplier tube (F_{340}/F_{380}). Background-subtracted

F_{340}/F_{380} emission ratios were calculated with Ion Wizard software (IonOptix) and recorded continuously throughout the experiment with simultaneous measurement of inner diameter from bright-field images as described previously (26).

Pressure-Response Curves

Luminal pressure was increased from 20 to 180 mmHg using a servo-controlled peristaltic pump. Myogenic tone was allowed to develop for a minimum of 5 minutes at each 40 mmHg pressure step. For constrictor studies, arteries were subsequently incubated with Ca^{2+} free PSS for 60 minutes, and the pressure curve repeated to determine passive diameter at each pressure. Myogenic tone was then calculated as ((Ca free diameter)-(Ca containing diameter)/(Ca free diameter))*100.

Fluo-4 Imaging

Arteries used for fluo-4 studies were incubated in a fluo-4 AM (10 μmol/L, Invitrogen) solution containing 0.25% pluronic acid in HEPES buffer ([in mmol/L] 134 NaCl, 6 KCl, 1 $MgCl_2$, 2 $CaCl_2$, 10 HEPES, 0.026 EDTA, and 10 glucose) for 60 min at 28°C prior to cannulation. After loading with fluo-4, arteries were transferred to a vessel chamber, cannulated as described above, and pressurized to 60 mmHg. After 5 minutes equilibration in oxygenated PSS at 32°C, fluo-4 loaded arteries were excited at 488 nm by a solid state laser and emitted light > 500 nm was collected using an Olympus IX71 microscope with a 60X water-immersion lens and a spinning-disk confocal scanning unit (Andor). A 75 X 50 μm area was imaged at 50-60 Hz using a laser power of 15%.

Spark Analysis

Spark movies were analyzed using SparkAn software, developed by A. D. Bonev and M. T. Nelson (University of Vermont). Ten images without spark activity were

averaged to determine background fluorescence levels (F_0). Regions of interest of 25 pixels^2 (3 μm^2) were used to detect sparks with a minimum F/F_0 of 1.2. Each image contained 10-20 cells, and spark frequency was averaged for all cells visible.

Western Blot Analysis

Isolated mesenteric arteries (1st order to 5th order) were homogenized in lysis buffer [1X RIPA lysis and extraction buffer (Pierce), 1X Complete protease inhibitor cocktail (Santa Cruz Biotechnology), 1X Halt phosphatase inhibitor cocktail (Pierce), 2 mmol/L phenylmethanesulfonylfluoride] on ice. Protein concentration was determined in the supernatant using BCA assay (Pierce) as recommended by the manufacturer. Supernatants (5 μg/lane) were resolved by SDS-PAGE, and proteins were transferred to polyvinylidene difluoride membranes. After being blocked for nonspecific binding with blocking buffer (LI-COR), the membranes were incubated with primary anti-CSE antibody (mouse monoclonal,1 ug/mL; Abcam) or anti-β-actin antibody (1:10000; Sigma) at 4°C overnight, washed, and incubated with IRDye fluorescent secondary antibody (LI-COR) for 1 h at room temperature. Specifically bound antibody was detected using an Odyssey infrared imaging system (LI-COR). Relative content of the antigen protein was evaluated using Odyssey software (LI-COR). Band densities were normalized to total protein loaded per lane as assessed by β-actin levels.

Quantitative Real-time Polymerase Chain Reaction (qRT-PCR)

Mesenteric arteries from Sham and IH rats were stored in RNAlater (Ambion). Total RNA was isolated using the RNeasy Mini kit (Qiagen) following the manufacturer's protocol using the QIAcube system. Total RNA was reverse-transcribed to cDNA using High Capacity cDNA Archive Kit (Applied Biosystems). For real time

detection of CSE (Rn00567128_m1) transcripts and reference gene β-actin (4352931E), TaqMan Gene Expression Assays were used. PCR was performed using Applied Biosystems 7500 Fast Real-Time PCR System. The normalized gene expression method (2-ΔΔCT) for relative quantification of gene expression was used (24; 31) with GAPDH as endogenous control.

Statistical Analysis

Constriction, Ca^{2+} concentration, and spark frequency were analyzed using 2-way repeated-measures ANOVA with Student-Newman–Keuls post hoc analysis for differences between groups, concentrations, and interactions. Western blot and real-time PCR data were analyzed using Student's *t* test. $P<0.05$ was considered statistically significant for all analyses.

Results

IH impairs Ca^{2+} spark activation

Ca^{2+} spark frequency in arteries from Sham rat mesenteric arteries was increased by 10 μM NaHS (H_2S donor), 15 mM KCl, or an increase in pressure from 20 to 100 mmHg. However, Ca^{2+} spark frequency in arteries from IH rats did not significantly increase with any of these treatments (Fig. 1). IBMX (40 μM, phosphodiesterase inhibitor), however, increased Ca^{2+} spark frequency in Sham and IH arteries (Fig. 1B). Starting Ca^{2+} spark frequency was not different between groups. Ca^{2+} spark amplitude and duration were not affected by IH treatment (Fig. 2).

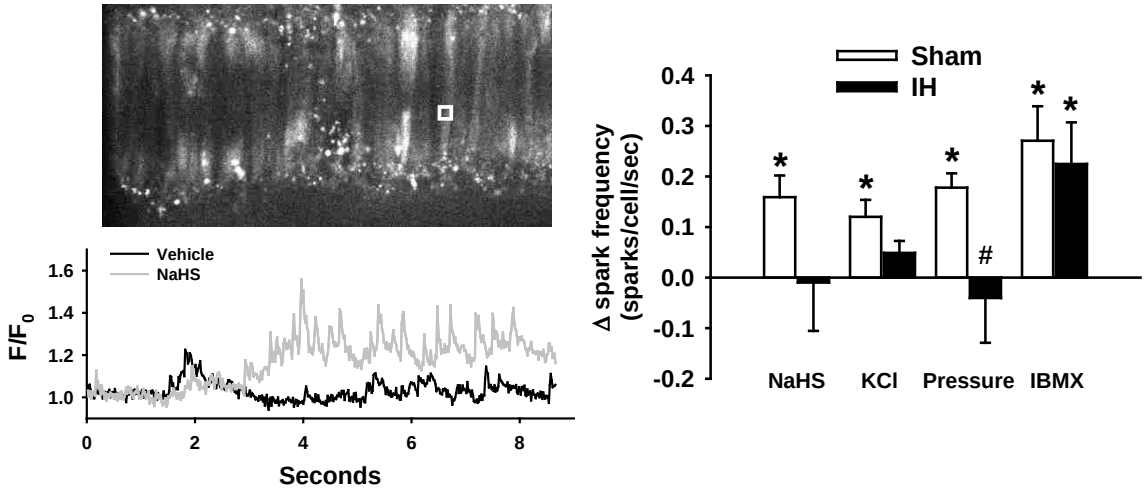

Figure 1.

Effect of IH treatment on Ca^{2+} spark activation. A: Example trace of sparks in a region of interest (ROI) before and after NaHS (10 μM) in a Sham artery. B: Summary data of spark activation over baseline (measured as Δ spark frequency) in Sham and IH arteries to NaHS (10 μM), KCl (15 mM), luminal pressure increase (20-100 mmHg), and IBMX (40 μM). C: Ca^{2+} spark amplitude and duration were not affected by treatments. n = 5-6 per group. * $p<0.05$ vs. baseline. #$p<0.05$ vs. Sham within treatment.

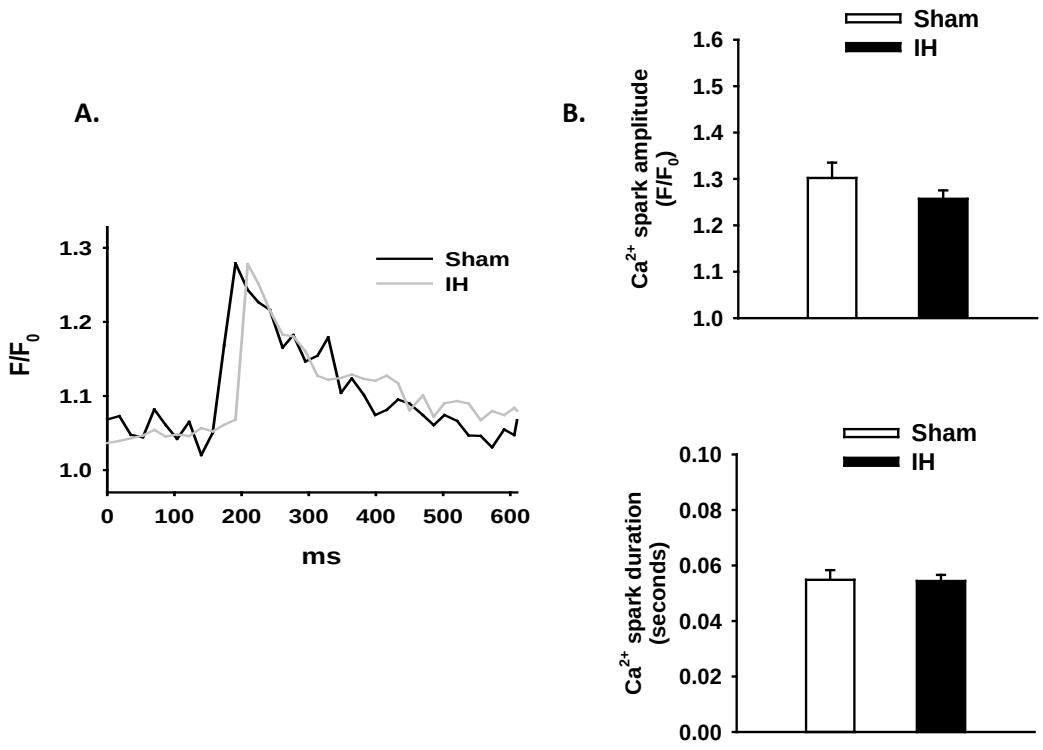

Figure 2.

Effect of IH treatment on Ca^{2+} spark frequency and duration. A: example sparks from Sham and IH superimposed. B: Summary data of spark frequency and duration in Sham and IH arteries. n = 5-6 per group.

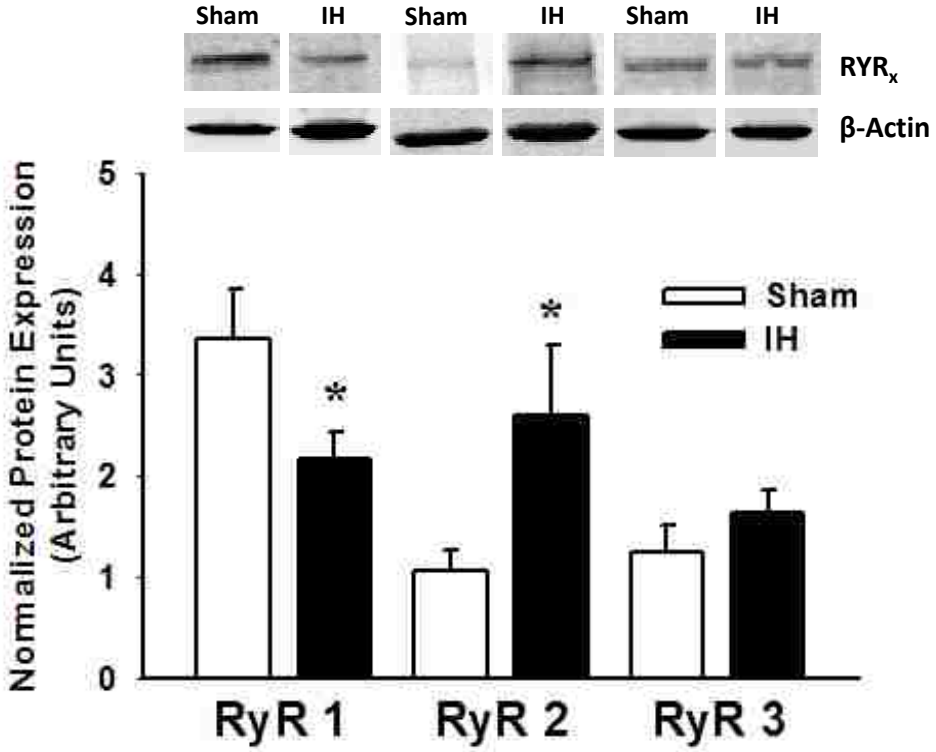

Figure 3.

Effect of IH treatment on expression of RyR isoforms in mesenteric arteries. Protein level probed by western blot and expressed in arbitrary units. n = 5 per group. *$p<0.05$ vs. Sham.

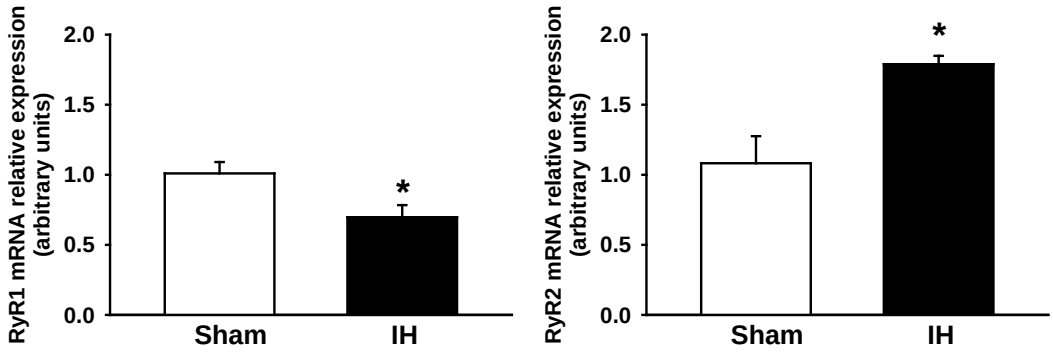

Figure 4.

Effect of IH treatment on RyR mRNA expression in mesenteric arteries. mRNA quantification normalized to GAPDH. n = 5 per group. *p<0.05 vs. Sham.

IH modifies ryanodine receptor expression

In western blots of RyR protein , there was less RyR1 expression but more RyR2 expression in IH compared to Sham mesenteric arteries (Fig. 3). RyR3 expression was not different between groups. Quantitative real-time PCR of RyR mRNA from mesenteric arteries showed that RyR1 mRNA expression was lower in IH arteries, whereas RyR2 mRNA was greater than that in Sham arteries (Fig. 4).

IH reduces ryanodine receptor regulation of myogenic tone

Blockade of RyR using ryanodine (10 μM) enhanced myogenic tone and VSMC $[Ca^{2+}]$ as measured by fura-2 in small mesenteric arteries from Sham rats but not in those from IH rats (Fig. 5). Myogenic tone in arteries from IH rats was greater than tone in arteries from Sham rats as described previously (13).

Discussion

This study establishes that IH reduces Ca^{2+} spark activation by known regulators of these Ca^{2+}-release events. Ca^{2+} sparks are thought to be important regulators of vascular function through activation of BK_{Ca} channels (27), which largely set VSMC membrane potential (4). The activation of a cluster of BK_{Ca} channels by Ca^{2+} sparks causes a spontaneous transient outward current, or STOC (29). These STOCs sum to cause a steady state E_m hyperpolarization of 10 mV or greater (20). Hypoxia has been previously shown to affect Ca^{2+} sparks. Acute hypoxic exposure causes an uncoupling of Ca^{2+} sparks to BK_{Ca} channels, thus reducing their hyperpolarizing effect (38). This effect was, however, caused by a reduced Ca^{2+} sensitivity of the BK_{Ca} channels, with no effect

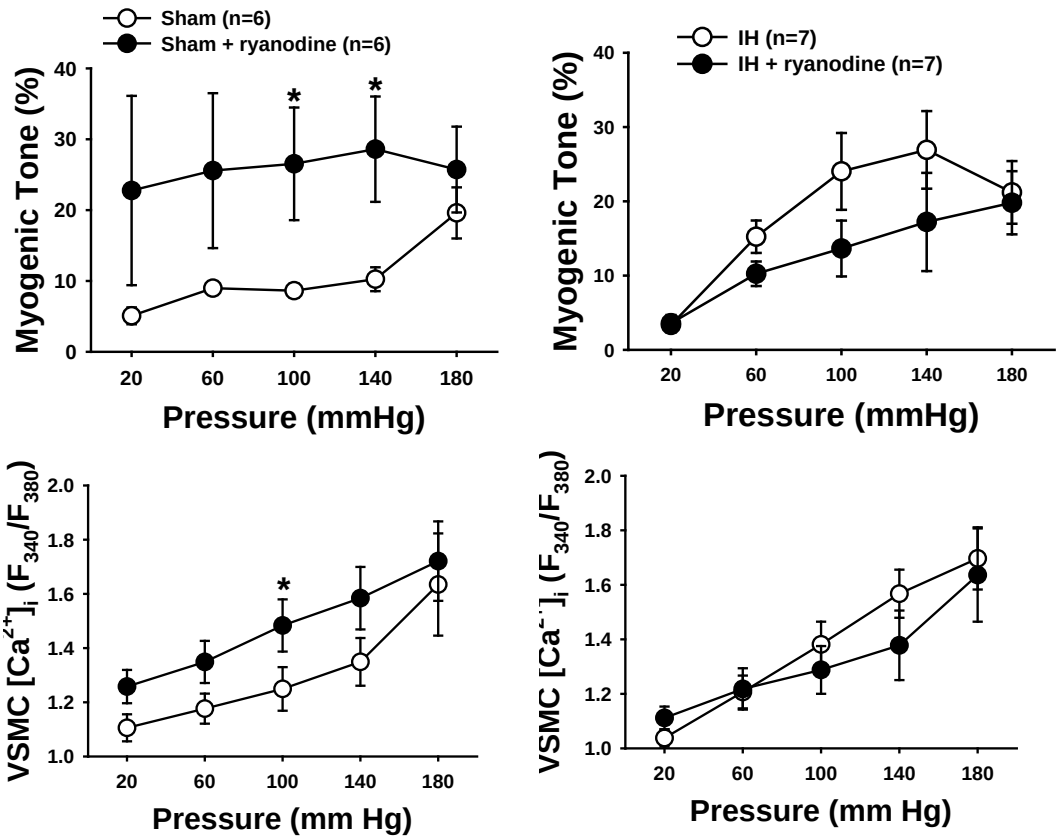

Figure 5.

Effect of ryanodine (10 μM) on myogenic tone and VSMC $[Ca^{2+}]_i$ in mesenteric arteries from Sham and IH rats. VSMC $[Ca^{2+}]_i$ was measured by ratio of fura-2 fluorescence. n = 6-7 per group. *$p<0.05$ vs. vehicle.

on Ca^{2+} spark frequency. Thus the effects of an acute hypoxic exposure versus two weeks of intermittent hypoxia (~1960 exposures) appear to be distinct. Furthermore, the effects of IH on Ca^{2+} sparks are persistent in the normoxic conditions under which the present experiments were performed, whereas the effects of hypoxia on Ca^{2+} spark-BK_{Ca} coupling are seen only during the hypoxic exposure.

In order to determine whether IH alters RyR expression as a possible mechanism of reduced Ca^{2+} spark activity, we measured levels of RyR protein in mesenteric arteries from Sham and IH rats. We found that IH reduces RyR1 expression but enhances RyR2 expression. In agreement with these findings, 6 hours of hypoxia has been shown to elevate RyR2 expression in the kidney (17). The experimental model in that study, however, was sustained hypoxia (8% O_2). Thus the effects of two weeks of IH and ischemia relatively short chronic hypoxia are likely to be different. This difference, as well as the more expansive range of cell types probed in the whole kidney, may explain the lack of effect on RyR1 in this hypoxia model that is apparent in our studies in mesenteric arteries. This RyR isoform switch in IH may indeed mediate the insensitivity to multiple Ca^{2+} spark activators.

The evidence for RyR isoform-specific function in VSMC is currently unconvincing, due primarily to the lack of pharmacological agents specific for the different isoforms. In addition, genetic knock-out of either RyR1or RyR2 is lethal (7). In cultured rat portal vein myocytes, antisense oligonucleotide injection demonstrated that both RyR1 and RyR2 are required for depolarization-induced Ca^{2+} spark activation (5). In contrast, RyR3 knockdown had no effect on sparks. This suggests that smooth muscle Ca^{2+} spark activation is perhaps mediated by interactions between RyR1 and RyR2. In

agreement with this, embryonic urinary bladder myocytes from RyR1 -/- mice show spontaneous Ca^{2+} spark activity, but do not display depolarization-induced increases in spark frequency (10). Furthermore, embryonic pulmonary artery VSMCs from RyR1 -/- mice displayed reduced spontaneous and caffeine-evoked spark activity but depolarization-induced spark activity was not examined (23). FK506 binding protein 12.6 (FKBP12.6) is thought to interact exclusively with RyR2 and inhibit its function. Thus FKBP12.6 -/- mice should have enhanced RyR2 activity. As predicted, urinary bladder myocytes from FKBP12.6 -/- mice display enhanced basal and depolarization-induced STOC frequency compared to wild type myocytes, thus demonstrating a role for RyR2 in spark production in this tissue (16).

Thus it seems that both RyR1 and RyR2 can be responsible for depolarization-induced Ca^{2+} spark activation in smooth muscle, but what role each plays in specific tissues is far from clear. Our results suggest that RyR1 may be more important for the response in mesenteric artery myocytes, since a decrease in expression of this channel was associated with loss of Ca^{2+} spark activation. Ca^{2+} sparks are generated from clusters of approximately 10 RyR channels (14), and perhaps the requirement for both RyR1 and RyR2 in the depolarization-induced spark activation indicate that these clusters are heteromeric composites of both channels. In this model, one isoform senses the depolarization, presumably through L-type VGCC activation. Then the Ca^{2+} released through this isoform activates the whole RyR cluster through Ca^{2+}-induced Ca^{2+} release and/or allosteric coupled gating mechanisms (33). Our results seem to suggest that RyR1 is the depolarization sensor, since reduced expression of this isoform abolishes

depolarization-induced spark activation. This is a speculative model, at the moment and future work is required to test these predictions.

It is interesting that IH VSMC Ca^{2+} sparks also do not respond to H_2S. Presumably KCl-induced depolarization and increases in luminal pressure share the mechanism of L-type VGCC activation, but H_2S is not known to activate these channels. H_2S does, however, cause dilation through activation of cytochrome P450 epoxygenase (Jackson-weaver et al., in review), which activates sparks through 11,12 EET-mediated opening of TRPV4 channels (6). Perhaps TRPV4 and L-type VGCC activation stimulate spark activity through similar mechanisms. Alternatively, the RyR receptor isoform switch may not play a role in the lack of spark activation in IH. It is possible that an altered expression of cytochrome P450 epoxygenases or TRPV4 channels could cause this effect. Future work again is needed to resolve these questions.

It is possible that the isoform switch in IH arteries has no effect on IBMX-induced spark activation because PKA and PKG do not directly affect the ryanodine receptor. In mice in which phospholamban was genetically ablated, forskolin-induced increases in cAMP did not alter Ca^{2+} spark frequency, whereas myocytes from wild type mice showed a normal increase (37). This suggests that IBMX may enhance SR Ca^{2+} load through PKA and PKG with a subsequent increase in Ca^{2+} spark frequency due to the RyR activation by SR Ca^{2+} (8). Alternatively, IH may not affect IBMX stimulation of Ca^{2+} spark frequency because PKA and PKG affect RyR1 and RyR2 similarly and the fall in RyR1 expression is offset by RyR2 increases.

These results have potential implications for sleep apnea-induced hypertension. Treatment-resistant hypertension is highly prevalent in patients with hypertension as well

as sleep apnea, highlighting a need for novel treatment options in this population (28). The alteration of RyR isoform expression in IH may affect the efficacy of future antihypertensive treatments that target, either indirectly or directly, Ca^{2+} spark activation. NO and H_2S have both been shown to activate Ca^{2+} sparks to mediate vasodilation (25; 30; and Jackson-Weaver et. al., in review), and both are potential targets for future antihypertensive therapies. Thus it may be that novel antihypertensive treatments in patients with sleep apnea will prove more efficacious if continuous positive airway pressure (CPAP) therapy is co-administered to alleviate IH-mediated transcriptional alterations in RyR expression.

In summary, this study provides evidence that IH impairs Ca^{2+} spark activation by depolarization, luminal pressure increases, and H_2S administration, leading to enhanced myogenic tone in small mesenteric arteries. These effects are accompanied by an isoform switch from RyR1 to RyR2 suggesting future studies are needed to elucidate the mechanism by which RyR isoform expression affects Ca^{2+} spark sensitivity to these stimuli.

Author contributions: O.J.W. performed Ca^{2+} spark, PCR, and myogenic tone experiments and wrote the manuscript, D.A.P. performed western blot experiments, A.M.I. performed PCR experiments, L.V.G.B., B.R.W., and N.L.K. designed the experiments, interpreted data, and edited the manuscript.

Sources of Funding

OJW (HL7736, 10PRE4050028, American Heart Association); LGB (HL088151); BRW (HL95640); NLK (EPA STAR award PHS 83186, HL82799 and is an established investigator of the American Heart Association)

Conflicts of Interests/Disclosures

None

Reference List

1. **Allahdadi KJ, Duling LC, Walker BR and Kanagy NL**. Eucapnic intermittent hypoxia augments endothelin-1 vasoconstriction in rats: role of PKCdelta. *Am J Physiol Heart Circ Physiol* 294: H920-H927, 2008.

2. **Bao G, Metreveli N, Li R, Taylor A and Fletcher EC**. Blood pressure response to chronic episodic hypoxia: role of the sympathetic nervous system. *J Appl Physiol* 83: 95-101, 1997.

3. **Bers DM**. Cardiac excitation-contraction coupling. *Nature* 415: 198-205, 2002.

4. **Brayden JE and Nelson MT**. Regulation of arterial tone by activation of calcium-dependent potassium channels. *Science* 256: 532-535, 1992.

5. **Coussin F, Macrez N, Morel JL and Mironneau J**. Requirement of ryanodine receptor subtypes 1 and 2 for Ca(2+)-induced Ca(2+) release in vascular myocytes. *J Biol Chem* 275: 9596-9603, 2000.

6. **Earley S, Heppner TJ, Nelson MT and Brayden JE**. TRPV4 forms a novel Ca2+ signaling complex with ryanodine receptors and BKCa channels. *Circ Res* 97: 1270-1279, 2005.

7. **Essin K and Gollasch M**. Role of ryanodine receptor subtypes in initiation and formation of calcium sparks in arterial smooth muscle: comparison with striated muscle. *J Biomed Biotechnol* 2009:135249. Epub;%2009 Dec 8.: 135249, 2009.

8. **Essin K, Welling A, Hofmann F, Luft FC, Gollasch M and Moosmang S**. Indirect coupling between Cav1.2 channels and ryanodine receptors to generate Ca2+ sparks in murine arterial smooth muscle cells. *J Physiol* 584: 205-219, 2007.

9. **Fletcher EC, Orolinova N and Bader M**. Blood pressure response to chronic episodic hypoxia: the renin-angiotensin system. *J Appl Physiol* 92: 627-633, 2002.

10. **Fritz N, Morel JL, Jeyakumar LH, Fleischer S, Allen PD, Mironneau J and Macrez N**. RyR1-specific requirement for depolarization-induced Ca2+ sparks in urinary bladder smooth muscle. *J Cell Sci* 120: 3784-3791, 2007.

11. **Gjorup PH, Sadauskiene L, Wessels J, Nyvad O, Strunge B and Pedersen EB**. Abnormally increased endothelin-1 in plasma during the night in obstructive sleep apnea: relation to blood pressure and severity of disease. *Am J Hypertens* 20: 44-52, 2007.

12. **Herrera GM, Heppner TJ and Nelson MT**. Voltage dependence of the coupling of Ca(2+) sparks to BK(Ca) channels in urinary bladder smooth muscle. *Am J Physiol Cell Physiol* 280: C481-C490, 2001.

13. **Jackson-Weaver O, Paredes DA, Gonzalez Bosc LV, Walker BR and Kanagy NL**. Intermittent hypoxia in rats increases myogenic tone through loss of hydrogen sulfide activation of large-conductance Ca(2+)-activated potassium channels. *Circ Res* 108: 1439-1447, 2011.

14. **Jaggar JH, Porter VA, Lederer WJ and Nelson MT**. Calcium sparks in smooth muscle. *Am J Physiol Cell Physiol* 278: C235-C256, 2000.

15. **Ji G, Barsotti RJ, Feldman ME and Kotlikoff MI**. Stretch-induced calcium release in smooth muscle. *J Gen Physiol* 119: 533-544, 2002.

16. **Ji G, Feldman ME, Greene KS, Sorrentino V, Xin HB and Kotlikoff MI**. RYR2 proteins contribute to the formation of Ca(2+) sparks in smooth muscle. *J Gen Physiol* 123: 377-386, 2004.

17. **Jurkovicova D, Sedlakova B, Lacinova L, Kopacek J, Sulova Z, Sedlak J and Krizanova O**. Hypoxia differently modulates gene expression of inositol 1,4,5-trisphosphate receptors in mouse kidney and HEK 293 cell line. *Ann N Y Acad Sci* 1148:421-7.: 421-427, 2008.

18. **Kanagy NL, Walker BR and Nelin LD**. Role of endothelin in intermittent hypoxia-induced hypertension. *Hypertension* 37: 511-515, 2001.

19. **Kato M, Roberts-Thomson P, Phillips BG, Haynes WG, Winnicki M, Accurso V and Somers VK**. Impairment of endothelium-dependent vasodilation of resistance vessels in patients with obstructive sleep apnea. *Circulation* 102: 2607-2610, 2000.

20. **Knot HJ, Standen NB and Nelson MT**. Ryanodine receptors regulate arterial diameter and wall [Ca2+] in cerebral arteries of rat via Ca2+-dependent K+ channels. *J Physiol* 508 (Pt 1): 211-221, 1998.

21. **Lamb GD**. Excitation-contraction coupling in skeletal muscle: comparisons with cardiac muscle. *Clin Exp Pharmacol Physiol* 27: 216-224, 2000.

22. **Lanner JT, Georgiou DK, Joshi AD and Hamilton SL**. Ryanodine receptors: structure, expression, molecular details, and function in calcium release. *Cold Spring Harb Perspect Biol* 2: a003996, 2010.

23. **Li XQ, Zheng YM, Rathore R, Ma J, Takeshima H and Wang YX**. Genetic evidence for functional role of ryanodine receptor 1 in pulmonary artery smooth muscle cells. *Pflugers Arch* 457: 771-783, 2009.

24. **Livak KJ and Schmittgen TD**. Analysis of relative gene expression data using real-time quantitative PCR and the 2(-Delta Delta C(T)) Method. *Methods* 25: 402-408, 2001.

25. **Mandala M, Heppner TJ, Bonev AD and Nelson MT**. Effect of endogenous and exogenous nitric oxide on calcium sparks as targets for vasodilation in rat cerebral artery. *Nitric Oxide* 16: 104-109, 2007.

26. **Naik JS, Earley S, Resta TC and Walker BR**. Pressure-induced smooth muscle cell depolarization in pulmonary arteries from control and chronically hypoxic rats does not cause myogenic vasoconstriction. *J Appl Physiol* 98: 1119-1124, 2005.

27. **Nelson MT, Cheng H, Rubart M, Santana LF, Bonev AD, Knot HJ and Lederer WJ**. Relaxation of arterial smooth muscle by calcium sparks. *Science* 270: 633-637, 1995.

28. **Pedrosa RP, Drager LF, Gonzaga CC, Sousa MG, de Paula LK, Amaro AC, Amodeo C, Bortolotto LA, Krieger EM, Bradley TD and Lorenzi-Filho G**. Obstructive sleep apnea: the most common secondary cause of hypertension associated with resistant hypertension. *Hypertension* 58: 811-817, 2011.

29. **Perez GJ, Bonev AD, Patlak JB and Nelson MT**. Functional coupling of ryanodine receptors to KCa channels in smooth muscle cells from rat cerebral arteries. *J Gen Physiol* 113: 229-238, 1999.

30. **Porter VA, Bonev AD, Knot HJ, Heppner TJ, Stevenson AS, Kleppisch T, Lederer WJ and Nelson MT**. Frequency modulation of Ca2+ sparks is involved in regulation of arterial diameter by cyclic nucleotides. *Am J Physiol* 274: C1346-C1355, 1998.

31. **Shahar E, Whitney CW, Redline S, Lee ET, Newman AB, Javier NF, O'Connor GT, Boland LL, Schwartz JE and Samet JM**. Sleep-disordered breathing and cardiovascular disease: cross-sectional results of the Sleep Heart Health Study. *Am J Respir Crit Care Med* 163: 19-25, 2001.

32. **Snow JB, Kitzis V, Norton CE, Torres SN, Johnson KD, Kanagy NL, Walker BR and Resta TC**. Differential effects of chronic hypoxia and intermittent hypocapnic and eucapnic hypoxia on pulmonary vasoreactivity. *J Appl Physiol* 104: 110-118, 2008.

33. **Stern MD, Song LS, Cheng H, Sham JS, Yang HT, Boheler KR and Rios E**. Local control models of cardiac excitation-contraction coupling. A possible role for allosteric interactions between ryanodine receptors. *J Gen Physiol* 113: 469-489, 1999.

34. **Takeshima H, Iino M, Takekura H, Nishi M, Kuno J, Minowa O, Takano H and Noda T**. Excitation-contraction uncoupling and muscular degeneration in mice lacking functional skeletal muscle ryanodine-receptor gene. *Nature* 369: 556-559, 1994.

35. **Troncoso Brindeiro CM, da Silva AQ, Allahdadi KJ, Youngblood V and Kanagy NL**. Reactive oxygen species contribute to sleep apnea-induced hypertension in rats. *Am J Physiol Heart Circ Physiol* 293: H2971-H2976, 2007.

36. **Vgontzas AN, Papanicolaou DA, Bixler EO, Kales A, Tyson K and Chrousos GP**. Elevation of plasma cytokines in disorders of excessive daytime sleepiness: role of sleep disturbance and obesity. *J Clin Endocrinol Metab* 82: 1313-1316, 1997.

37. **Wellman GC, Santana LF, Bonev AD and Nelson MT**. Role of phospholamban in the modulation of arterial Ca(2+) sparks and Ca(2+)-activated K(+) channels by cAMP. *Am J Physiol Cell Physiol* 281: C1029-C1037, 2001.

38. **Zhao G, Adebiyi A, Xi Q and Jaggar JH**. Hypoxia reduces KCa channel activity by inducing Ca2+ spark uncoupling in cerebral artery smooth muscle cells. *Am J Physiol Cell Physiol* 292: C2122-C2128, 2007.